AD-A153 121 A CLOSED LOOP ANALYSIS OF POGO INSTABILITY(U) AIR FORCE 1/2
INST OF TECH WRIGHT-PATTERSON AFB OH SCHOOL OF
ENGINEERING D A ROSENBERG DEC 84 AFIT/GA/AA/84D-9
UNCLASSIFIED F/G 21/9.1 NL

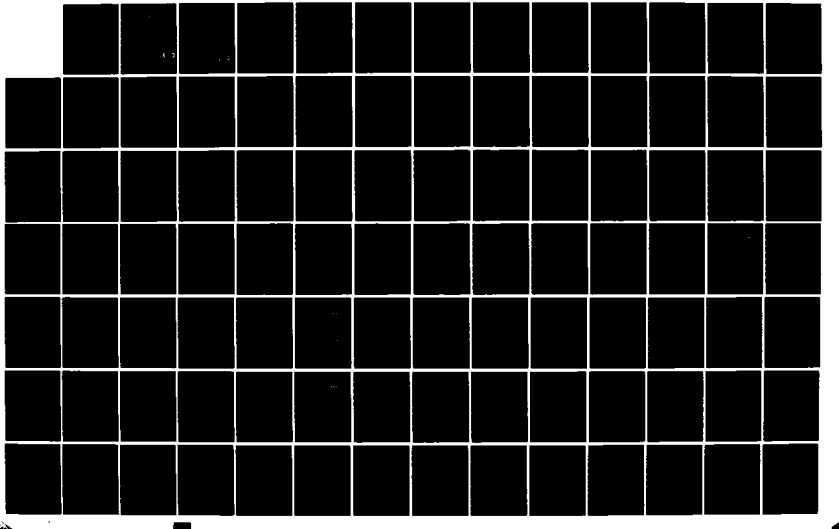

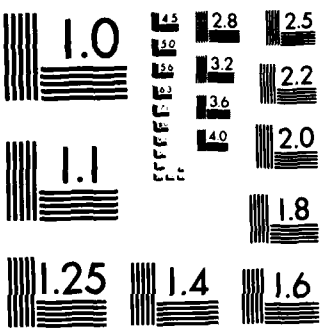

MICROCOPY RESOLUTION TEST CHART
NATIONAL BUREAU OF STANDARDS-1963-A

(1)

A CLOSED LOOP ANALYSIS OF POGO INSTABILITY

THESIS

David A. Rosenberg
Second Lieutenant, USAF

AFIT/GA/AA/84D-9

DEPARTMENT OF THE AIR FORCE
AIR UNIVERSITY
AIR FORCE INSTITUTE OF TECHNOLOGY

Wright-Patterson Air Force Base, Ohio

AFIT/GA/AA/84D-9

A CLOSED LOOP ANALYSIS OF POGO INSTABILITY

THESIS

David A. Rosenberg
Second Lieutenant, USAF

AFIT/GA/AA/84D-9

Approved for public release; distribution unlimited

AFIT/GA/AA/84D-9

A CLOSED LOOP ANALYSIS OF POGO INSTABILITY

THESIS

Presented to the Faculty of the School of Engineering

of the Air Force Institute of Technology

Air University

In Partial Fulfillment of the

Requirements for the Degree of

Master of Science in Astronautical Engineering

David A. Rosenberg, B.S.

Second Lieutenant, USAF

December 1984

Preface

The purpose of this investigation was to develop and verify a generalized computer model for POGO instability. The solution of POGO and other self-excited instability problems is of paramount concern in the design of any liquid rocket system. Furthermore, improved liquid rocket systems will almost certainly be a major development item for the support of future Air Force space systems, as well as for the NASA space station.

A non-linear approach employing the method of characteristics in conjunction with component models from numerous sources was used in generating a digital computer code to determine both the transient and steady state responses of a typical bipropellant liquid rocket to sinusoidal thrust oscillations. Since the goal of this study was to create the computer code and not to perform an exhaustive parametric analysis, the programs were written in the BASIC language and implemented on a personal computer. However, this code could easily be transported to a main frame system (such as a CYBER) and a thorough design study would be most enlightening.

I wish to thank my advisor, Dr. M.E. Franke for his help in establishing the overall direction and organization of this work. Also, the steady state results were very time consuming and would not have been possible without the computer time donated by my fellow section members Captains Henry Baird, Dave Thomin, Steve Moore, and Mario Borja, as well as my friends Thomas Black and Josè Flores. Finally, I thank my wife Julia for her proofreading of this thesis and her infinite patience and understanding during the many evenings and weekends on which I was chained to my computer terminal.

David A. Rosenberg

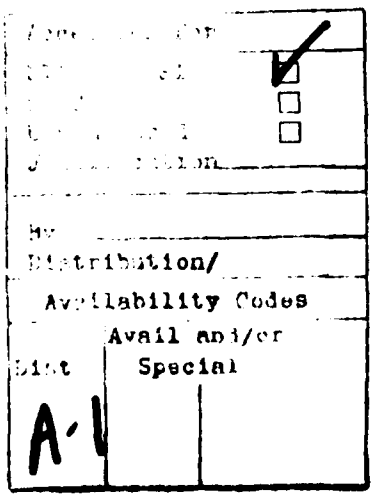

Table of Contents

List of Figures

Notation

A:	Element Cross Sectional Area	a:	Sonic Velocity
A^*:	Dorsch Pump Parameter	B_{inj}:	Dorsch Injector Constant
$B0$:	Pump Coefficient	$B1$:	Pump Coefficient
$B2$:	Pump Coefficient	$B3$:	Pump Coefficient
B^*:	Dorsch Pump Parameter	C^*:	Effective Exhaust Velocity
C_0^*:	Nominal Exhaust Velocity	C_{slope}^*:	Local Slope of C^*
C_M:	Backward Characteristic Value	C_p:	Forward Characteristic Value
C_T:	Thrust Coefficient	C^*:	Dorsch Pump Parameter
D:	Effective Pipe Diameter	E_c:	Valve Closure Parameter
F:	Thrust	F_o:	Nominal Thrust
f:	Friction Factor	g:	Local Acceleration
i_{max}:	Number of Single Pipe Sections	K:	Fluid Bulk Modulus
L^*:	Chamber Characteristic Length	M:	Mass
$\dot{M}$:	Mass Flow Rate	MR:	Mixture Ratio
NS:	Number of Sections in Element	P:	Pressure
P_C:	Combustor Pressure	P_{Po}:	Nominal Pump Inlet Pressure
R:	Gas Constant (exhaust gas)	T_C:	Combustor Temperature
t_{cut}:	Valve Closure Time	V:	Velocity
Vol:	Cavitation "Bubble" Volume	Vol_o:	Initial "Bubble" Volume
V_{Po}:	Nominal Pump Flow Velocity	x:	Displacement

β:	Area Ratio	γ:	Pipe Material Young's Modulus
ΔH_{inj}:	Dorsch Injector Pressure Drop	ΔP:	Pump Pressure Rise
ΔP_0:	Nominal Pump Pressure Rise	Δt:	Time Increment
Δx:	Section Separation	θ:	Grid-Mesh Ratio
θ_g:	Gas Residence Time	ρ:	Density
τ:	Orifice Flow Constant	τ_C:	Chamber Dead Time
ω:	Circular Frequency	ω_n:	Natural Frequency
ζ:	Grid Parameter		

Subscripts

C:	Combustor	D:	Downstream
Dischg:	Discharge Line	F:	Fuel System
Feed:	Feed Line	inj:	Injector
Ox:	Oxidizer System	P:	Pump
T:	Tank	U:	Upstream
Ull:	Ullage		

Pressure and Velocity Indices

Pressure and velocity terms for the systems modeled in this study are designated with indices and qualifying subscripts. The indicies, 1 thru 7 refer to the Figs. 4.1B, 4.3B, and 4.6B and the single pipe, monopropellant, and bipropellant systems, respectively. Qualifying identifiers are found in the subscripts list.

Abstract

In this thesis, a generalized computer code for the simulation of POGO instability in liquid rockets was generated and verified. The term POGO refers to the out of phase motion of the ends of a liquid rocket, which can build to a dangerous magnitude due to propulsion feed back. The elimination of any POGO instability will be of great importance in the development of future liquid rocket systems such as ~~OTV's and OMV's~~. The model detailed in this investigation is based on a method of characteristics solution of the simplified Navier-Stokes equations. The resulting non-linear differential equations were solved using first order finite difference methods. This solution was applied to the fluid lines of several liquid rocket systems. Boundary conditions, based on component models used generally throughout the literature were developed to link these fluid lines.

The computer routines were verified by comparison with published results from several sources. The results of numerous runs agreed quite well with the published data, even in very non-linear systems with large disturbance amplitudes.

As an aid to future investigators the routines developed in this thesis were applied to a typical bipropellant liquid rocket system. Both the transient and the steady state responses of this system to sinusoidal thrust perturbations were obtained. A relatively limited parametric study was performed and indicated that this particular system was very stable and showed no sign of POGO instability. Two factors were most important in the system's stability: the pump operating points and the chamber dead time; the stability of the system being greatly enhanced by the the stable range in which the pumps operated and the selection of a relatively short combustor dead time.

A user's guide was compiled to detail the software developed in this investigation. Its purpose is to facilitate the application of these routines to other systems by future investigators.

Orifice in Line. Applying the standard pressure flow equation at the orifice:

$$V_D = \tau\sqrt{P_U - P_D} \qquad [3.7]$$

Combining with the compatibility and continuity relations

$$P_U = C_P - \rho a_U V_U; \quad P_D = C_M + \rho a_D V_D$$

$$A_U V_U = A_D V_D$$

Solving for V_D in terms of quadratic coeficients,

For V_D:

$$B = \tau^2 \rho(\beta a_U - a_D) \qquad [3.8]$$

$$C = \tau^2(C_M - C_P); \quad \beta = \frac{A_D}{A_U}$$

The quadratic coefficients **A**, **B**, and **C** are used with [3.6] in determining **V**. The other unknowns may now be computed. This boundary condition is similar to the section area change except that a specified loss is implied by Eq. [3.7].

Relative Component Motion. Fig. 3.3 depicts relative motion between two system elements. If the areas and orientations of the two elements are dissimilar, there will in general be a finite rate of fluid storage at their interface due to the relative motion. Equating the rate of storage to the rate of inflow minus the rate of outflow at the interface[1:9]

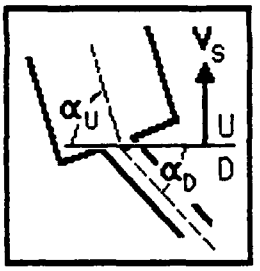

Figure 3.3
Relative component motion.

$$V_U A_U - V_D A_D = -V_S(A_U \sin\alpha_U - A_D \sin\alpha_D) \qquad [3.9]$$

Using the simple continuity relation for an incompressible fluid[14]:

$$A_U V_U = A_D V_D \qquad [3.3]$$

Assuming no energy dissipation (i.e. assuming no losses) at the interface[14:37] and equating the total pressure at either side of the interface:

$$P_U + \tfrac{1}{2}\rho V_U^2 = P_D + \tfrac{1}{2}\rho V_D^2 \qquad [3.4]$$

There are now four equations in four unknowns. Solving in terms of the downstream velocity:

$$AV_D^2 + BV_D + C = 0 \qquad [3.5]$$

where: $\beta = \frac{A_D}{A_U}$ $\qquad A = (1 - \beta^2)$

$$B = 2(a_D + \beta a_U) \qquad C = \frac{2}{\rho}(C_M - C_P)$$

The unsubscripted terms, **A**, **B**, and **C** are quadratic coefficients. From the sense of Fig. 3.2, **A** will be a positive quantity. Thus to obtain a positive flow velocity, the positive square root should be applied in the quadratic formula:

$$V_D = \frac{-B + \sqrt{B^2 - 4AC}}{2A} \qquad [3.6]$$

Note that other boundary conditions will be described in terms of quadratic coefficients (the identifiers **A**, **B**, and **C** will be used in each case). Unless otherwise stated, use of the positive form of the quadratic equation ([3.6]) will be assumed. It is now possible to solve for the other quantities. This completely specifies conditions at both end points. Note that the only assumption made was to neglect energy dissipation at the interface. For the typical liquid rocket, this is a reasonable assumption due to the relatively small velocities in the feed system as well as the streamlined geometries involved[1:5].

Known Pressure Upstream or Downstream. If the pressure at the upstream or downstream end of a conduit is a known function of time F(t), this relation can be combined with Eqs. [2.16] or [2.17] to fix the endpoint conditions[14]. For the upstream and downstream cases

Known Pressure Upstream

$$P_U = F(t);\quad P_D = P_U;\quad P_D = C_M + \rho a_D V_D \qquad [3.1]$$

Known Pressure Downstream

$$P_D = F(t);\quad P_U = P_D;\quad P_U = C_P - \rho a_U V_U$$

Note that the subscripts U and D refer to points infinitessimally upstream and downstream of the end in question, not to the end itself. Combining the equations to find the velocity at either end of the pipe:

$$V_D = \frac{F(t) - C_M}{\rho a_D} \quad [3.1] \qquad V_U = \frac{C_P - F(t)}{\rho a_U} \quad [3.2]$$

Eqs. [3.1] and [3.2] give the velocities at either end of the pipe. Since the pressure has already been specified, the boundary conditions are completely fixed. Both the upstream and downstream elements in this system will affect each other. Thus, the dynamic effects of each element in a complex system will propagate both upstream and downstream.

Section Area Change. Fig. 3.2 depicts the interface between lines of constant area. Each line is modeled as in the previous section and it is necessary to develop the relations which connect them. Applying a compatibility equation at each pipe end

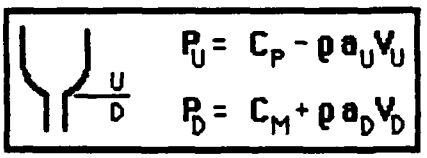

Figure 3.2
Section area change.

III. Elements and Boundary Conditions

In this section, the major components of a typical liquid rocket will be examined with the aim of applying the knowledge of their dynamic behavior (taken from various sources in the literature) to the problem of mating them to their connecting fluid lines. First however, it will be necessary to describe the connection between these external elements and the finite difference equations which model the pipe flow portion of the problem. That is, a general form for the various types of boundary conditions in the system must be determined.

Boundary Conditions

At either end of a single pipe only one of the compatibility equations (Eqs. [2.16] or [2.17]) is available. This situation is depicted in Fig. 3.1[14:36]. At the upstream end of the pipe, only the backward difference equation (Eq. [2.17]) is available; the situation is reversed at the downstream end. To determine the pressure and velocity at the ends, it will be necessary to develop auxillary equations (boundary conditions) based on end conditions.

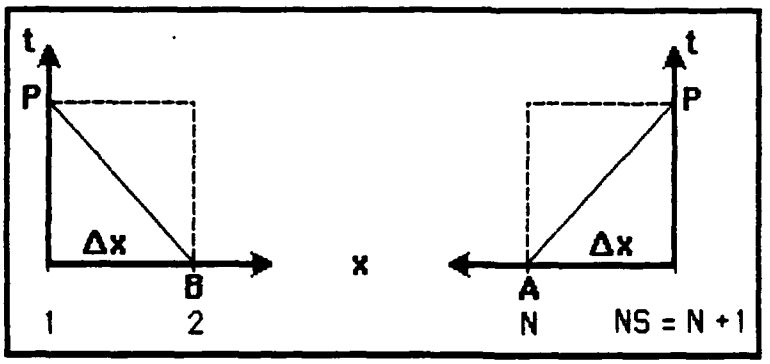

Figure 3.1
Pipe end conditions.

To maintain convergence, the Courant condition[14] must be satisfied, namely

$$\theta \leq \frac{1}{V+a}; \quad \zeta \leq \frac{a}{V+a} \qquad [2.27]$$

This simply implies that in Fig. 2.1, the points **R** and **S** fall between **A** and **B**. Finally, combining Eqs. [2.16] and [2.17] and solving for the pressure at point **P**[14]:

$$P_P = \frac{C_P + C_M}{2} \qquad [2.28]$$

Either of Eqs. [2.16] or [2.17] can be used to compute the velocity. This completely establishes the state at all internal points in the pipe. Note that a linear interpolation has been used. In order to maintain the accuracy of the non-linear results, the values of ζ and θ should approach the Courant limits, implying only a small interpolation. The pipe flow problem is completely solved at this point, however the problem of establishing the boundary conditions at the end points (where either **Cp** or **Cm** are unknown) remains.

Importance of Boundary Condtions

The equations developed in this section allow the computation of the pressure and velocity at essentially arbitrary points inside a conduit. Unfortunately, a liquid rocket is more than a simple collection of pipes. Indeed, the boundary conditions make up the most active components of the system. In the next section, boundary conditions which link the pipe elements of a rocket propulsion system will be developed.

highly deformable tubes or compressible fluids, the variation in Δt would greatly complicate a complex system with multiple elements since boundary conditions must be passed from one element to the next. For this reason constant time steps will be used.

Specified Time Intervals. Rearranging Eqs. [2.12] and [2.14][14]:

$$P_P = C_P - \rho a_R V_P \qquad [2.16]$$

$$P_P = C_M - \rho a_S V_P \qquad [2.17]$$

$$C_P = P_R + \rho a_R V_R \left[1 + \frac{g}{V_R}\Delta t \sin\alpha - \frac{f\Delta t|V_R|}{2D}\right] \qquad [2.18]$$

$$C_M = P_S + \rho a_S V_S \left[1 + \frac{g}{V_S}\Delta t \sin\alpha - \frac{f\Delta t|V_S|}{2D}\right] \qquad [2.19]$$

From Fig. 2.1 it is apparent that

$$\frac{x_C - x_R}{x_C - x_A} = \frac{V_C - V_R}{V_C - V_A} \qquad [2.20]$$

Noting that

$$V_R = \frac{V_C - \zeta_R(V_C - V_A)}{1 + \theta_R(V_C - V_A)} \qquad [2.21]$$

$$\theta = \frac{\Delta t}{\Delta x} \qquad [2.22] \qquad \zeta = \frac{\Delta t}{\Delta x} a = \theta a \qquad [2.23]$$

Similarly,

$$V_S = \frac{V_C - \zeta_S(V_C - V_B)}{1 + \theta_S(V_C - V_B)} \qquad [2.24]$$

$$P_R = P_C - (V_R \theta_R + \zeta_R)(P_C - P_A) \qquad [2.25]$$

$$P_S = P_C + (V_S \theta_S + \zeta_S)(P_C - P_A) \qquad [2.26]$$

The pressure and velocity at points A, C, and B which occur at time t are known (either from the last time-step iteration or from steady state results). Conditions at points R and S occur at time t but must be calculated from known relationships. The state at point P occurs at time $t+\Delta t$. Our approach is to use Eqs. [2.8]-[2.10] to compute the conditions at P. Multiplying by the differential time dt, and integrating (to first order):

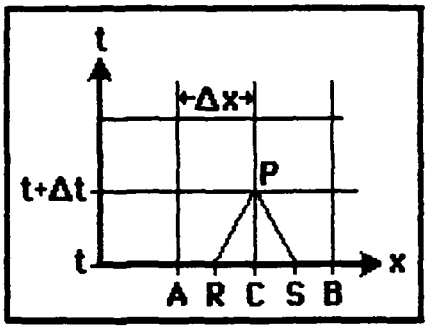

Figure 2.1
Time-displacement grid.

$$P_P - P_R + \rho a_R (V_P - V_R) - \rho a_R g \sin\alpha \; (t_P - t_R) + \rho a_R \frac{f V_R |V_R|}{2D} (t_P - t_R) = 0 \qquad [2.12]$$

$$x_P - x_R = (V_R - a_R)(t_P - t_R) \qquad [2.13]$$

$$P_P - P_S - \rho a_S (V_P - V_S) + \rho a_S g \sin\alpha \; (t_P - t_S) - \rho a_S \frac{f V_S |V_S|}{2D} (t_P - t_S) = 0 \qquad [2.14]$$

$$x_P - x_S = (V_S - a_S)(t_P - t_S) \qquad [2.15]$$

There are two possible approaches in obtaining a numerical solution to these equations: the use of a grid of characteristics or the use of specified time intervals. With the grid of characteristics, the time-step is chosen so that the points R and S fall on points A and B respectively. While this can lead to improved accuracy (relative to the use of specified time intervals) in

[2.1] and [2.2]. If the appropriate selections are made, simplification is possible. In particular, since P and V are functions of x and t, regarding x as a function of t, then

$$\frac{dP}{dt} = P_x \frac{dx}{dt} + P_t ; \quad \frac{dV}{dt} = V_x \frac{dx}{dt} + V_t \qquad [2.4]$$

This can be accomplished if

$$\frac{dx}{dt} = V + \frac{1}{\lambda \rho} = V + \rho a^2 \lambda \qquad [2.5]$$

Now, Eq. [2.3] becomes the ordinary differential equation

$$\lambda \frac{dP}{dt} + \frac{dV}{dt} - g \sin\alpha + \frac{f V|V|}{2D} \qquad [2.6]$$

Solving Eq. [2.5]

$$\lambda = \frac{1}{\rho a} ; \quad \frac{dx}{dt} = V + a$$
$$\lambda = -\frac{1}{\rho a} ; \quad \frac{dx}{dt} = V - a \qquad [2.7]$$

Substituting Eq. [2.7] into [2.6] produces the following total differential equations:

$$\frac{dP}{dt} + \rho a \frac{dV}{dt} - \rho a g \sin\alpha + \rho a \frac{f V|V|}{2D} = 0 \qquad [2.8]$$

$$\frac{dx}{dt} = V + a \qquad [2.9]$$

$$\frac{dP}{dt} - \rho a \frac{dV}{dt} + \rho a g \sin\alpha - \rho a \frac{f V|V|}{2D} = 0 \qquad [2.10]$$

$$\frac{dx}{dt} = V - a \qquad [2.11]$$

Finite Difference Equations

Traditionally, a finite difference approach is used to solve these decidedly non-linear equations. Fig. 2.1 is a time-displacement grid depicting the fluid conditions at various points in a pipe at times t and $t+\Delta t$.

II. Method of Characteristics

The method of characteristics transforms partial differential equations for which no general solution exists (such as those describing liquid flow in a conduit) into particular total differential equations. The resulting non-linear equations may then be integrated using numerical methods employing finite difference equations.

In this section, the equations describing continuity and momentum for incompressible fluids will be transformed into total differential equations. Forward and backward finite difference equations will then be developed for implementation with constant time-step computations.

Equations of Motion

The hydraulic equations embodying the principles of conservation of momentum and continuity in a one dimensional pipe are respectively[14]

$$\frac{P_x}{\rho} + V V_x + V_t - g \sin\alpha + \frac{f V|V|}{2D} = 0 \qquad [2.1]$$

$$P_t + P_x V + \rho a^2 V_x = 0 \qquad [2.2]$$

These general equations can be combined with an unknown multiplier λ, to yield

$$\lambda\left[P_x\left(V + \frac{1}{\lambda\rho}\right) + P_t\right] + \left[V_x\left(V + \rho a^2 \lambda\right) + V_t\right] - g \sin\alpha + \frac{f V|V|}{2D} = 0 \qquad [2.3]$$

Any choice of two real, distinct values of λ will again yield two independent equations in terms of P and V that are still equivalent to Eqs.

Bipropellant Liquid Rocket. The methods developed in this investigation will be applied to a complete, closed loop, liquid rocket burning liquid hydrogen and oxygen propellants. The system analyzed is intended to be a typical one and will serve as a base line for future investigators.

Results. The data resulting from the single pipe and monopropellant computer models will be compared with published data to establish the accuracy of the routines generated in this thesis. The transient and steady state response of the bipropellant rocket to various inputs will be presented. An exhaustive parametric analysis of these responses is beyond the scope of this study.

Conclusions. The overall perfomance of the models used in this investigation will be examined in the light of the objectives of this thesis. Future uses for the routines developed in this thesis will be recommended.

Approach

This thesis may best be broken up into five sections. The intent is to provide both a step-by-step derivation of the system model and a reference for future implementations of the programs developed here.

Method of Characteristics Solution. To provide a framework for a finite difference solution, the necessary equations to model fluid flow in feed lines will be derived using the method of characteristics[14]. These equations form the very heart of this analysis. With a clear understanding of the pipe flow component of this problem, the other parts become simple boundary conditions.

Boundary Conditions. In order to complete the feed line solutions obtained using the method of characteristics, boundary conditions must be specified. These conditions take on a definite physical significance in describing the valves, pumps, accumulators, and other components which make up a liquid rocket. In this study, we will employ "typical" models, i.e., element models which have been extensively used in the literature. Specific knowledge of a given component is of great importance in improving the overall accuracy of any predictive tool. Future investigators will undoubtedly wish to employ more complex boundary conditions to improve the overall model accuracy.

Systems Analysis. In this section, the results derived above will be used to model several systems. In each case, a system model will be assembled and implemented in the BASIC computer language.

Single-Pipe System. A single-pipe system will be designed and several different boundary conditions will be applied in order to gain physical insight into their effects. In the next section, results will be compared with those of Wylie and Streeter[14], who analyzed an identical system.

Monopropellant System. A complex open loop system first analyzed by Dorsch, Wood and Lightner[1] will be modeled with relations developed in this paper. This model will be used subsequently for verification by comparison with published results.

propellant feed components including lines, valves, and orifices with the aim of applying these techniques to high frequency combustion instability. He showed that disturbances led to large (i.e. unlimited) amplitude waves in closed pipe systems and to limited amplitudes in pipe flow systems such as liquid rocket motors.

In 1965, Fashbaugh and Streeter[7] used the method of characteristics with various boundary conditions to form one of the first complete models of a propellant feed system in the analysis of the observed POGO instability of the Titan II missile. The authors used finite difference methods to simulate the transients involved on a digital computer. Fashbaugh and Streeter concluded with the suggestion that the fluid system results could be coupled with engine thrust relations and structural dynamic equations to complete the closed-loop system. The major thrust of this paper is to close the loop and obtain the overall transient and steady state response of a liquid rocket to arbitrary thrust oscillations.

More recently, Dorsch et al.[1] of the NASA Lewis Research Center have employed the wave plan, a pulse synthesis method, fundamentally similar to the method characteristics, to examine the response of a simple monopropellant feed system. Boundary conditions for important feed system components were developed and the authors also published a great deal of experimental results for a monopropellant system.

Objectives

The purpose of this investigation is three fold: to develop a closed loop model of POGO instability from the well established method of characteristics, to verify the model by comparison with results published by other analysts, and to provide a reference and computer routines for future investigators of similar systems. These objectives will be achieved only if the routines generated here are both accurate enough to be a useful design tool, and flexible enough to handle a varied group of systems.

This can result in a large closed loop gain and the build-up of dangerously large vibrations. Most OTV and OMV designs differ radically from current vehicles. Since OTV's and OMV's are designed to function solely outside of the atmosphere, they have a much lower profile, being relatively short and squat. The magnitude of POGO instability in these vehicles will be of great interest.

Previous Work

The POGO phenomenon and its associated complications have been the subject of considerable study. Two basic types of analysis have been performed to date: linearized network analyses and time-step simulations. Linear network analyses employ perturbation techniques on linearized impedances at mean operating conditions, while time-step methods employ a non-linear method of characteristics solution solved using a finite difference approach.

Linearized Models. Network methods of analysis have been employed by Ryan[2], Rubin[3,10], Holster and Astleford[5], and Zielke[6] (superscripts designate references given at the end of the paper). These investigators used linear mathematical models to establish transfer functions for stability analysis. Network methods are ideal for the analysis of complex, but primarily linear, systems. After the component transfer functions are determined, a conventional analysis (generally using the Nyquist stability criterion) can be performed. The simplifications involved are usually valid for the purposes of making closed loop stability predictions where the growth or decay of small sinusoidal perturbations is considered. Because of the extremely nonlinear nature of liquid rocket systems, linearized models cannot be used to find the wave shapes of large amplitude pressure and flow disturbances, nor can they find the response associated with events such as valve closures[1,2].

Time-Step Methods. In an early work, Woods[4] used a method of characteristics formulation to model flow fluctuations in a number of

A CLOSED LOOP ANALYSIS OF POGO INSTABILITY

I. Introduction

The development of high performance interorbital transfer vehicles will enable a major expansion of space utilization and dramatically reduce the overall cost of space operations. To accomplish objectives such as these, OTV's (Orbital Transfer Vehicles) and OMV's (Orbital Maneuvering Vehicles) are being designed to provide a new level of performance in chemical rockets. These vehicles will support future Air Force systems and NASA's space station well into the 21st century.

Propulsion systems utilizing liquid oxygen and hydrogen offer significant inherent advantages over other technologies. They can easily achieve higher performance (principally higher specific impulse) and versatility than solid propellant systems. Furthermore, they represent more mature technologies than exotic systems such as ion, arcjet and plasmajet concepts. There are, of course, many technical difficulties involved in achieving gains in performance. As always, a thorough understanding of these difficulties is prerequisite to their solution.

A significant difficulty in the development of any liquid rocket system is the elimination of self-excited instability. One of the pricipal concerns is the clear understanding and reduction of so called "POGO" instabilities. The name POGO is derived from the similarity observed between the out of phase motion of the ends of a rocket vehicle and the motion of a Pogo stick. This vibration arises from the interactions of the propellant feed system, the system thrust function, and the rocket component structures. These oscillations have been observed in a number of important launch vehicles including the Titan II, Thor/Agena, and Saturn SIIB. During a POGO event, thrust variation, typical in the normal operation of virtually all liquid rockets, leads to structural and propellant oscillations which further intensify the original disturbance.

The structural velocity, V_s is assumed to be directed vertically, while the fluid velocities, V_U and V_D are directed longitudinally with their respective fluid lines (at orientation angles α_U and α_D). Thus, V_S, V_U, and V_D are scalars. Using Eqs. [2.16] and [2.17], and noting that the pressure is essentially constant across the interface:

$$P_U = C_P - \rho a_U V_U; \quad P_D = C_M + \rho a_D V_D$$

$$P_U = P_D$$

Solving these equations simultaneously:

$$V_U = \beta V_D - V_S(\sin\alpha_U - \beta \sin\alpha_D) \qquad [3.10]$$

where: $\beta = \dfrac{A_D}{A_U}$

The other unknowns may now be readily determined. This completes the description of the fluid dynamics of relative motion.

Accumulator in Line. An accumulator (as in Fig. 3.4) adds a localized compliance to the interface between two elements. Since an accumulator is an energy storage device (the total energy and fluid storage being a function of pressure) the local pressure will be described by a differential equation. The compliance of an accumulator is defined by[1:8]

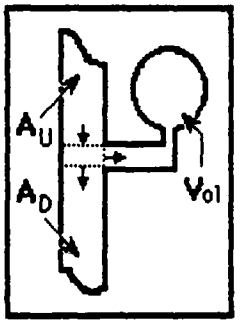

Figure 3.4
Accumulator in line.

$$a' = \frac{dV_{ol}}{dt} \qquad [3.11]$$

where: a' = compliance

As in the relative motion case, the fluid storage rate in the accumulator is equal to the inflow rate minus the outflow rate[1:11]:

$$V_U A_U - V_D A_D = \frac{dV_{ol}}{dt} \qquad [3.12]$$

Applying the calculus and substituting

$$\frac{dV_{ol}}{dt} = \frac{dV_{ol}}{dP}\,\frac{dP}{dt} = a'\,\frac{dP}{dt}$$

Therefore

$$\frac{dP_U}{dt} = \frac{V_U A_U - V_D A_D}{a'} \qquad [3.13]$$

This gives the time history of the pressure at the accumulator as a function of the flow rates. The pressure may be found using any of several numerical integration schemes (a simple first order integration is used in this analysis). Once the pressure is determined, the boundary condition is exactly the same as that for a known pressure.

Instantaneous Pressure Change. The action of a pump may be approximated by a lumped pressure rise of magnitude ΔP if the pump's dimensions are small compared to the other system elements. The resulting boundary condition is very similar to the known pressure case:

$$P_U = C_P - \rho a_U V_U \;;\; P_D = C_M + \rho a_D V_D$$
$$P_D = P_U + \Delta P \quad ;\; A_U V_U = A_D V_D$$

Solving simultaneously

$$V_D = \frac{C_P - C_M + \Delta P}{\rho(\beta a_U + a_D)} \qquad [3.14]$$

Again, the other quantities can readily be calculated. Note that no loss term has been used at the interface. Any actual losses should be taken into account when assigning a functional form to ΔP.

System Components

A typical liquid rocket system consists of several different components which give rise to the boundary conditions described above. The models found in this section are used generally throughout the literature.

Tank Pressurization. The oxidizer and fuel tanks will be pressurized to a specified pressure known as the ullage pressure. This is done to ensure that a minimum pressure (net positive suction head) is maintained in the feed system in order to avoid excessive pump inlet cavitation. For purposes of this analysis, the ullage pressure will be assumed constant. Thus the boundary condition consists of a simple known pressure.

Valves. A valve can accurately be modeled as an orifice with a variable flow constant τ. The boundary condition associated with the valve is precisely the same as that developed for the orifice.

Pump Inlet Cavitation. This phenomenon is very poorly understood. Various authors have used differing approaches, most simply adjusting the sound speed in the pump inlet so that the numerical analysis matched experimentally observed resonance conditions[2-7]. Others have modeled a hypothetical accumulator at the pump inlet to account for the locally high compliance of the cavitation "bubble"[1,10] (this should not be confused with pump cavitation and the surge phenomena as a small volume of vapor is normally present in any cryogenic pump inlet[3,4]). The latter approach is used in this analysis simply because it seems less artificial. One must recognize however, that this is still an approximation and the only meaningful criterion to be used in judging the success of this model is comparison with experimental results. The relative amount of inlet compliance must be adjusted so that the results are in agreement with experimental data.

The compliance associated with the formation of vapor bubbles (due to their isothermal expansion and contraction) in the pump inlet is given by Dorsch, et al.[1:8] as

$$a' = \frac{P_0 V_{01_0}}{P^2} \qquad [3.15]$$

This relation need only be substituted into Eq. [3.13] to obtain the

boundary condition

$$\frac{dP_U}{dt} = \frac{P_U^2(V_U A_U - V_D A_D)}{P_o V_{ol_o}} \qquad [3.16]$$

Thus, the accumulator is positioned at the end of the upstream pipe. Again, this highly non-linear equation is solved using a first order numerical integration technique. Specifcally, P_U is integrated to first order while the right hand side of [3.16] is evaluated at mean conditions for the time step. These mean conditions are determined by iteration (using a modified form of Newton's method).

Injector Dome Compliance. The injector is housed in a dome with a compliance due to the cavitation of the cryogenic propellant. For this reason, Dorsch, et al. modeled this compliance in exactly the same way as the pump inlet compliance[1:11] (i.e. with an isothermal vapor bubble expansion model). The same analysis will be used in this investigation.

Pump Pressure Rise. The dynamic pressure output of a turbo pump is generally similar to Figs. 3.5 and 3.6. These depict the variation of pump output pressure with output velocity (or flow for incompressible fluids) and suction pressure, respectively. The normal operating point is near the peak in Fig. 3.5 and well away from the cavitation point in Fig. 3.6. An excellent curve fit for such pump characteristics is given by Fashbaugh and Streeter[7:1014] as

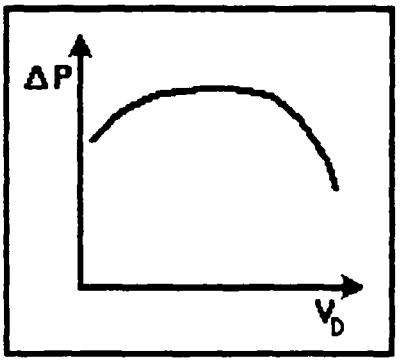

Figure 3.5
Pressure rise-flow characteristic.

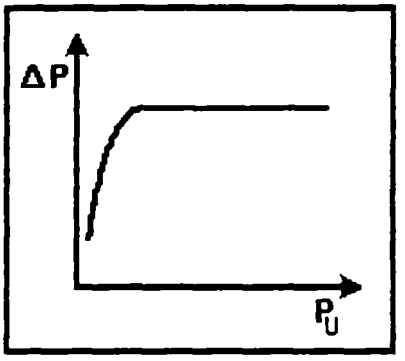

Figure 3.6
Pressure rise-inlet pressure characteristic.

$$\Delta P = \Delta P_o - B_0(V_D - V_{D_o})^2 - \left(B_1 - \frac{(P_U - P_{U_o})}{B_2 + B_3(P_U - P_{U_o})}\right) \qquad [3.17]$$

The coefficients above are determined from the characteristic plots (Figs. 3.5 and 3.6). The boundary condition associated with the pump has been derived previously.

Combustor. The thermochemistry of the combustor is relatively well understood. Several authors have devised a composite time-lag theory; a complete description of which is beyond the scope of the present work[1,4,7,9,10,18,20]. Dorsch, et al.[1:11] used a two-part time-lag, associating a constant dead time with the burning of the propellant and a residence time (a function of chamber geometry, exhaust velocity, and temperature) with propellant injection. The chamber pressure rate of change is given by

$$\frac{dP_C}{dt} = \frac{L^* C^*}{\theta_g V_{ol_C}} \dot{m}(t - \tau_C) - \frac{P_C}{\theta_g} \qquad [3.18]$$

$$\theta_g = \frac{L^* C^*}{R T_C} \qquad [3.19]$$

In applying these equations to a bipropellant system the total injector mass flow rate will be the sum of the mass flow rates for the fuel and the oxidizer. This differential equation establishes another boundary condition to be numerically integrated. For purposes of this analysis the effective

exhaust velocity, C^* is considered a linear function of the instantaneous mixture ratio, MR[4]:

$$C^* = C_o^* + C^*_{slope} (MR - MR_o) \qquad [3.20]$$

In reality, for a bipropellant liquid rocket the effective exhaust velocity is a very complex function of mixture ratio as well as chamber pressure and temperature. This simplification is justified, however, if the range of instantaneous mixture ratios is sufficiently small as will be the case in the bipropellant system analyzed in this investigation.

Implementation

The boundary conditions associated with the various elements described in this section will be combined with the fluid flow model of Section II to dynamically model a liquid rocket. Various simple systems will first be implemented to gain insight into the behavior of each component before they are combined in more complex arrangements.

IV. Systems Analysis

In this section, the finite difference equations and boundary conditions detailed previously will be used to model three complete systems of increasing complexity. A very simple, single pipe system will be modeled to verify the accuracy of a digital computer program written using the equations given in Sections II and III by comparison with published results. Various boundary conditions will then be applied to this simple model to gain an understanding of the effects of several parameters.

A more complex monopropellant rocket system first modeled by Dorsch, et al.[1] will next be examined. The POGO analysis rouines developed in this investigation will be applied to this system and results will be generated for comparison with those published by Dorsch, et al.

Finally, to demonstrate a more general application of the software developed in this investigation to systems of arbitrary complexity, a hypothetical bipropellant liquid rocket system will be designed and modeled with these POGO analysis routines. A very limited parametric analysis will be performed to determine those factors important in POGO instability (see Section V).

Single Pipe Models

Fig. 4.1A depicts a simple pipe flow problem with a constant pressure reservoir upstream and a valve downstream. Table 4.1 lists values for the parameters involved.

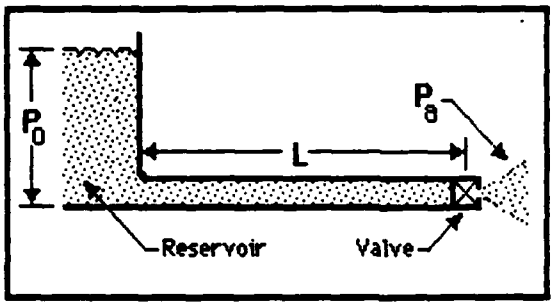

Figure 4.1A
Single pipe flow system.

Table 4.1	
Single Pipe Parameters	
a=1,200 m/s	L=600 m
D=0.5 m	P_0=1.4715 MPa
τ_0=0.00205	f=0.018
τ_{cut}=2.1 s	E_c=1.5
P_a=0 MPa	

The values in Table 4.1 were taken from an identical system modeled by Wylie and Streeter[14:38]. Initially, the system is assumed to have reached steady state conditions (with the valve open; its flow constant being taken as τ_0). These steady state conditions are easily calculated using the simplified Navier-Stokes equations [2.1] through [2.2] since the partial temporal derivatives are zero here by definition (see results in Section V). At time equal to zero, the valve is shut according to the following exponential law:

$$\tau = \tau_0 \left(\frac{1-t}{\tau_{cut}}\right)^{E_c} \qquad [4.1]$$

This system (in a vertical rather than horizontal orientation with respect to the local acceleration vector) and two other sytems adding a time-varying reservoir pressure and variable acceleration magnitude (simulating the effects of rocket thrust variation) are also examined in response to a sinusoidally varying reservoir pressure. For these responses, the orifice

flow constant, τ is taken as the constant, τ_0 (implying that the valve remains open).

Boundary Conditions. In order to model the system using the finite difference equations of Section II boundary conditions from Section III must be applied. Fig. 4.1B schematically depicts the single pipe and its two interfaces (with the reservoir and valve):

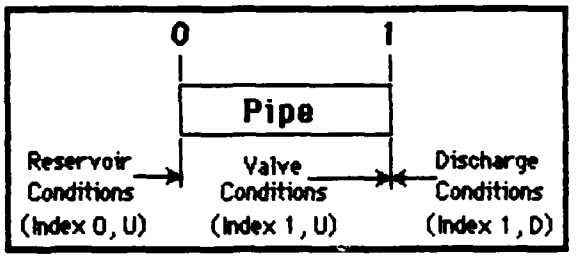

Figure 4.1B
Single pipe interfaces.

Note that by the index notation of the figure, the reservoir pressure and velocity of the system are denoted $P_{0,U}$ and $V_{0,U}$, respectively while the valve pressure is $P_{1,U}$ and the valve flow velocity is $V_{1,D}$. The destinction between conditions just upstream and downstream of an interface is necessary since some of the boundary conditions in Section III involve spatial discontinuities in pressure and flow velocity.

Boundary Condition at Interface 0. This is the known upstream pressure condition described by equations [3.1] and [3.2]. In terms of Fig. 4.1A indices

$$P_{0,D} = P_{0,U} = P_o$$
$$V_{0,D} = V_{0,U} = \frac{P_o - C_M}{\rho a} \qquad [4.2]$$

Note that C_M is always available since conditions inside the pipe are known (either from the previous time step or from the steady state solution).

Boundary Condition at Interface 1. This condition is a combination of the known downstream pressure condition of [3.1] and [3.2] and the orifice condition described by [3.7] (with flow constant modeled by [4.1]). For the case at hand

$$\text{For } V_{1,D}:$$

$$A = 1 \qquad B = \tau^2 \rho a \beta$$

$$C = -\tau^2 C_P \quad \beta = \frac{A_{inj}}{A_{pipe}} = 1 \qquad [4.3]$$

$$V_{1,U} = \beta V_{1,D} \quad P_{1,U} = P_{1,D} + \frac{V_{1,D}^2}{\tau^2} \quad P_{1,D} = 0$$

Note, $V_{1,D}$ is given in terms of quadratic coefficients for solution by [3.6].

Other Single Pipe Models. To examine some of the effects of boundary conditions more typical of a liquid rocket, another single pipe system was modeled. The system is based on that taken from Wylie and Streeter (Fig. 4.1A,B) but differs as noted below.

Single Pipe Compliant System. For this system the valve transient response is deleted and the reservoir pressure is given the following sinusoidal form (oscillating at frequency ω)

$$P_o = 1.4715 \text{ MPa} + 100 \text{ KPa} \cdot \text{Sin}\omega t \qquad [4.4]$$

An accumulator is placed in line with the valve to model the effects of valve inlet cavitation. The isothermal expansion model (see [3.15]) was used for the compliance. This changes the boundary condition at interface 1 to a combination of the known downstream pressure ([3.1] and [3.2]), orifice ([3.7]), and the accumulator ([3.13]) conditions ($P_{1,U}$ becomes the accumulator pressure which must be integrated numerically). In terms of the pressures and velocities of Fig. 4.1A:

$$P_{1,u}\Big|_{t+\Delta t} = P_{1,u}\Big|_{t} + \Delta t \frac{P_{1,U_{avg}}^2}{P_{a_0} Vol_{a_0}} \pi D^2 \left[\frac{C_{P_{avg}} - P_{1,U_{avg}}}{\rho a} \tau \sqrt{P_{1,U_{avg}}} \right] \quad [4.5]$$

Note that the average values which are used in the first order integration of the accumulator pressure are determined by iteration (see Appendix A for a source code listing of this routine). P_{a_0}, the initial bubble pressure, was taken as the steady state pressure at the valve, 143 kPa. Three different initial accumulator volumes were examined: 1, 0.1, and 0.01 m^3. The purpose of these changes is to produce the kind of response to pressure variations seen at the injectors of a liquid rocket (the injectors are housed in a dome with a cavitation compliance).

Program Flow. Any finite element routine will involve a great many repetitive calculations, necessitating an organized approach. The flow diagram for the problem at hand is depicted in Fig. 4.2:

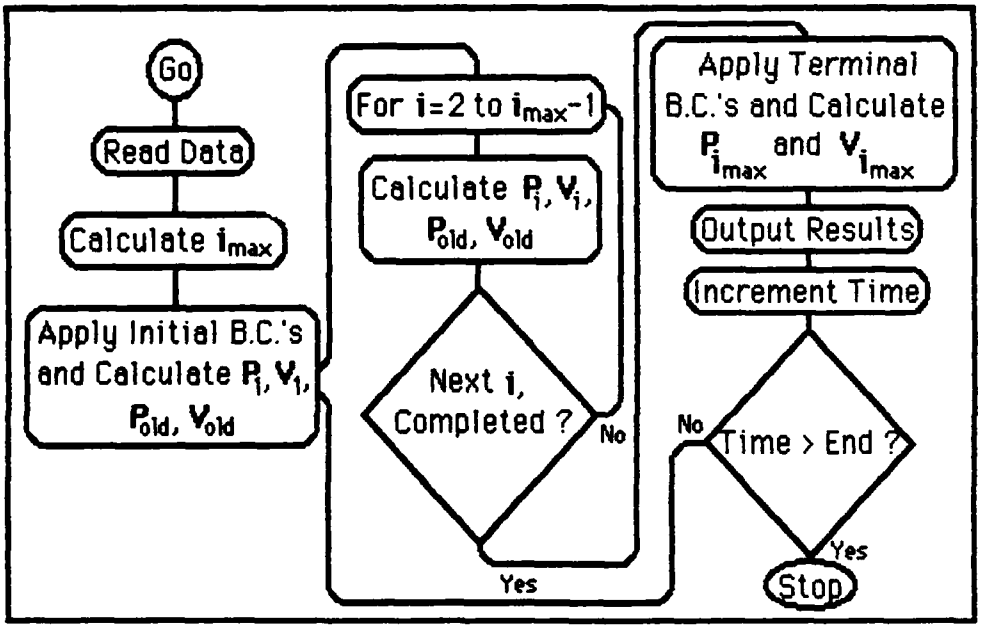

Figure 4.2
Single pipe computer flow diagram.

The program consists of four main parts: initialization, initial boundary conditions, interior sections, and terminal boundary conditions. The initialization includes reading in constants and steady state results from a simple static analysis. The pressure and velocity at the first point in the pipe are calculated using the constant pressure boundary condition. Note that the old pressure and velocity must be available for the calculation of conditions at the next element; they are therefore held in memory. The state at each interior section is calculated next, updating the old pressures and velocities at each point. Finally, the state at the last pipe element is calculated using the orifice boundary condition. See the Appendix for a source code listing.

Monopropellant Liquid Rocket

Dorsch, et al.[1] analyzed a liquid rocket system using the so-called "wave plan" developed at the NASA Lewis Research Center. This pulse synthesis approach is closely related to the method of characteristics used in this study and a comparison of results from the model of this monopropellant system developed in this section with those of Dorsch, et al. will verify the accuracy of the routines detailed in Appendix A. The system is depicted in Fig. 4.3A.

The System. The monopropellant system consists of the following components: fuel tank, feed line, turbo pump, throttle valve, discharge line, injector, and combustor. A cavitation bubble is hypothesized to exist in the pump inlet and has a compliance modeled with the isothermal expansion results of Section III. The system is assumed to be at equilibrium initially, then it is excited by the forced sinusoidal motion of the propellant tank and pump. As there is no propulsion loop feed back and the dynamic nature of the pump and tank motions is ignored, the system may be considered to be open.

Parameter Values. Parameter values describing the monopropellant system are displayed in Table 4.2 . These values were taken from Dorsch, et

al.[1:17], and represent a typical monopropellant liquid rocket. Note that the sonic velocity is different in each pipe due to varying degrees of pipe elasticity. The acoustic velocity within a pipe is given by[4:1563]

$$a = \sqrt{\frac{K}{\rho\left(1+\frac{KD}{Et}\right)}} \qquad [4.7]$$

Other parameters in Table 4.2 are defined as

$$\text{Combustion Parameter} = \left(\frac{C^* L^*}{Vol_C\, g\, \theta_g}\right) \Delta H_p$$

$$\text{Pump Pressure Rise, } \Delta H_p = A + BQ + CQ^2$$

$$\text{Injection Velocity, } V_{inj} = B_{inj}\sqrt{\Delta H_{inj}}$$

Boundary Conditions. The component interfaces for the monopropellant liquid rocket which must be modeled with boundary conditions are depicted in Fig. 4.3B:

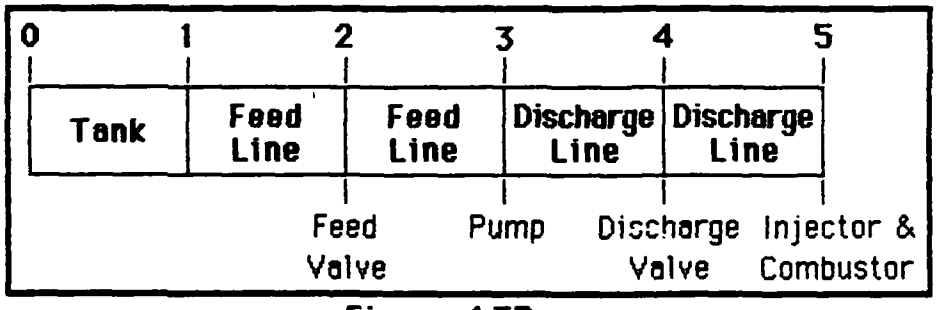

Figure 4.3B
Monopropellant system component interfaces.

Interface 0 (Ullage Pressure-Propellant Tank). This is a known upstream pressure condition (the tank ullage pressure is assumed constant) modeled exactly as interface 0 of the single pipe system.

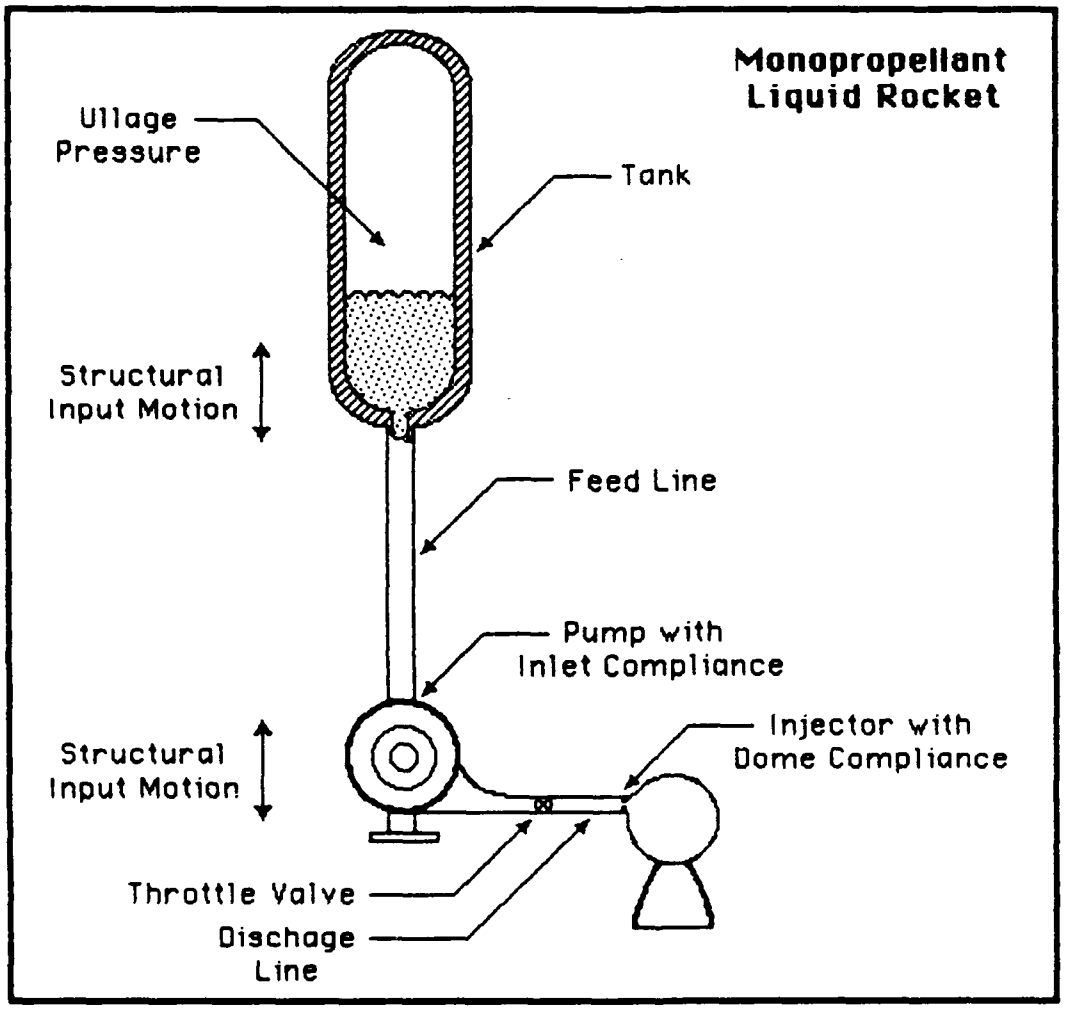

Figure 4.3A

Monopropellant liquid rocket fluid system.

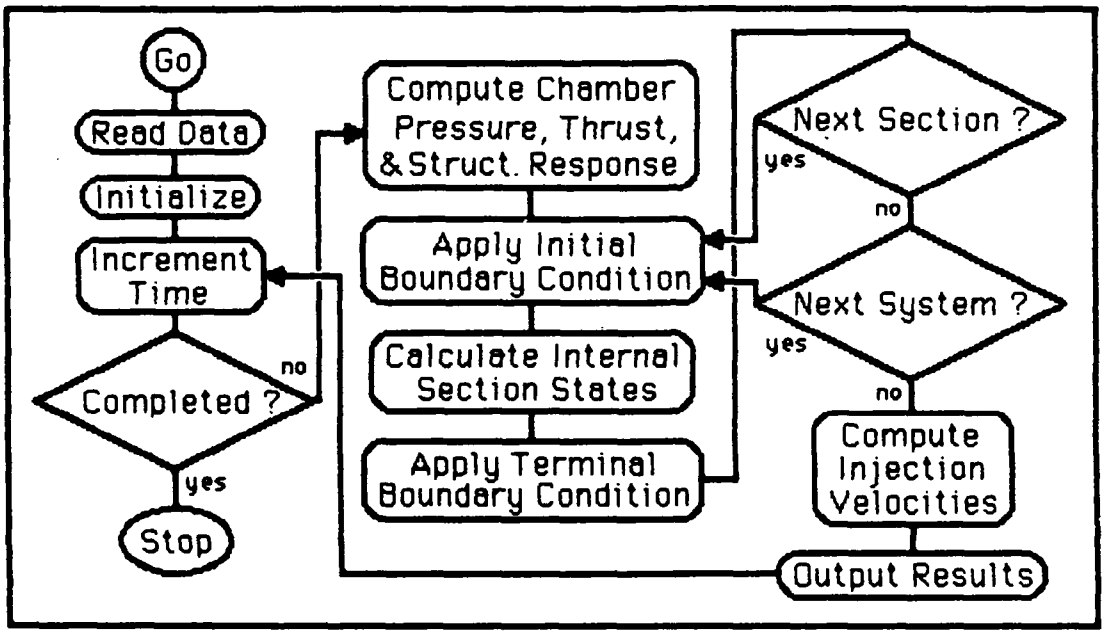

Figure 4.10

Bipropellant liquid rocket system flow diagram.

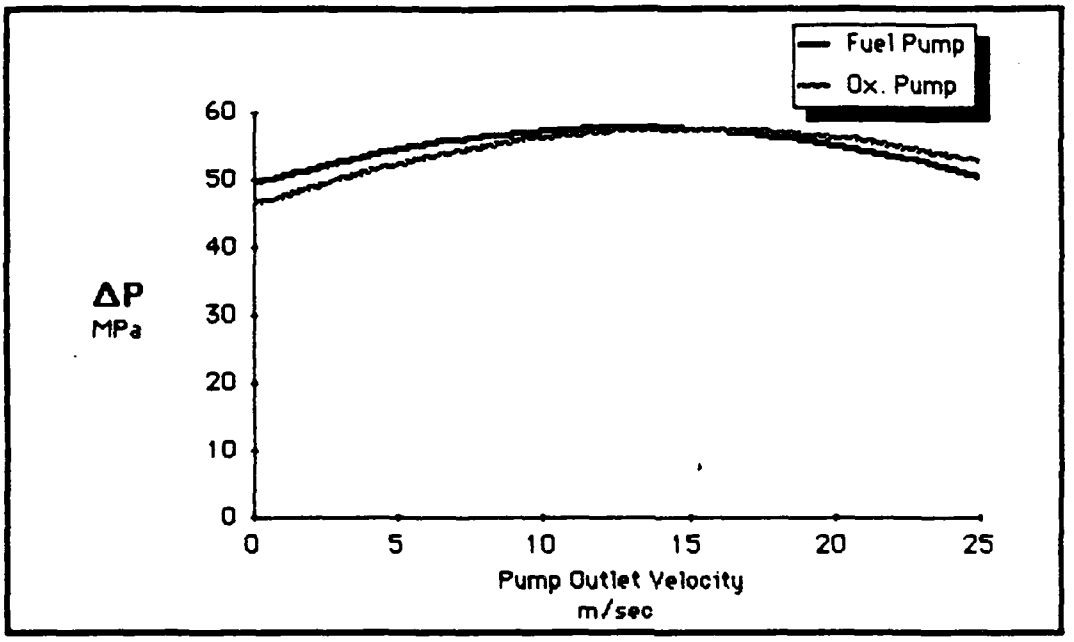

Figure 4.8
Pump pressure rise response to pump flow variation.

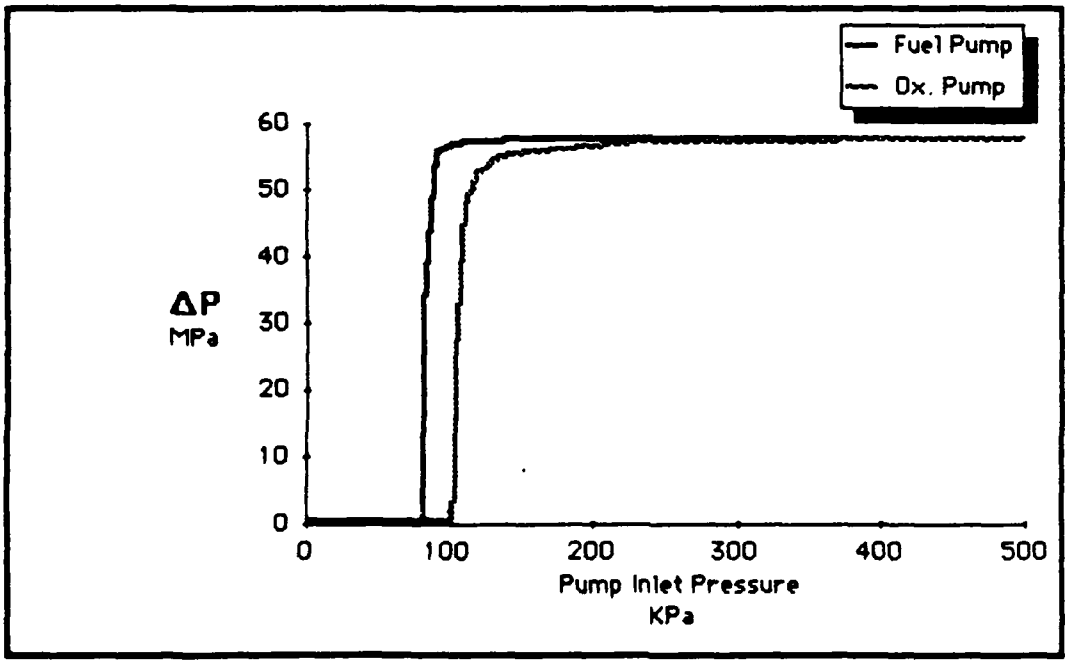

Figure 4.9
Pump pressure rise response to inlet pressure variation.

Table 4.4

Bipropellant Structural Parameters

Structural Properties

Natural Frequency (Undamped) 10 Hz Damping Factor 0.1

	Mass (Kg)	Spring Constant (MN/m)	Damping Constant (KN·sec/m)
Structure	3000	——	——
Tank			
Fuel	3236	12.774	40.663
Ox.	19414	76.643	243.96
Pump			
Fuel	100	0.39478	1.2566
Ox.	100	0.39478	1.2566

Table 4.5

Bipropellant System Calculated Parameters

Char. Length, L^* 7 m Chamber Vol., Vol_C 0.1 m^3
Chamber Temp., T_C 3500 K Gas Constant, R_g 5.8867 J/Kg·K
Nom. Accel., g 19.32 m/sec^2

	Fuel		Oxidizer	
Mass Flow Rate	16.18	Kg/sec	97.07	Kg/sec
Injector Constant	$29.664 \cdot 10^{-3}$	$(m^3/Kg)^{1/2}$	$30.787 \cdot 10^{-3}$	$(m^3/Kg)^{1/2}$
Injector Diameter	45	mm	27	mm
Nominal Pump Pressure Rise, ΔP_0	58.153	MPa	58.006	MPa
Nominal Pump Flow Velocity, V_{P_0}	12.896	m/sec	15.006	m/sec
Nominal Pump Inlet Pressure, P_{P_0}	180.24	KPa	326.93	KPa
Pipe Wall Thickness				
Tank	2.0448	mm	1.9245	mm
Feed Line	0.64437	mm	0.30505	mm
Discharge Line	1.9718	mm	0.50658	mm
Pump Coefficients				
B0	50000	Kg/m2	50000	Kg/m2
B1	0	Pa	0	Pa
B2	0.5	Pa	0.5	Pa
B3	$5 \cdot 10^{-6}$		$5 \cdot 10^{-6}$	

Table 4.3

Bipropellant Fluid System Parameters

Combustor Properties

Thrust	500 KN	Exhaust Velocity, C^* (Effective)	4415 m/sec at 6:1 4562 m/sec at 8:1
Nominal Mixture (Ox./Fuel Mass Rates)	6:1		
Thrust Coef., C_T	0.999	Chamber Pressure, P_C	35 MPa
Residence Time, θ_g	1.5 msec	Dead Time, τ_C	4 msec

Material Properties

Young's Modulus, Y (Pipe Material) 10 GPa

	Fuel ($L H_2$)	Oxidizer (LOx)
Density, ρ (Fluid)	71 Kg/m^3	1140 Kg/m^3
Bulk Modulus, K	102.2 MPa	1.641 GPa

Fluid System Properties

Injector Pres. Drop 40% Injection Velocity 150 m/sec

Ullage Pressure 150 KPa

Tank	Length (m)	Diameter (cm)	Sound Speed (m/sec)	Friction Factor	Alpha (Deg)
Fuel	6.448	300	300	0.03	90
Ox.	2.409	300	75	0.03	90
Feed Line					
Fuel	8	30	500	0.03	90
Ox.	3	17	125	0.03	90
Discharge Line					
Fuel	1	15	900	0.002	0
Ox.	1	8.5	225	0.002	0

described by [3.20]. The system thrust must also be calculated and is given by[20:357]

$$F = C_T C^* (\dot{M}_{5,D,F} + \dot{M}_{5,D,Ox}) \qquad [4.13]$$

Tank and Pump Motions. The motions of the tanks and pump depicted in Fig. 4.7 are described by the following total differential equations (these follow directly from Newton's third law):

$$\begin{aligned}
M_S \ddot{X}_S &= X_{T,F} k_{T,F} + \dot{X}_{T,F} c_{T,F} + X_{T,Ox} k_{T,Ox} + \dot{X}_{T,Ox} c_{T,Ox} \\
&\quad + X_{P,F} k_{P,F} + \dot{X}_{P,F} c_{P,F} + X_{P,Ox} k_{P,Ox} + \dot{X}_{P,Ox} c_{P,Ox} \\
M_{T,F}(\ddot{X}_S + \ddot{X}_{T,F}) &= -X_{T,F} k_{T,F} - \dot{X}_{T,F} c_{T,F} \\
M_{T,Ox}(\ddot{X}_S + \ddot{X}_{T,Ox}) &= -X_{T,Ox} k_{T,Ox} - \dot{X}_{T,Ox} c_{T,Ox} \\
M_{P,F}(\ddot{X}_S + \ddot{X}_{P,F}) &= -X_{P,F} k_{P,F} - \dot{X}_{P,F} c_{P,F} \\
M_{P,Ox}(\ddot{X}_S + \ddot{X}_{P,Ox}) &= -X_{P,Ox} k_{P,Ox} - \dot{X}_{P,Ox} c_{P,Ox}
\end{aligned} \qquad [4.14]$$

It is convenient to integrate these equations numerically at each time step (although several sub time steps are used for improved accuracy) to obtain the component velocities (for use in the relative component motion boundary conditions) and the structure acceleration, g_v (for use in the finite difference equations).

Program Flow. Fig. 4.10 is the computer flow diagram for the bipropellant rocket POGO analysis routine. It bears considerable similarity to the monopropellant case, except for the thrust determination and structural feed back routines. A user's guide to this program is available in Appendix A.

4.9 depict the pump pressure rise, ΔP, response to pump flow velocity, $V_{3,D}$, and pump inlet pressure, $P_{3,U}$, variations respectively. These curves arise from the choice of pump coefficients for use with [3.17]. The rationale behind this choice of coefficients is to provide a stable range of pump operation for this analysis (see Appendix B).

Boundary Conditions. Fig. 4.6B defines the component interfaces for the purpose of establishing boundary conditions for the bipropellant POGO analysis routine.

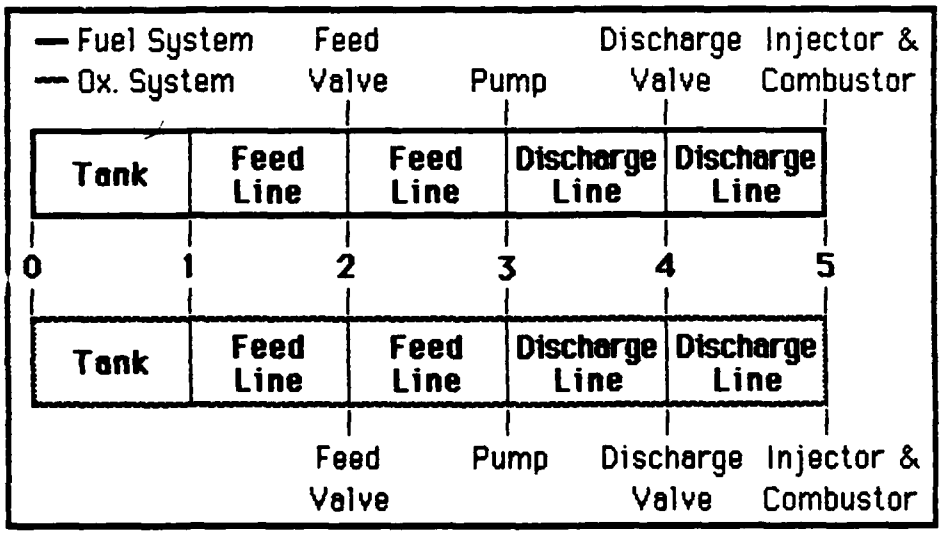

Figure 4.6B
Bipropellant system component interfaces.

A comparison with Fig. 4.3B shows that the fluid elements of the bipropellant system are exactly the same as those of the monopropellant system (for which boundary conditions have already been developed), except that the bipropellant system contains both fuel and oxidizer subsystems. In fact, the boundary conditions for the bipropellant system can be obtained by simply adding the subscripts F and Ox to each term employing indices from Fig. 4.3B i.e. $P_{1,U}$ becomes $P_{1,U,F}$ and $P_{1,U,Ox}$. The combustor conditions are the same except that the total mass flow rate (fuel plus oxidizer) must be substituted for the monopropellant mass flow rate, and the effective exhaust velocity is a function of the instantantaneous mixture ratio as

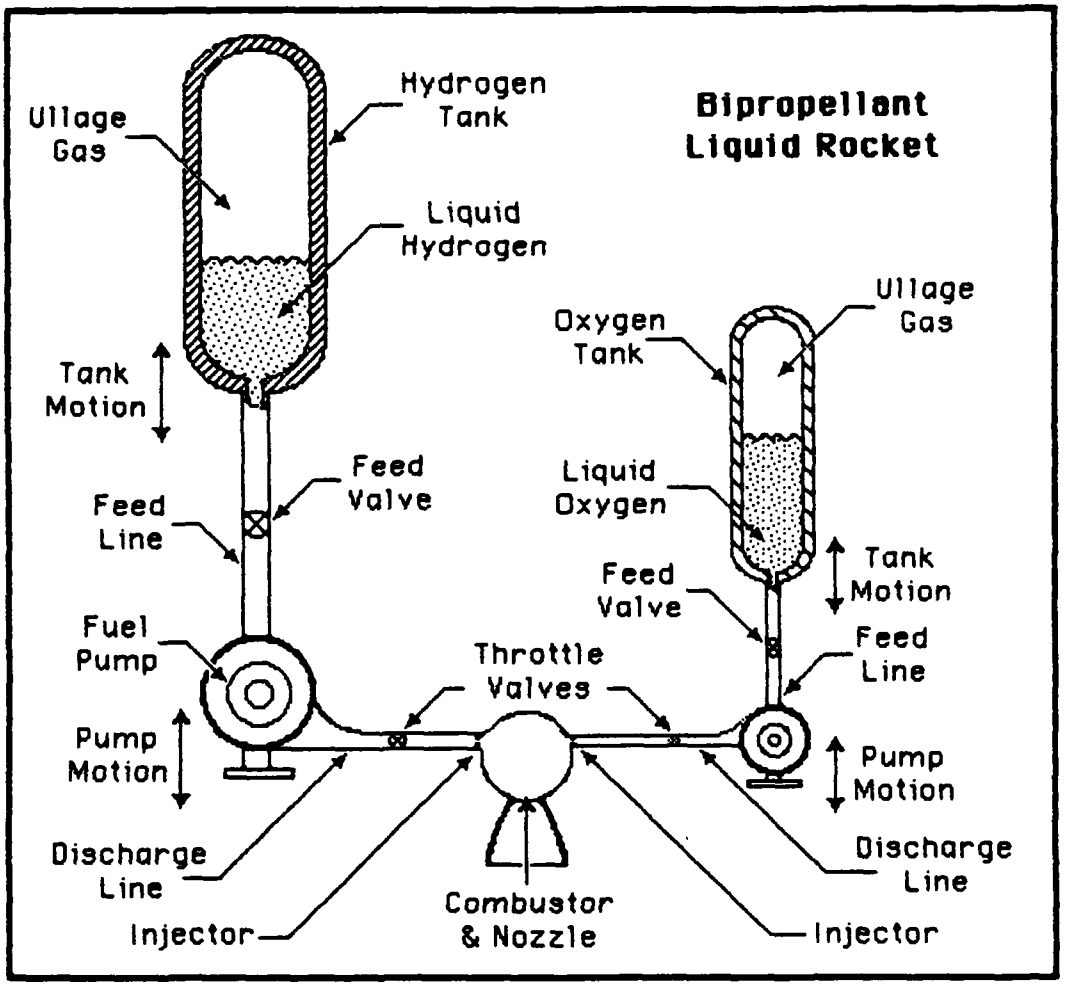

Figure 4.6A

Bipropellant liquid rocket fluid system.

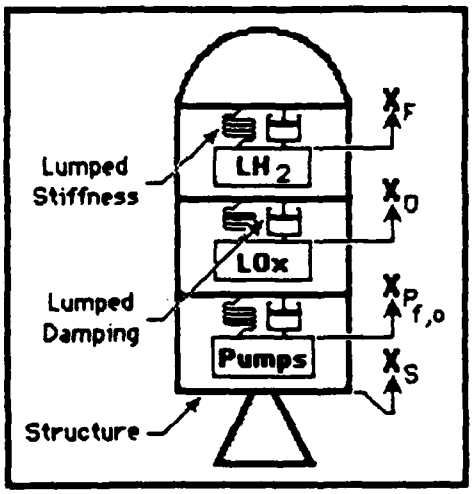

Figure 4.7

Structure-component interactions.

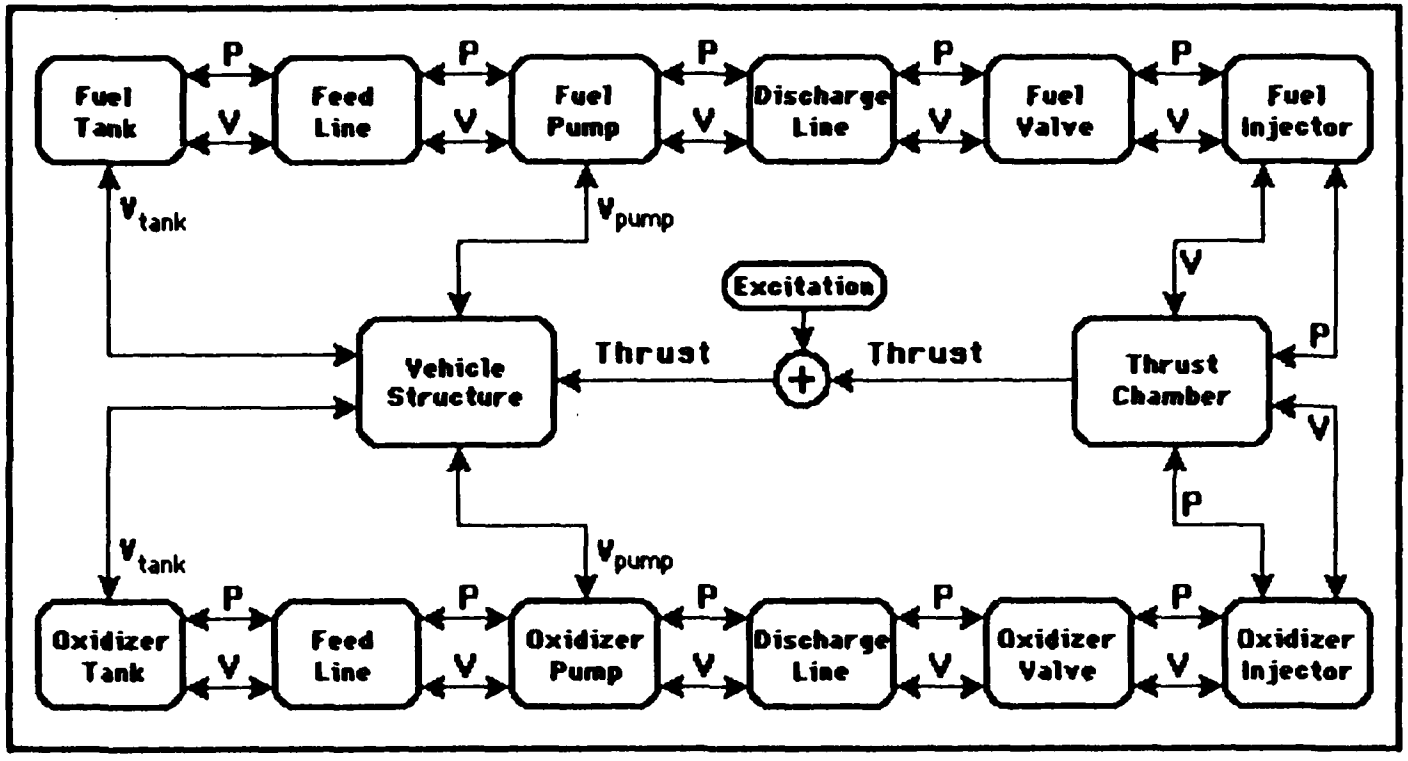

Figure 4.5

Bipropellant rocket system schematic.

in visualizing the complex interactions between model components. Note that the thrust feedback closes the propulsion-structural vibrations loop. The only new problems are the thrust calculation and dynamic response of the floating (relative to the vehicle structure) tanks and pumps. The system thrust is related to the total injection mass flow rate as well as to the chamber specific impulse (itself a function of the instantaneous mixture ratio). The thrust variation feeds back through the structure to drive the propellant tank and pump oscillations.

Model Components. Fig. 4.6A is a simplified view of the bipropellant feed system. It is quite similar to two monopropellant models in parallel, having both fuel and oxidizer components. Fig. 4.7 depicts the bipropellant structural system. This is a five degree of freedom model allowing pump and tank motions relative to the structure. The "structure" (denoted by the subscript "s") includes all elements except the pumps and tanks (i.e. all other fluid lines, vehicle structure, and any payload).

Choice of Parameters. Before a numerical analysis may be made, values must be chosen for all system parameters. Tables 4.3 and 4.4 give values chosen for this bipropellant system. These values represent a "typical" system and do not correspond to any physical implementation. Table 4.5 gives values for other parameters calculated from Tables 4.3 and 4.4 using simple steady state relationships[1,14], the details of this static analysis as well as the reasons for all parameter values chosen are available in Appendix B. The fuel (liquid hydrogen) and oxidizer (liquid oxygen) components of the bipropellant system are quite similar, except that the oxidizer is more than ten times as dense as the fuel[20] and the sonic velocities in the oxidizer lines are much less than those for the fuel component due to the relative compliance (i.e. the wall elasticity of the fluid lines compared to the bulk modulus of the fluid) of the oxidizer pipes. These contrasting values were selected primarily to demonstrate the effects of sonic velocity on the performance of each (fuel and oxidizer) fluid system. The fuel and oxidizer pump parameters will prove to be of principal importance in determining the systems over all POGO stability. Figs. 4.8 and

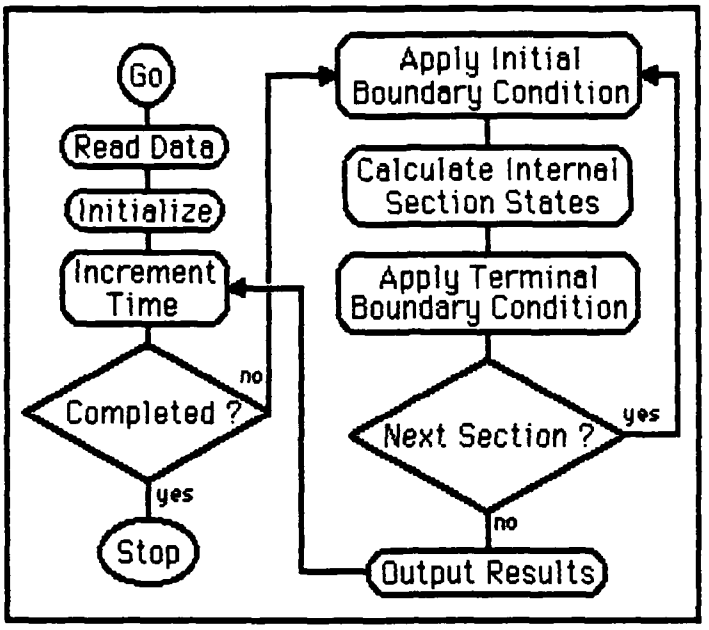

Figure 4.4

Monopropellant system computer flow diagram.

Bipropellant Liquid Rocket

In order to illustrate the application of the routines and principles detailed in this thesis, a closed loop model for a typical liquid rocket was developed. Each fluid system (fuel and oxidizer) of the bipropellant model is similar to the monopropellant system of Dorsch, et al. with several important differences:

1. The system thrust is calculated from chamber conditions and is fed back into the system resulting in a time-varying acceleration[7].

2. The propellant tanks and pumps are modeled dynamically as separate mass-spring-dashpot systems[3,4,7]. Their relative motions are driven by variations in the vehicle acceleration.

3. The system is driven by sinusoidal thrust variations imposed upon (simply added to) item 1 above[7].

Schematic. The system schematic diagram, Fig. 4.5, is given as an aid

Interface 5 (Discharge Line-Combustion Chamber). The combustor pressure is solved for separately (at the beginning of each time step) and can be considered known, thus this condition involves the orifice equation, [3.7], a compatibility equation, [2.16], the section area change equation, [3.3] (the discharge line area is quite different than the injector area), and the accumulator equation, [3.13], to model injector dome compliance. Combining these equations and integrating the injector inlet pressure

$$P_{5,U}\Big|_{t+\Delta t} = P_{5,U}\Big|_{t} + \Delta t \frac{P_{5,U_{avg}}^2}{P_{a,I_o} Vol_{a,I_o}} \left[\frac{(C_{P_{avg}} - P_{5,U_{avg}})}{\rho a_{5,U}} A_D - \tau_{inj} \left[\frac{P_{5,U_{avg}} - P_{C_{avg}}}{2} \right]^{1/2} A_{inj} \right] \quad [4.12]$$

The other unknowns are readily determined. Note that the average combustor pressure, $P_{C\ avg}$ is simply the mean of the current and most recent (the result of the last time step) combustor pressures.

Combustor Pressure. The combustor pressure is numerically integrated using [3.18]. This is relatively straight forward since the injector mass flow rate can be determined from old values of the injector velocity, $V_{5,D}$ (see [3.18]). These old values are available from a first-in-first-out (FIFO) queue which is maintained by the routine. This queue holds a complete set of injection velocities for a time period equal to the chamber dead time, τ_c.

Program Flow. Fig. 4.4 is a greatly simplified flow diagram for the routine used to model the monopropellant rocket system. The fuel tank, feed line, and the two discharge lines (separated by the throttle valve), are modeled as simple, one-dimensional pipes. The flow through each of these lines is treated exactly as in the single pipe example, except that the initial boundary condition of one line is the terminal boundary condition of the next. The results from this program will be compared with those of Dorsch, et al.[1] in Section V.

compliance and relative motion. This involves the compatibility relations, [2.16] and [2.17], the accumulator equation, [3.13] (to model the pump inlet cavitation) modified by the relative component motion equation, [3.9], and the instantaneous pressure change equation, [3.14]. In terms of Fig. 4.3B indices, these are

$$A_{Feed} V_{3,U} = A_{Dischg} V_{3,D} \qquad P_{3,U} = C_P - \rho a_{3,U} V_{3,U}$$

$$P_{3,D} = C_M + \rho a_{3,D} V_{3,D} \qquad P_{3,D} = P_{3,U} + \Delta P \qquad [4.10]$$

$$\frac{dP_{3,U}}{dt} = \frac{1}{a_P^2}\left[V_{3,U} A_{3,U} - V_{3,D} A_{3,D} + V_S(A_{Feed} \sin\alpha_{3,U} - A_{Dischg} \sin\alpha_{3,D})\right]$$

These constitute a set of four equations in four unknowns. Solving and integrating $P_{3,U}$ to first order

$$P_{3,U}\big|_{t+\Delta t} = P_{3,U}\big|_t + \Delta t \frac{P_{3,U_{avg}}^2}{P_{\theta,P_0} Vol_{\theta,P_0}} A_F \cdot (V_{in} - \beta V_{out} + V_S(\sin\alpha_{3,U} - \beta \sin\alpha_{3,D})) \qquad [4.11]$$

Where:

$$V_{in} = \frac{(C_{P_{avg}} - P_{3,U_{avg}})}{\rho a_{3,U}} = V_{3,U}$$

$$V_{out} = \frac{(P_{3,U_{avg}} + \Delta P - C_{M_{avg}})}{\rho a_{3,D}} = V_{3,D}$$

The pump output pressure, $P_{3,D}$ is determined from [3.14]. The average values must be found through an iterative process.

Interface 4 (Discharge Line-Discharge Line). This boundary condition is exactly the same as for interface 2 with the subscript 4 substituted for subscript 2.

Interface 1 (Propellant Tank-Feed Line). This boundary condition involves the section area change equations, [3.2] through [3.4] except that the simple incompressible continuity relation, [3.3], is replaced by the relative component motion continuity equation , [3.9]. Combining these equations and solving for $V_{1,D}$ in terms of quadratic coefficients (for subtitution into [3.6])

$$A = 1-\beta^2 \quad \beta = \frac{A_{Feed}}{A_{Tank}}$$

$$B = 2(a_{1,D} + \beta a_{1,U} + \beta V_{Tank}(\sin\alpha_{1,U} - \beta\sin\alpha_{1,D})) \qquad [4.8]$$

$$C = 2\frac{(C_M - C_P)}{\rho} - V_{Tank}^2(\sin\alpha_{1,U} - \beta\sin\alpha_{1,D})^2 - 2a_{1,U}V_{Tank}(\sin\alpha_{1,U} - \beta\sin\alpha_{1,D})$$

After $V_{1,D}$ has been determined, the other unknowns at the boundary are readily calculated using [3.9], [3.4], and a compatibility relation (either [2.16] or [2.17]).

Interface 2 (Feed Line-Feed Line). This boundary condition is modeled as the simple orifice condition of [3.7] and [3.8] with an orifice constant equal to τ_{V1} (the feed valve flow constant). In terms of Fig. 4.3B

For $V_{2,D}$:

$$A = 1 \qquad \beta = \frac{A_{Feed}}{A_{Feed}} = 1 \qquad [4.9]$$

$$B = \tau_{V1}^2 \rho \beta (a_{2,U} - \beta a_{2,D}) \quad C = -\tau_{V1}^2 (C_M - C_P)$$

Again, $V_{2,D}$ is found by substitution into [3.6] and the other unknowns are determined using the compatibility equations, [2.16], and [2.17] and the orifice flow equation, [3.7].

Interface 3 (Feed Line-Discharge Line). This is a complex boundary condition which models the combined action of the pump and its inlet

Table 4.2

Monopropellant System Parameters

Combustor Properties

Dead Time, τ_c	3	msec	Residence Time, θ_g	1	msec
Combustor Parameter	370000	$1/ft^2$			

Flow System Properties

Density, ρ	53	lbm/ft^3	Steady State Flow Rate	4	ft^3/sec
Injector Head Drop, ΔH_{inj}	40	%	Injector Const., B_{inj}	2.8	ft/sec
Pump Pressure Rise Coefficients			Input Motion Amplitudes		
			Pump	0.8	ft/sec
			Tank	0.32	ft/sec
A^*	1208	ft			
B^*	668	sec/ft^2			
C^*	-109	$sec2/ft^5$			

	Sonic Velocity (ft/sec)	Length (ft)	Area (ft^2)	Friction Factor
Tank	1000	2	20	0
Feed Line	2000	40	0.2	0.032
Discharge Line	3000	6	0.05	0.042

Computer Requirements

Since only the values corresponding to the current time need be stored (plus a few old values and a small queue), the implementation of the routines developed in this investigation will run on a small system such as a micro (desk top) computer. In fact, all of the programs developed in this investigation were run on a micro computer (the Apple Macintosh™).

Single Pipe Model. This particular routine requires only about 10 K (10,000 bytes of storage) of memory for its source code and about 2 K for variables. Typical run times are on the order of one minute. A small system is well suited to this type of simple model.

Monopropellant System. This routine requires much more storage (15 K source code and 8 K variables) and run times (for transient responses) are about two hours. This type of performance is probably adequate for transient resonses (which need run for only a few cycles of the disturbance) but would not be adequate for steady state responses involving multiple runs of much greater duration.

Bipropellant System. This routine requires more than twice the storage of the monopropellant system. Transient response run times are about six hours and any useful parametric study should be carried out on either a "fast" mini computer or a mainframe. For comparison, this program was partially implemented on the ASD CYBER (CDC 6400) main frame computer. Run times were a very modest 200 CPU's (just a few seconds of real time). Future users of these routines would do well to transport them to a main frame computer (see Appendix A).

V. Results

In this section, results from the single pipe and monopropellant system models described in Section IV are analyzed and compared with published results. The effects of various parameter choices on the relative POGO stability of the monopropellant and bipropellant models developed in this investigation will also be examined.

Single Pipe Systems

Fig. 5.1 is a plot of data generated by the single pipe program described in Section IV. Fig. 5.2 was published by Wylie and Streeter[14:39] who originally modeled this system. Although they are in dissimilar units, a point by point conversion of values given by these plots shows an excellent agreement between the results generated by the routine developed in this study and Wylie and Streeter's published results. A number of other observations follows (note that pressure and velocity indices refer to Fig. 4.1B).

Valve Flow Velocity ($V_{1,D}$). The valve flow velocity falls off starting at time zero and is completely stopped in 2.1 seconds, according to the valve flow constant described by [4.1] (although the increasing valve inlet pressure modifies the shape of this curve).

Valve Inlet Pressure ($P_{1,U}$). At time zero, the fluid system is in steady state equilibrium with a downstream valve inlet pressure of 1.41 MPa (143 feet of head in Fig. 5.2). As the valve closes, a large pressure rise (due to the water-hammer effect) may be observed in both plots. After its peak, the pressure oscillates with a period of about 2 seconds which is the natural period of the system (4 times the transit time of the pressure pulse).

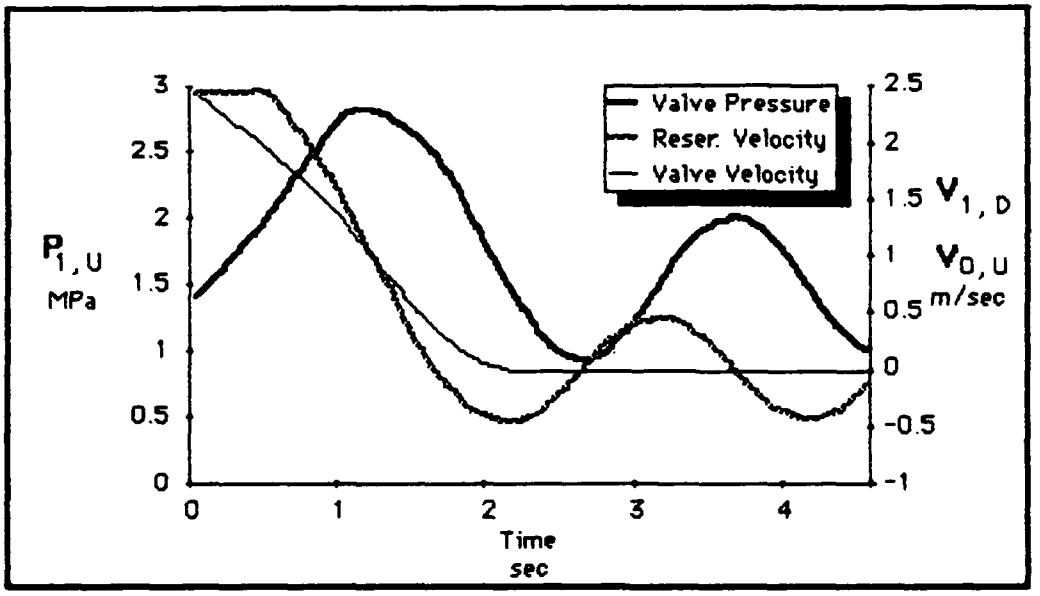

Figure 5.1
Single pipe program results.

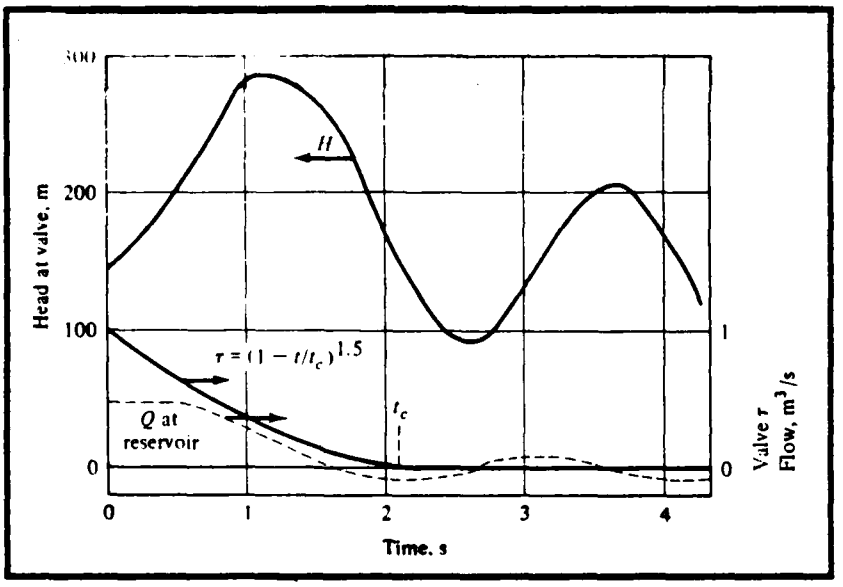

Figure 5.2
Single pipe results from Streeter and Wylie[14].

Reservoir Flow Velocity ($V_{0,u}$). The flow velocity at time zero is at the steady state condition of 2.45 m/sec. Due to the finite transfer time of the pressure pulse, there is approximately a half-second delay in the response at the upstream end of the pipe. The flow begins to fall off, eventually reversing and oscillating about the zero value (at the system's natural frequency).

Other Single Pipe Systems. Since the object of this thesis is to develop and document routines for the analysis of POGO instability in liquid rocket systems, several other boundary conditions were substituted for the simple valve and constant pressure reservoir of Wylie and Streeter's model. POGO instability occurs during the normal full throttle operation of a liquid rocket[1,1-7] and therefore the valve transient represented by [4.1] was deleted in favor of a constant valve flow constant. This flow constant was to be set to τ_0, the initial value used by Wylie and Streeter but was unintentionally set to $500 \cdot 10^{-6}$ $(m^3/Kg)^{1/2}$ which is 25% of τ_0.

POGO instability is caused by pressure oscillations (due to normal thrust variations) in the propellant feed system of a liquid rocket, which give rise to propellant injection variations, thereby causing greater thrust variations[1-7]. In an attempt to simulate this phenomenon in the single pipe model, the upstream pressure of the pipe, $P_{0,u}$ is given a sinusoidally oscillating variation (of frequency 0.5 Hz, the systems resonant frequency) from its mean value. This variation is described by [4.4]. The mean value is still taken as P_0, the same value as in Wylie and Streeter's model.

A hypothetical accumulator is also added to the valve inlet to simulate the cavitation compliance at the injector of a liquid rocket (see Sections III and IV for details). This compliance is modeled with the isothermal expansion result [3.15] with the initial bubble pressure taken as the valve inlet steady state pressure and the initial bubble volumes taken as 0 (effectively zero compliance), 0.01, 0.1 and 1 m^3. These volumes are representative of initial volumes used in the monopropellant system of

Dorsch, et al.[1]

Results. This single pipe compliant system is at the steady state condition (flow velocity of 480 mm/sec and valve pressure, $P_{1,U}$ of 1.45 MPa) when the 0.5 Hz pressure oscillations begin. Figs. 5.3 and 5.4 are plots of the pressure and velocity at the valve inlets and outlets ($P_{1,U}$ and $V_{1,D}$, respectively) of systems with initial cavitation bubbles as noted. Increasing amounts of valve cavitation compliance (increasing initial bubble volume) lead to decreased pressure and velocity perturbations. Also, the zero compliance responses are still building after 5 sec, while the compliant system responses are bounded. This is the main purpose of the compliant devices (i.e. accumulators and "fix"[1:3] devices) introduced in the pump inlets of most liquid rockets.

Fig. 5.5 plots steady state valve inlet pressure disturbance amplitudes (peak to peak) for initial valve inlet cavitation bubble volumes of 0 m^3 (zero compliance) and 1 m^3. For this plot, the inlet pressure oscillation frequency, ω is varied from 0.1 Hz to 3 Hz (0.63 to 18.9 rad/sec). Note the effect of the valve compliance (compliance increases with initial accumulator volume) is to shift the resonance phenomena down in frequency and to greatly decrease its overall amplitude.

Monopropellant Liquid Rocket

The monopropellant system model as detailed in Section IV was run with the same data as the system described by Dorsch, et al.[1] in order to verify the routines developed in this investigation. A number of runs were compared with those already published; three comparisons will be presented here. Before any meaningful comparisons can be made, however, performance criteria must be established. The two factors most important in POGO instability are pump inlet and combustion chamber conditions. Note that the indices of the pressures and velocities refer to Fig. 4.3B.

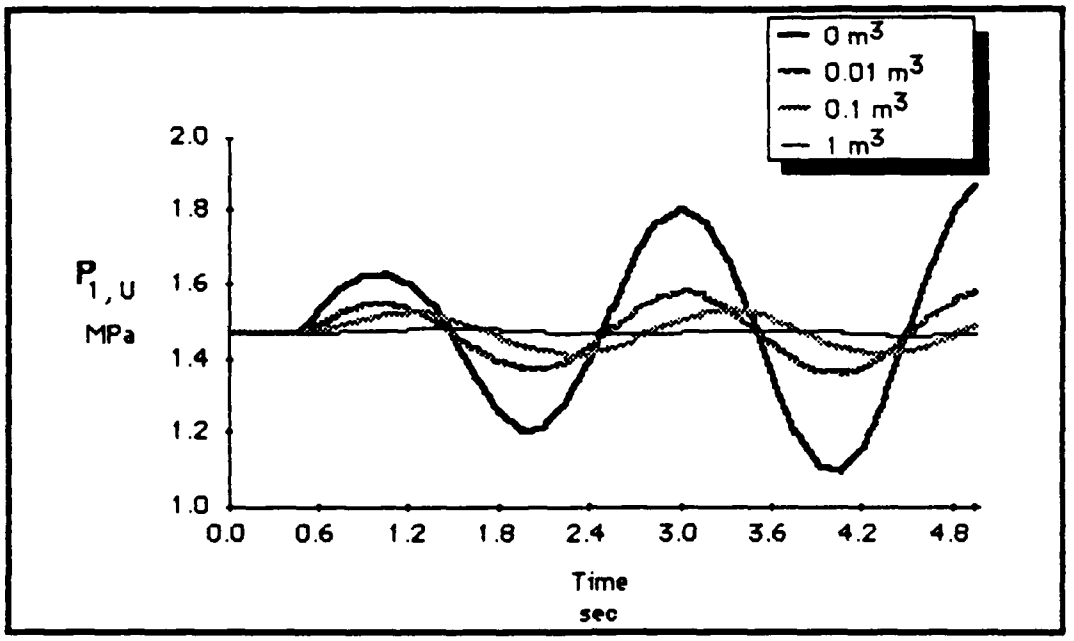

Figure 5.3

Single pipe valve pressures for various compliances.

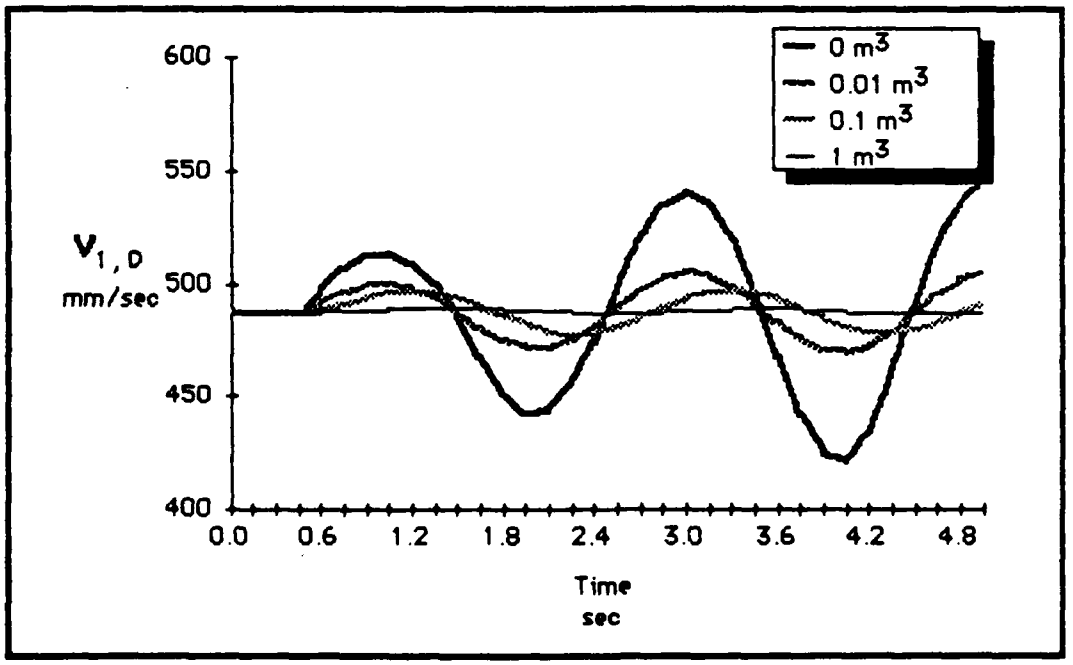

Figure 5.4

Single pipe valve flow velocities for various compliances.

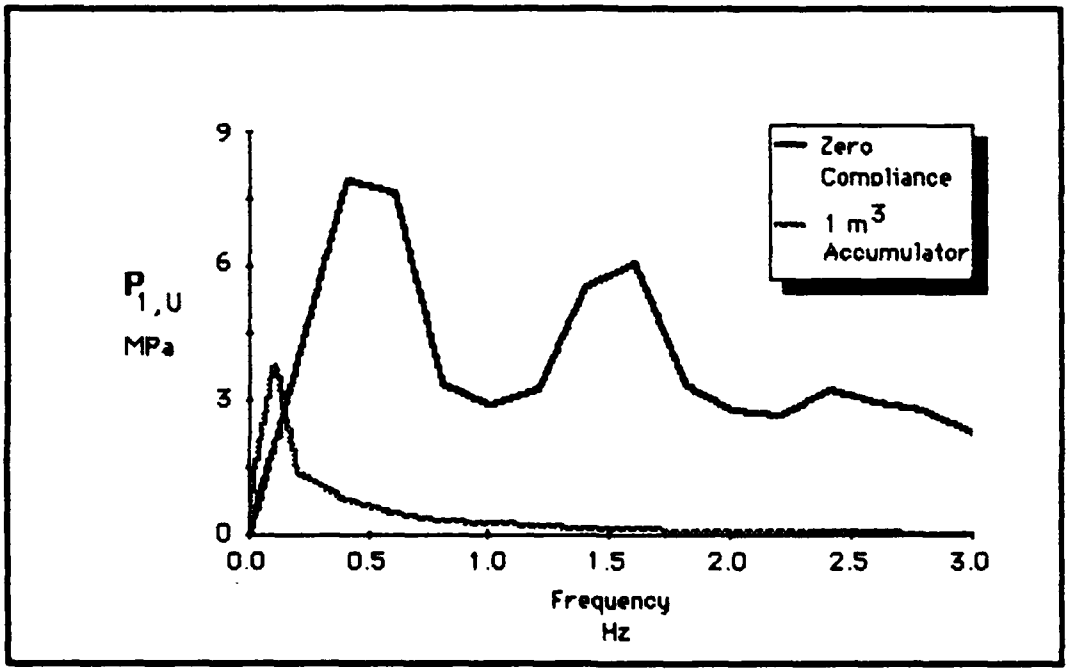

Figure 5.5

Frequency responses for zero and large compliances.

Pump Inlet ($P_{3,U}$ and $V_{3,U}$). The performance of the pump is directly related to the pump inlet pressure[1:18](see Table 4.2). The fluctuation of the pump inlet pressure due to the oscillatory pump and tank motions will therefore be a primary indicator of POGO instability (pump inlet flow variations will be of similar importance). If the inlet pressure minima drive the pump into cavitation (surge), the resulting pump output pressure will greatly magnify these minima, since the pump pressure rise is very much greater in magnitude (and therefor its variation will be much greater) than the pump inlet pressure. These pressure oscillations will lead to injector flow velocity variations which are in turn fed back into the system as variations in the vehicle acceleration, a_s[7:1015].

Combustor ($P_{5,D}$ and $V_{5,D}$). As previously stated, pump output pressure oscillations give rise to injector flow variations which are fed back into a real system (the monopropellant model employs a constant structural accleration and thus ignores this feed back) in the form of structural acceleration variations. The presence of large combustor pressure and flow oscillations (driven by pump output pressure oscillations) indicates POGO instability[1:22].

The pump inlet and combustor states were determined for several pump inlet compliance values. In each case examined, the agreement between the routines developed in this study and the analysis of Dorsch, et al. was striking.

Zero Compliance. As a basis upon which to compare later runs, Dorsch, et al.[1] examined the response of the monopropellant system with no accumulators to input sinusoidal pump and tank motions with amplitudes of 0.8 ft/sec and 0.32 ft/sec, respectively. The excitation frequency was chosen as 10 Hz.

Results. Fig. 5.6 plots the pump suction pressure ($P_{3,U}$) transient response of the monopropellant system as modeled using the routines detailed in this investigation. Fig. 5.7 plots the same response as published by Dorsch, et al.[1:19]. Although the scales and units of the two plots are

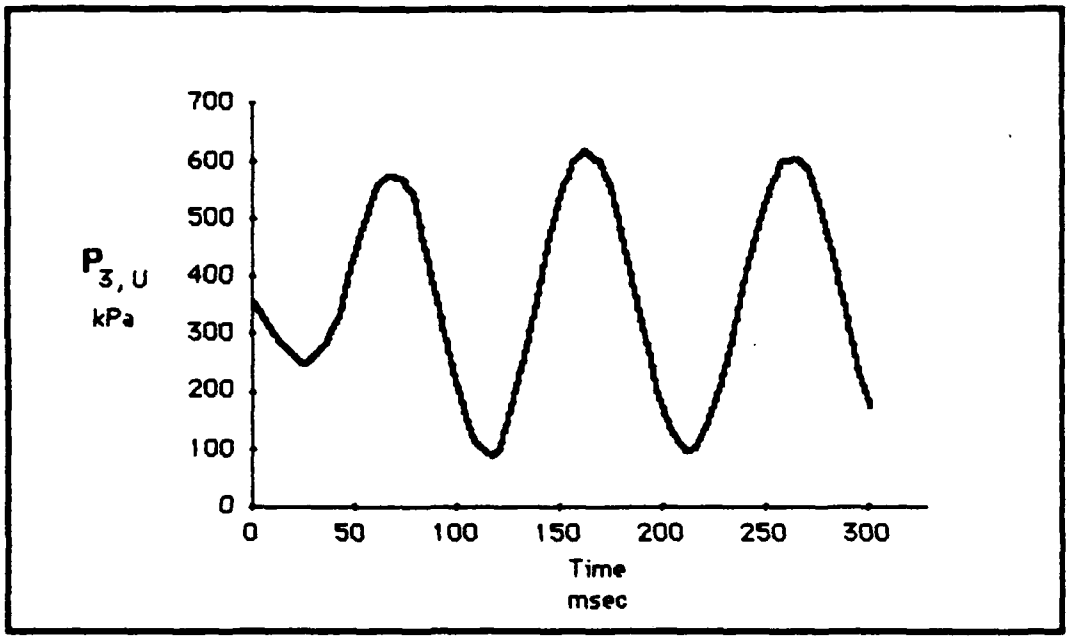

Figure 5.6

Program results for the monopropellant system pump inlet pressure (zero compliance).

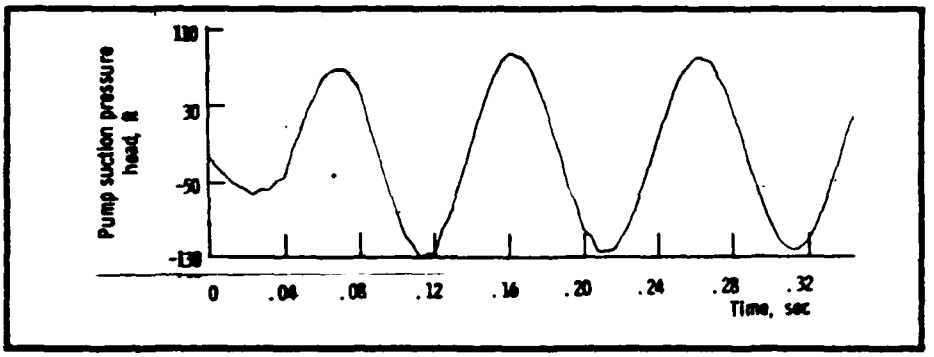

Figure 5.7

Pump inlet pressure results from Dorsch, et al.[1] (zero compliance).

dissimilar, a conversion of the units of Fig. 5.7 to those of Fig. 5.6 showed a quantitative agreement (to within approximately 2%). Note also the excellent agreement of the wave forms, both in the initial transient and in the final steady state amplitudes. Only a non-linear analysis (i.e. one based on the Navier-Stokes equations, [2.1] and [2.2]) could have reproduced these large amplitude responses since the pressure amplitudes are far to large as to be consistent with the assumptions used in a linear network analysis[1,3,14].

Low Compliance Pump Inlet. For this case, the pump inlet compliance was modeled with the isothermal expansion result of [3.15], the initial pressure taken as 1.47 MPa (150 feet of H_2O) and the initial volume as 113 cc. The applied excitation was the same as for the zero compliance case.

Results. Fig. 5.8 depicts the results from the program described in this investigation, while Fig. 5.9 shows published results[1:24] for the transient responses of the pump inlet velocity ($V_{3,0}$) and flow, respectively. There is a marked similarity between these very non-linear plots (again, although the units are dissimilar, they correspond very closely after conversion). Apparently, the introduction of the compliance at the pump inlet leads to very complex behavior when coupled with the relative pump motion and combustion chamber dynamics. This conclusion is supported by the fact that for the zero compliance case these same plots (not shown) were quite sinusoidal. Dorsch's analysis as well as the routines developed in this investigation provide both the complex transient response and the amplitude and wave form of the steady state oscillations. This is another advantage of finite difference based methods.

Large Compliance Pump Inlet. This case is similar to the previous low compliance case, except that the initial bubble volume is taken as 283 cc, and the excitation frequency as 6 Hz. The effect of the greater inlet compliance is to lessen the coupling between pump inflow and outflow.

Results. Fig. 5.10 is a plot of the combustion chamber pressure ($P_{5,0}$) as determined by the routine developed in this investigation, while Fig. 5.11 depicts the analogous published result[1:25]. After conversion to similar units, the plots were found to agree within approximately 2%. Notice

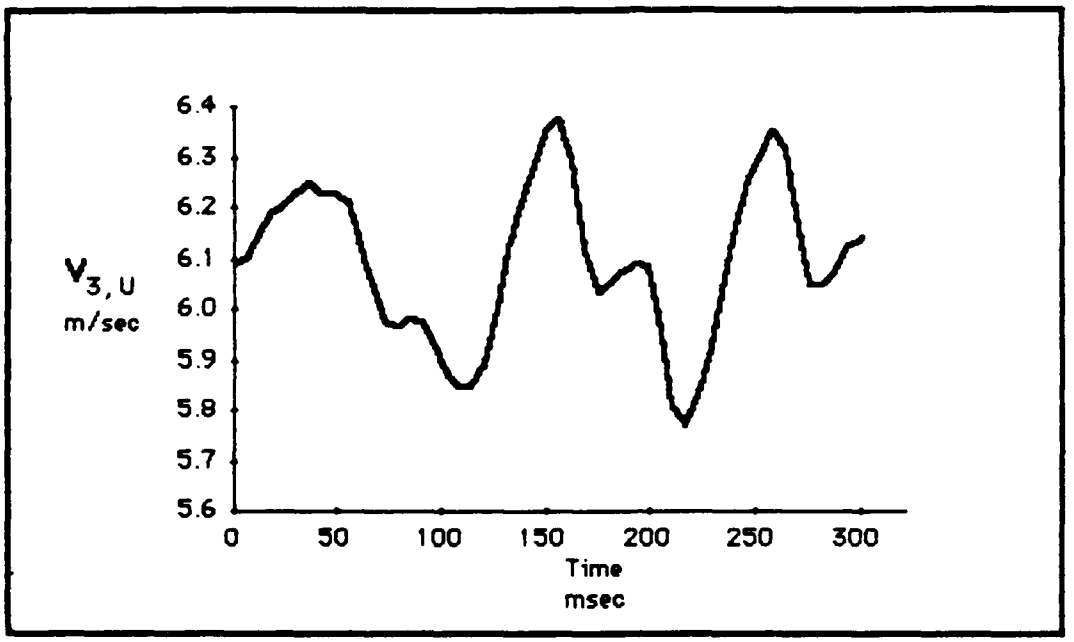

Figure 5.8

Program results for the monopropellant system pump inlet velocity (low compliance).

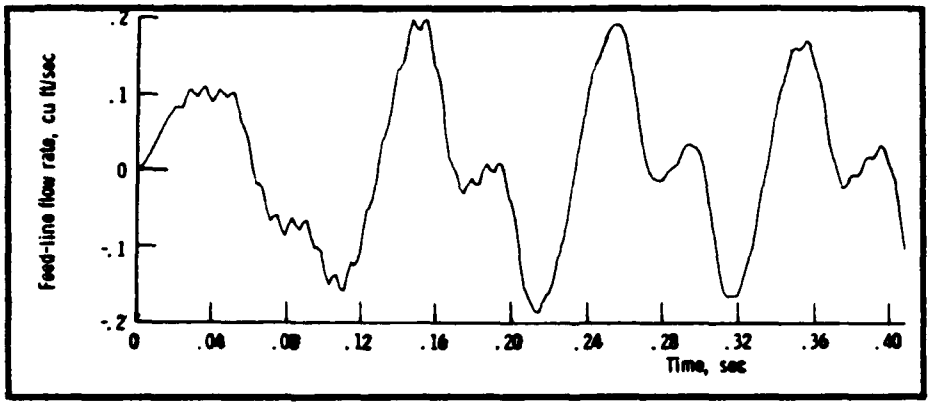

Figure 5.9

Pump inlet velocity results from Dorsch, et al.[1] (low compliance).

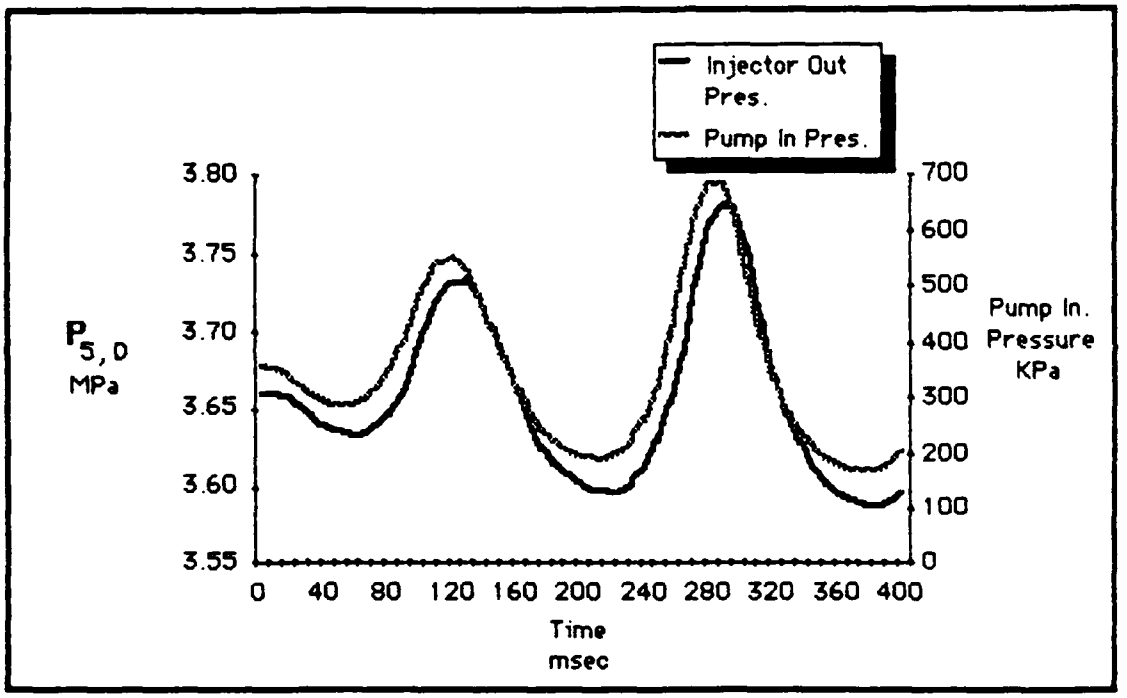

Figure 5.10

Program results for the monopropellant system combustor pressure (large compliance).

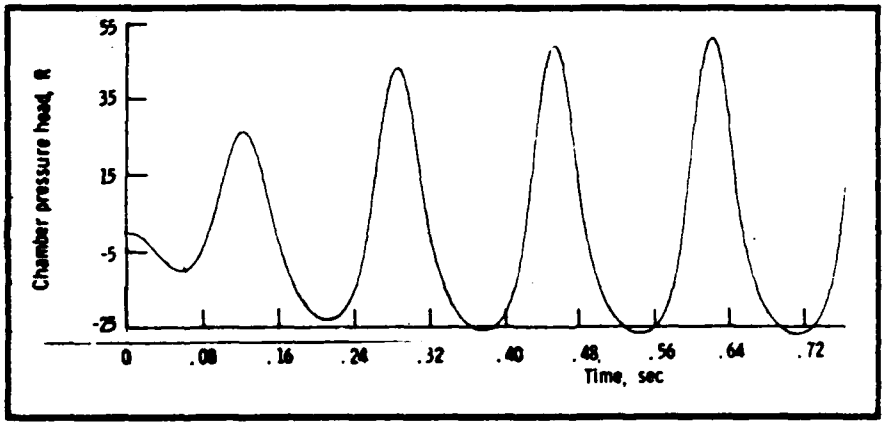

Figure 5.11

Combustor pressure results from Dorsch, et al.1 (large compliance).

the relatively sharp nature of the pressure peaks. This is due to the pump characteristics. As the inlet pressure drops, the pump begins to cavitate producing a rapidly decreasing pressure rise, causing the pump output pressure to exhibit an abrupt pressure minimum. When the inlet pressure is near its peak, the pump inlet pressure response is relatively flat leading to a more rounded pressure maxima in the pump's output pressure. These effects are propagated to the combustion chamber giving rise to Figs. 5.10 and 5.11.

Bipropellant Liquid Rocket

As a guide to the application of the software developed in this thesis by future investigators of more complex liquid rocket models, a typical liquid rocket system was examined. The closed loop (i.e., a system employing propulsion feed back) model was described in Section IV while its actual implementation in terms of digital computer code is described in Appendix A. In this section, the results obtained from this code will be discussed. The following plots are important in determining the relative POGO stability of a system (note that the indices of the pressures and velocities refer to Fig. 4.6B).

Pump Inlet Pressure and Velocity ($P_{3,U}$ and $V_{3,U}$). Just as for the monopropellant system, the pump inlet pressure variations are of paramount concern since they will be magnified by the pump inlet pressure response (see Fig. 4.7). The pump inlet velocity is an indicator of the magnitude of the feed line flow variation, as well as the relative pump structural motion. The presence of large (i.e. of much greater magnitude than the driving thrust oscillations) pump inlet pressure and velocity oscillations is indicative of a POGO instability[1:18].

Combustor Pressure and Velocity ($P_{5,D}$ and $V_{5,D}$). Since the bipropellant system thrust variations will be fed back as structural acceleration variations, the injection velocity oscillations are of great

importance. The combustor pressure is also examined since large chamber pressure variations would be consistent with large injection oscillations and since other modes of instability can be excited by excessive chamber pressure variations[1:22].

Component Displacements (X_T and X_p). During a POGO event, the tanks and pumps will oscillate with large displacement amplitudes[3,10] (presumably at or near their natural frequencies, 10 Hz in this case). These displacements may therefore be used to determine the presence of POGO instability.

Both the transient and steady state response (discussed at the end of this section) were determined for three different configurations with varying degrees of pump inlet and injector dome compliance.

System with Zero Compliance. As a basis for comparison, the compliances of the pump inlet and injector dome cavitation bubbles were taken as zero (accumulator initial volumes equal to zero). This implies that the pump and injector outflows equal their respective inflows (corrected for relative motion). The system was excited with a sinusoidal thrust variation of 50,000 N amplitude at a frequency of 12 Hz. This magnitude represents a modest 10% thrust variation (as defined in Appendix B, the nominal thrust is 500,000 N). The 12 Hz response is plotted since the system exhibited a resonance near this frequency (see steady state response).

Pump Inlet Pressures ($P_{3,U,F}$ and $P_{3,U,Ox}$). Fig. 5.12 depicts the transient response of the fuel and oxidizer pump inlet pressures to the sinusoidal thrust excitation. The fuel pump inlet exhibits an essentially sinusoidal response, while the much less reponsive oxidizer system shows a very non-linear response due to its lower natural frequency. This lower natural frequency occurs because the oxidizer lines are more compliant than the fuel lines (see Appendix B), the larger compliance causing a lower sonic velocity (and therefore natural frequency[14]) as defined by [4.7]. Note also that both the fuel and oxidizer pump inlet pressures are in the stable (i.e,. flat) region of Fig. 4.8. This indicates the relative stability of the system to the thrust variation. This would not necessarily be true if different pump

ummary

Single Pipe Models. The results from a single pipe model utilizing the omputer routines developed in this investigation compared favorably with ıe published results of Wylie and Streeter[14]. It was also shown that valve ılet compliance (modeled using [3.15]) attenuated the effects of inlet ressure disturbances.

Monopropellant System. A more complex system first modeled by orsch, et al.[1] was modeled using the software developed in this thesis. A ery favorable comparison with results published by Dorsch verified that the outines developed in this study produced reliable information.

Bipropellant System. A typical bipropellant system was designed sing a simple steady state analysis (see Appendix B) and the resulting model ras analyzed using the routines developed in this investigation. The ombination of a small excitation amplitude and conservative pump operating haracteristics yielded results that contra-indicated POGO instability. urthermore, a very limited parametric study of the effects of pump inlet nd injector dome compliances showed this system to be very insensitive to hese values due to the small input thrust variation and stable pump haracteristics.

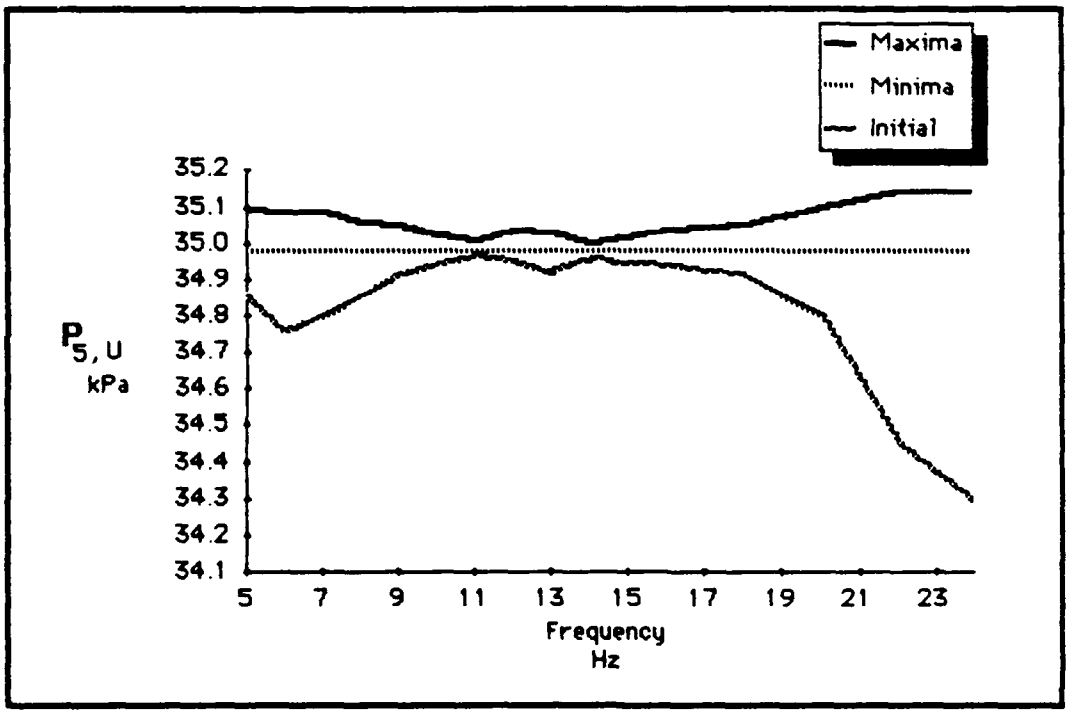

Figure 5.26

Chamber pressure frequency response (zero compliance).

System with Intermediate Compliance. This system produced pump inlet pressure responses (not shown) identical to those for the zero and large compliance cases.

Combustor Response. Fig. 5.26 plots the combustor pressure response amplitudes for the zero compliance case. The excitation was the same sinusoidal 50,000 N thrust variation used throughout this section. The curves for the large and intermediate compliance cases were identical to the zero compliance case and are not shown here. The zero compliance curve indicates amplitude (difference between maxima and minima) minima at approximately 11 Hz and 14 Hz with larger amplitudes at both higher and lower frequencies. Note that all amplitudes are very much smaller than the mean chamber pressure (much less than 1% of mean chamber pressure). This magnitude is considerably smaller than that for the pump inlet pressure (about 10% of mean pressure), giving another indication of the stability of the pump output pressures.

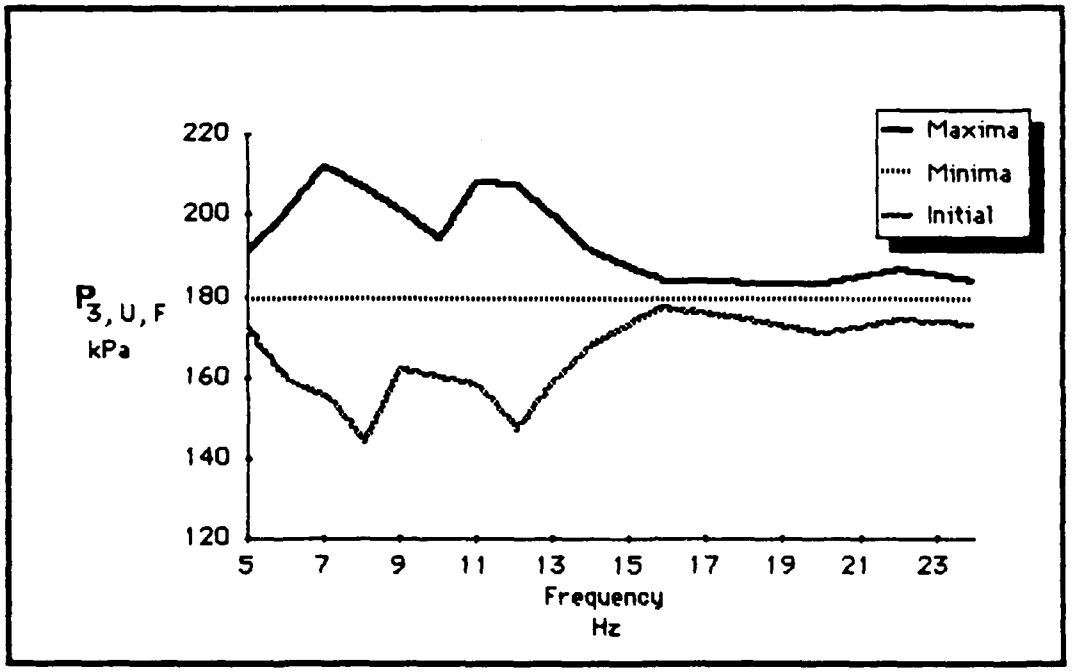

Figure 5.24

Fuel pump inlet pressure frequency response (large compliance).

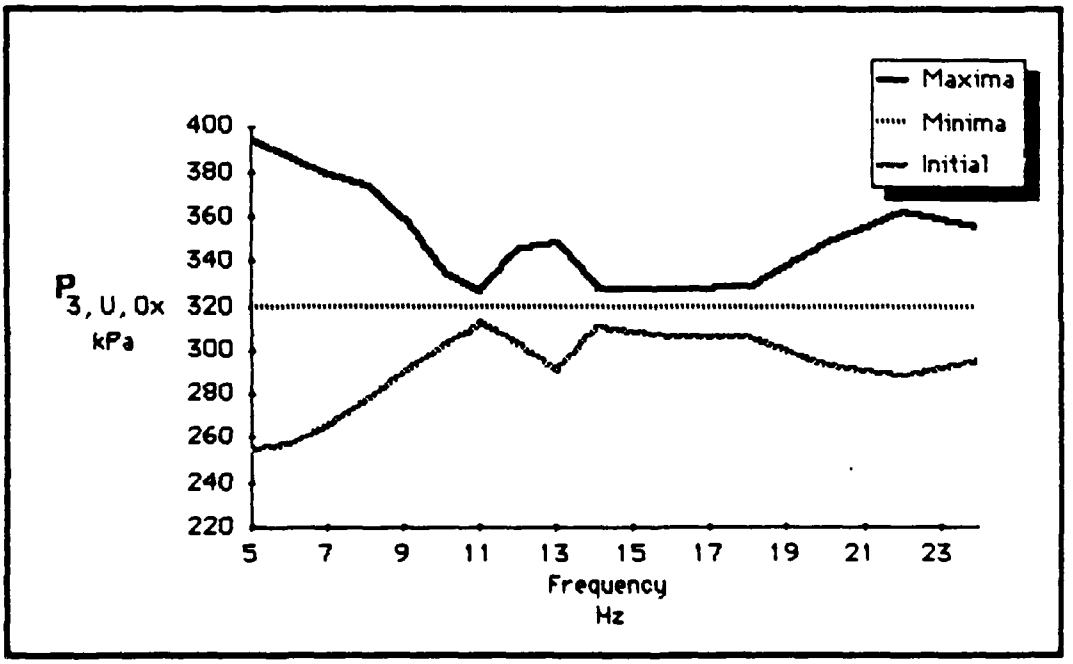

Figure 5.27

Ox. pump inlet pressure frequency response (large compliance).

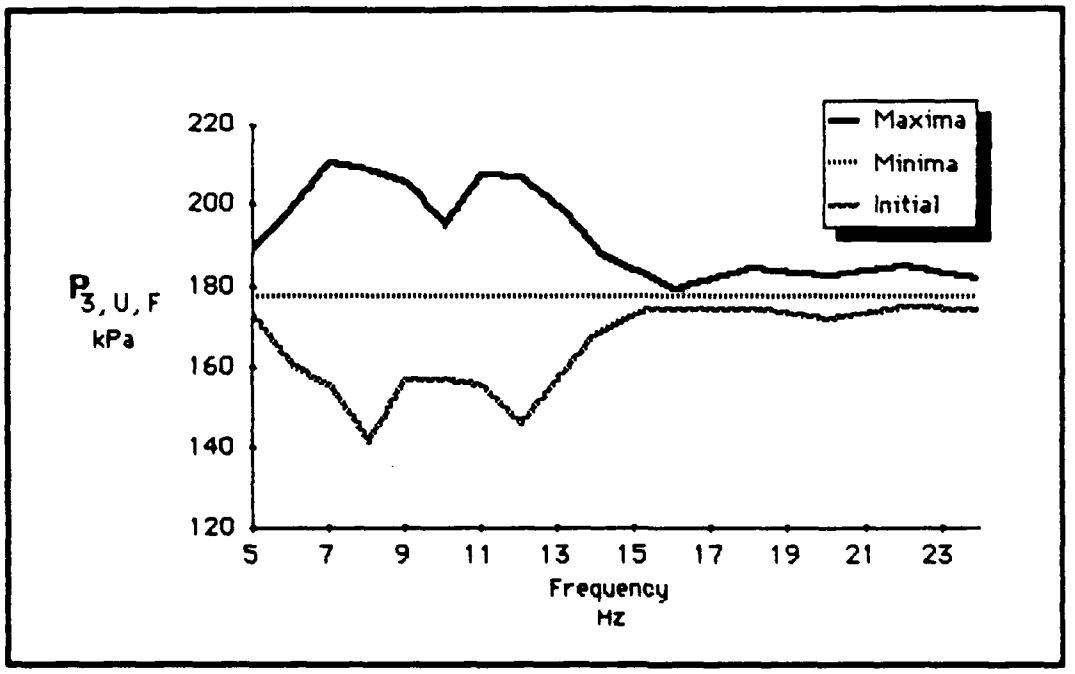

Figure 5.22

Fuel pump inlet pressure frequency response (zero compliance).

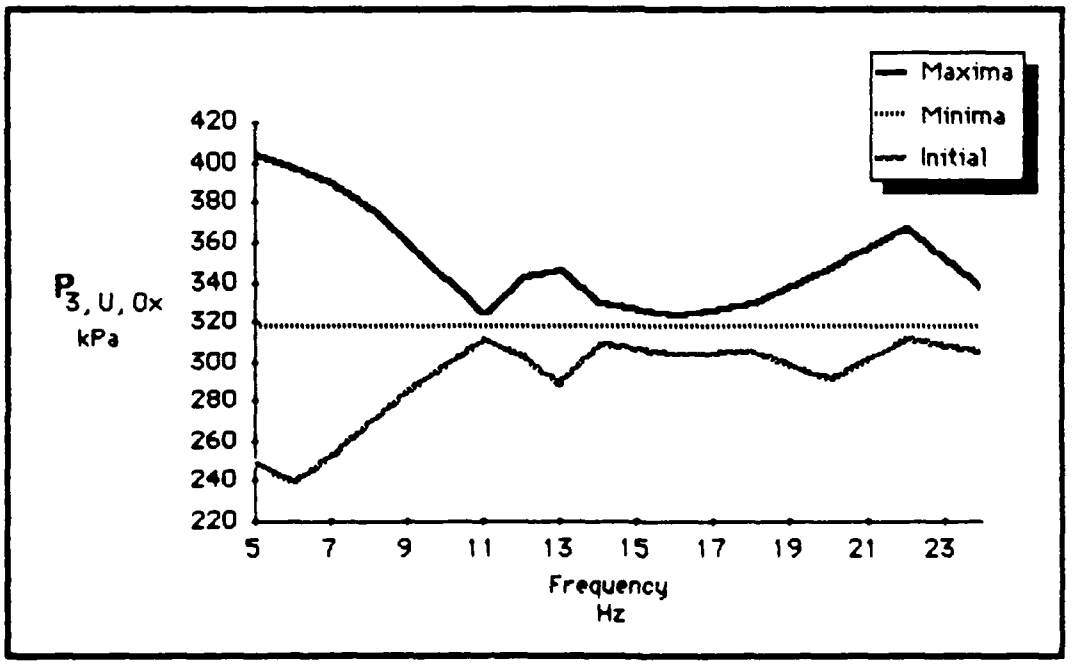

Figure 5.23

Ox. pump inlet pressure frequency response (zero compliance).

and velocity responses do not necessarily occur at component boundaries. If these values are important to a particular analysis, responses at points interior to a fluid lines could easily be obtained.

Pump Inlet Response ($P_{3,\,U}$). As was the case for the transient response, the steady state pump inlet pressure response is of great importance since low pressures can cause pump inlet cavitation and large pump output pressure disturbances. At a given frequency, the presence of large pump inlet pressure steady state amplitudes resulting in pressure minima lower than the stable operating point of the pump (Fig. 4.8), would indicate a POGO instability[1,3].

System with Zero Compliance. Figs. 5.22 and 5.23 depict the fuel and oxidizer pump inlet pressure response of the zero compliance system. On each plot, the upper curve represents the pressure maxima (i.e., the maximum steady state pressure exhibited at the given frequency), while the lower curve reflects the pressure minima (i.e., the minimum steady state pressure). The dashed line between the curves is the unperturbed (i.e,. initial) pressure. Note that the very non-linear nature of the plot is due in part to the small number of data points taken (15 per plot). The fuel pump traces have peaks at 8 and 12 Hz, and approach the mean value (nominal pump inlet pressure of 180 KPa) at high and low frequencies. The oxidizer pump inlet response is more complex and seems to indicate peaks near 6, 13, and 22 Hz, with decreasing response (difference between maxima and minima) at higher and lower frequencies. In neither case do the pressure minima approach the cavitation points in Fig. 4.7, thus it can be concluded that the system exhibits no POGO instability over the range of frequencies examined.

System with Large Compliance. Figs. 5.24 and 5.25 are the analogous plots for the system with 283 cc and 50 cc initial pump inlet and injector dome accumulator volumes respectively. These plots are virtually identical to the zero compliance plots (Figs. 5.24 and 5.25), indicating the insensitivity of the pump inlet pressures to inlet compliance values at this level of input thrust oscillation.

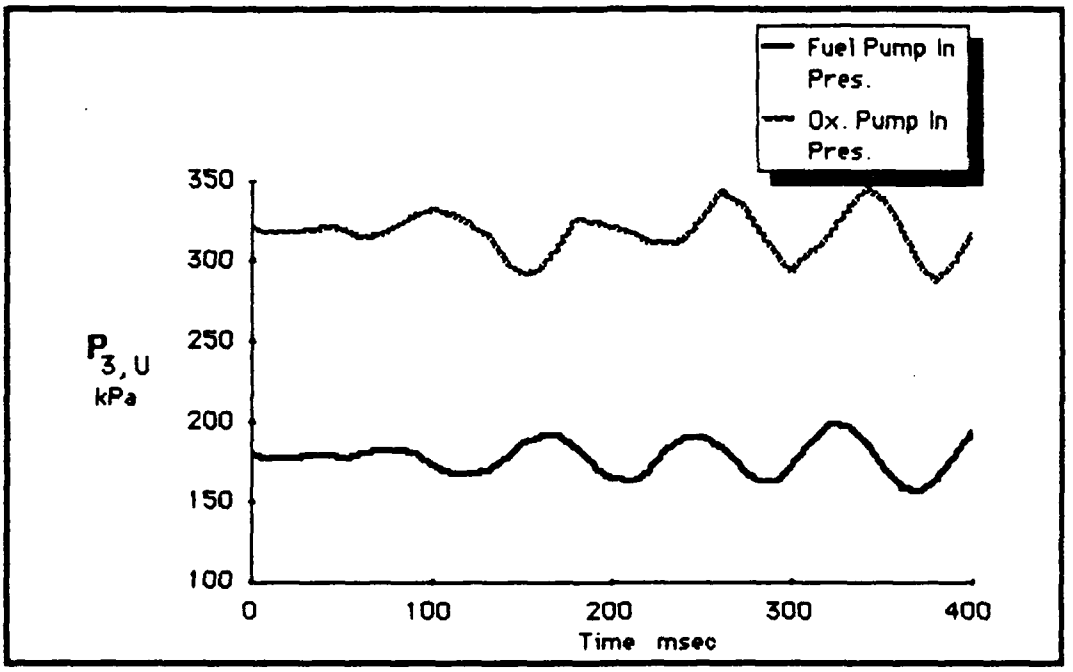

Figure 5.20

Bipropellant system pump inlet pressures (intermediate compliance).

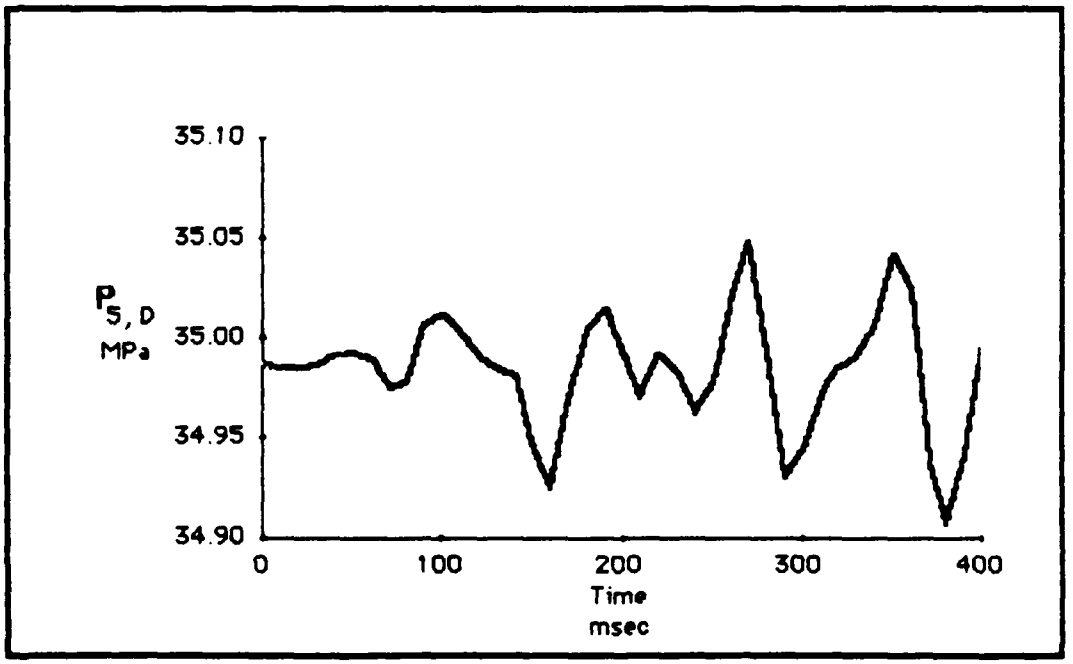

Figure 5.21

Bipropellant system combustor pressure (intermediate compliance).

System with Intermediate Compliance. For this case, the initial bubble volumes for the fuel and oxidizer inlets were lowered to 140 cc, while the fuel and oxidizer injector dome values were raised to 250 cc. Although the resulting data reflects both of these changes (making it difficult to judge their effects separately), the system has proven to be relatively insensitive to the localized compliance values. This model produced responses identical to the zero and large compliance cases. Two plots are given for comparison.

Pump Inlet Pressures. Fig. 5.20 is the graph of the fuel and oxidizer pump inlet velocites for the intermediate compliance case. They appear almost identical to the previous two cases, indicating the relative insensitivity of the inlet pressures to the compliance values (at this level of input disturbance).

Combustor Pressure. The combustor pressure is given in Fig. 5.21. Again the pressure fluctuation, though very complex in wave form, is very small. This particular system is indeed quite stable.

Steady State Response

A principal advantage of the method of characteristics based approach used in this analysis is the ability to obtain both the transient and the steady state responses. The steady state response is simply the final waveform and amplitude of the transient response plot after the transient has died out. This principle can be applied at all points in the system for arbitrary frequencies, resulting in the complete steady state description of the system's response to any input. However, due to the computational limitations of this analysis, only a small number of plots (pump inlet and combustor pressures) will be examined. Furthermore, only a small number of points (each corresponding to the response at a discreet frequency) will be taken. It should be noted that this is not an inherent limitation of the methods presented in this thesis and a more complete analysis of the pressure and velocity steady state responses at many more points in the system would be most useful. Note that the largest steady state pressure

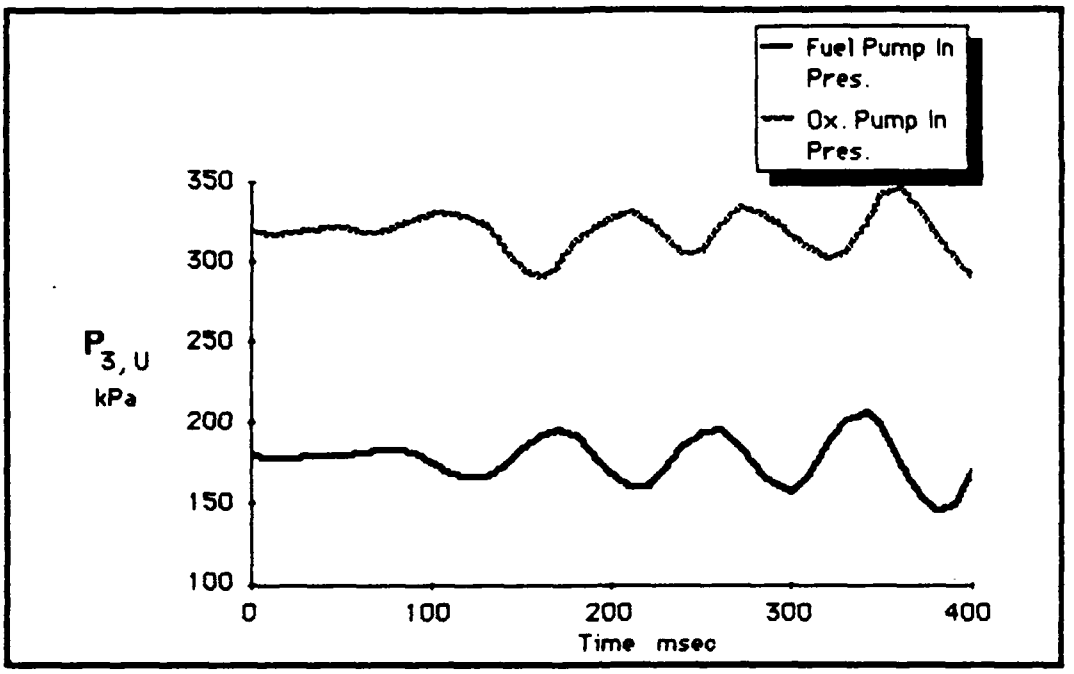

Figure 5.18

Bipropellant system pump inlet pressures (large compliance).

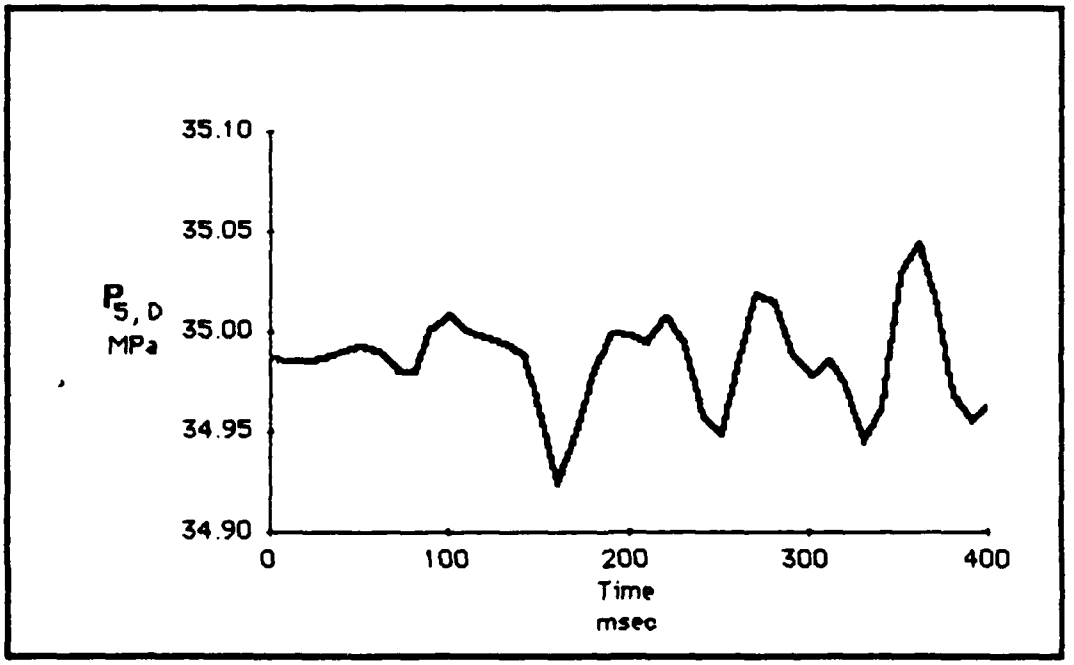

Figure 5.19

Bipropellant system combustor pressure (large compliance).

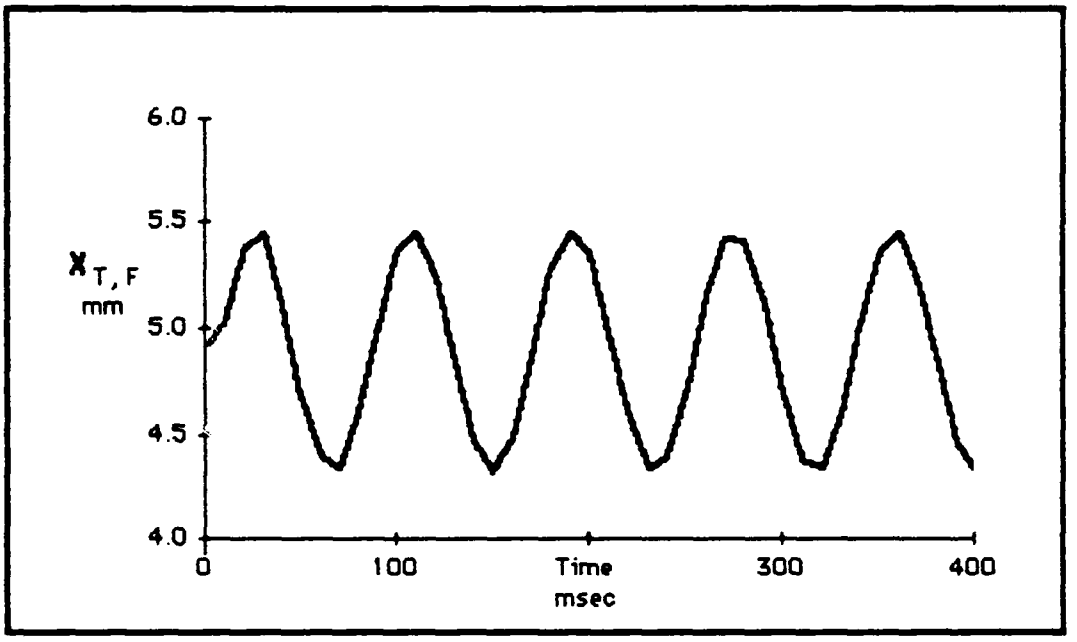

Figure 5.16

Bipropellant rocket system fuel tank displacement (zero compliance).

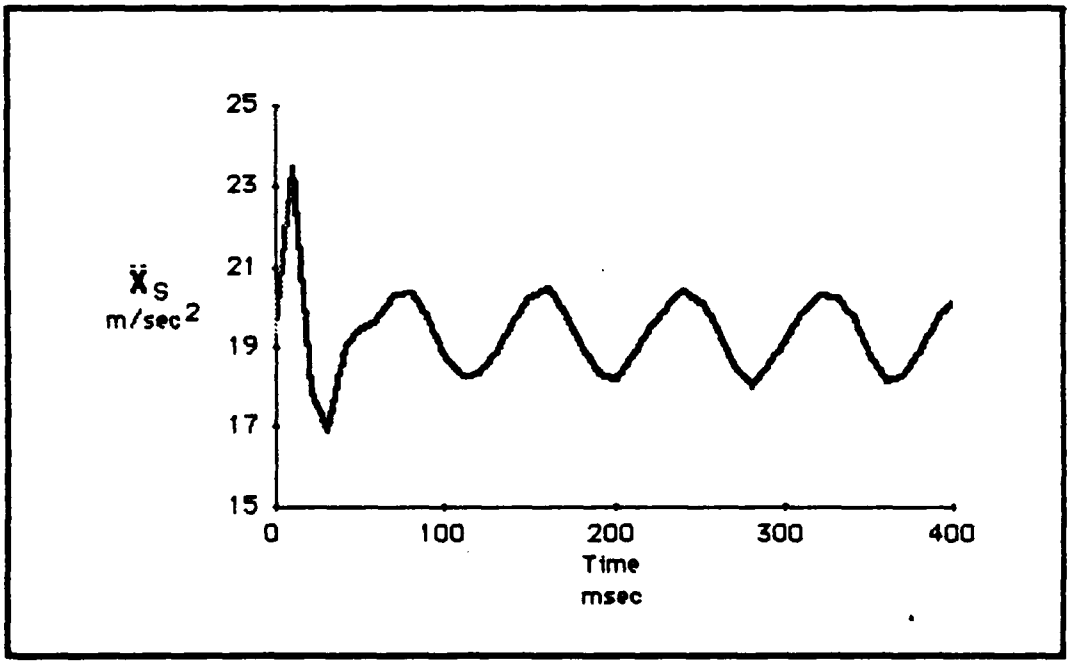

Figure 5.17

Bipropellant rocket system structural acceleration (zero compliance).

is about 0.5 mm which represents a 10% variation from the mean value (5 mm). Since the original thrust variation was 10%, a stable system is indicated[1,3,4].

Structure Acceleration. Fig. 5.17 gives the structural acceleration of the zero compliance system. Note that the structure includes all of the system components except the tanks and pumps (see Fig.4.7). A large start-up transient of approximately 80 msec duration is present. This is due to the small transient response of the component displacements, magnified by the fact that the structure is very light compared to the tanks. As in the case of the component displacements, the relative magnitude of the steady state structural acceleration is the same as the original disturbance (10%) indicating the system's stability.

System with Large Compliance. This system is the same as the zero compliance system except that the pump inlet and injector dome compliances were modeled with the isothermal expansion model (see Section II.). The initial bubble pressures were chosen as the steady state (nominal) pressures (Table 4.5). The initial fuel and oxidizer inlet bubble volumes were each 283 cc, while the initial fuel and oxidizer injector dome bubble volumes were 50 cc. This model produced results that were almost identical with the zero compliance case indicating that the initial thrust disturbance was too small to cause any significant pump ouput variations, and thus, no feed back in the form of flow velocity variations reached the combustion chamber. Two typical plots are given below.

Pump Inlet Pressures ($P_{3.\,U.\,F}$ and $P_{3.\,U.\,Ox}$). Fig. 5.18 details the time history of the fuel and oxidizer pump inlet pressures. There is a great similarity to the zero compliance case (Fig. 5.14), although Fig. 5.18 is slightly smoother in comparison. The localized pump inlet compliance seems to have little effect on this very stable system.

Combustion Chamber Pressure ($P_{5.\,D.\,F}$ and ($P_{5.\,D.\,Ox}$). The combustor pressure response is given in Fig. 5.19. Again this curve is almost identical to the zero compliance case, the resulting oscillation being very small. This indicates the lack of POGO instability.

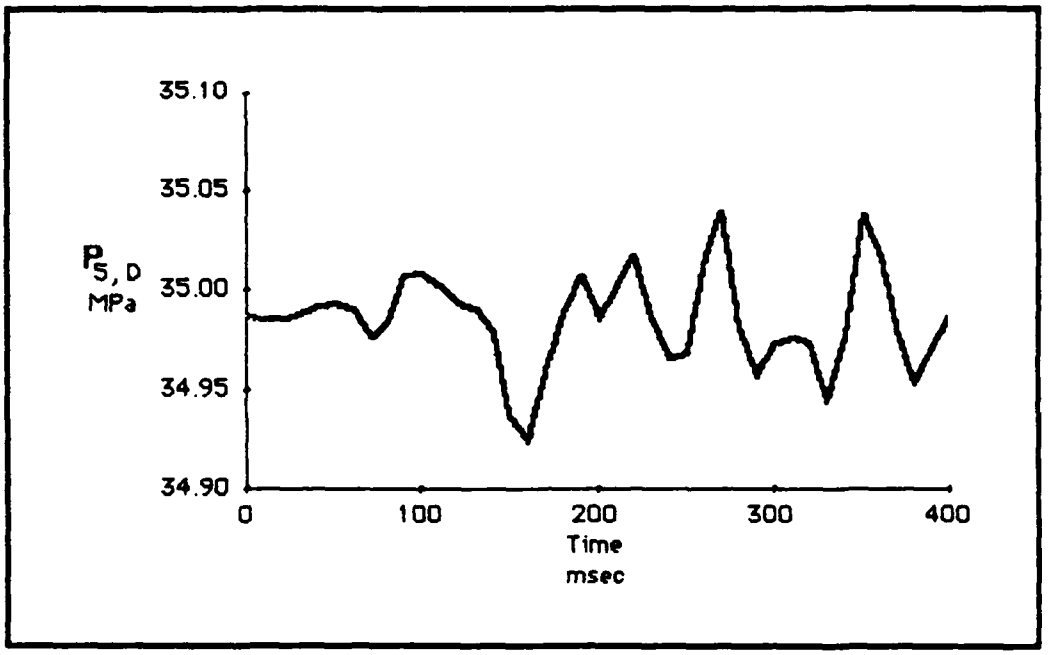

Figure 5.14
Bipropellant system combustor pressure (zero compliance)

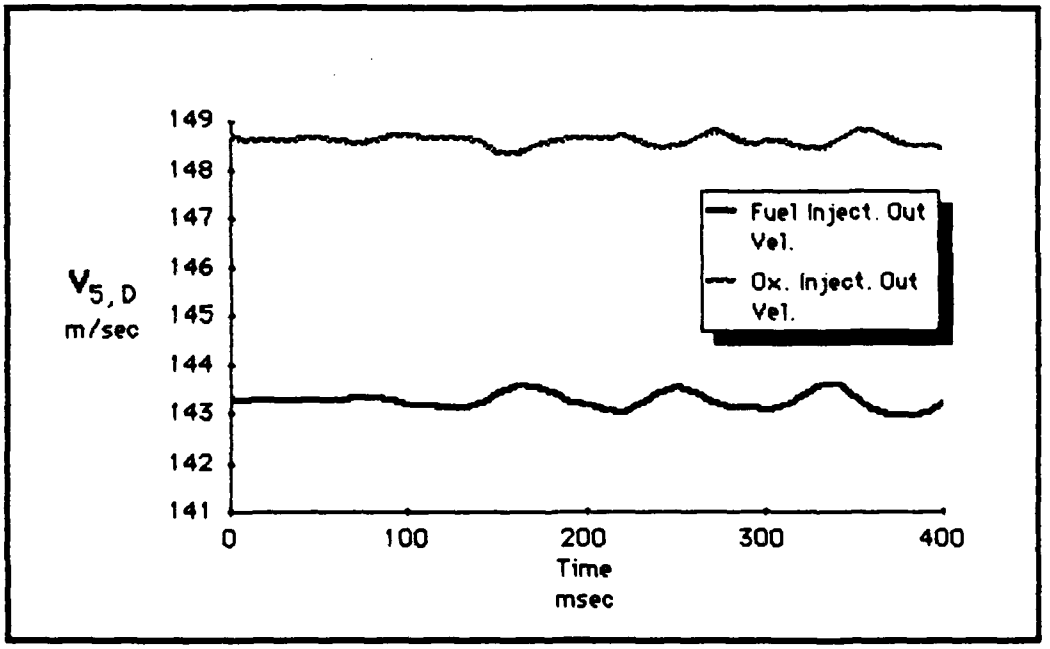

Figure 5.15
Bipropellant system injector velocities (zero compliance).

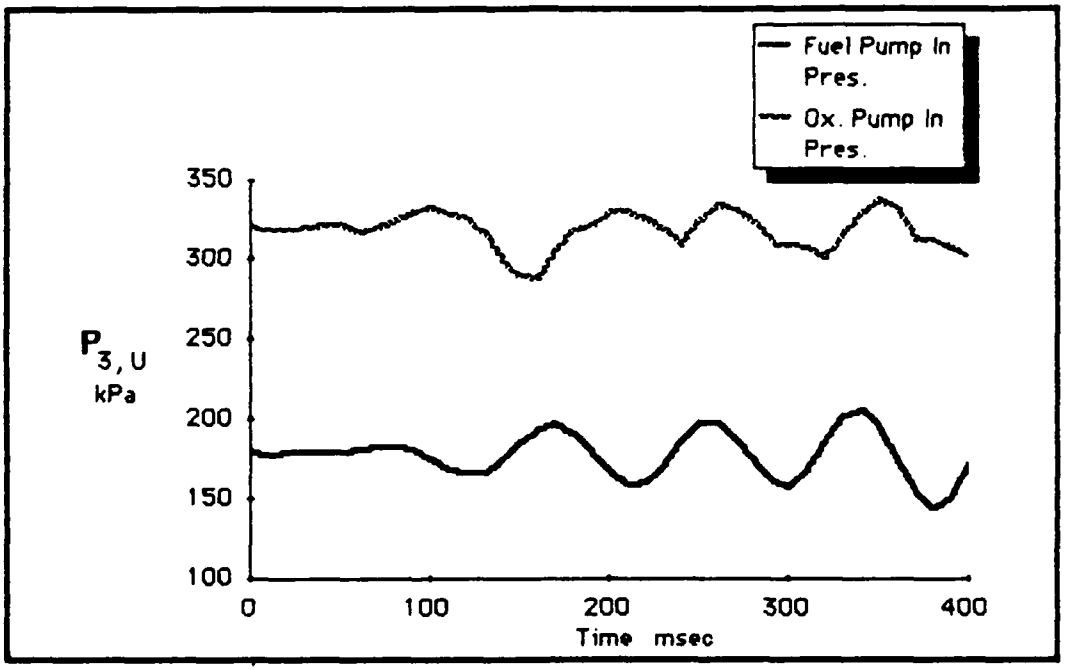

Figure 5.12

Bipropellant system pump inlet pressures (zero compliance).

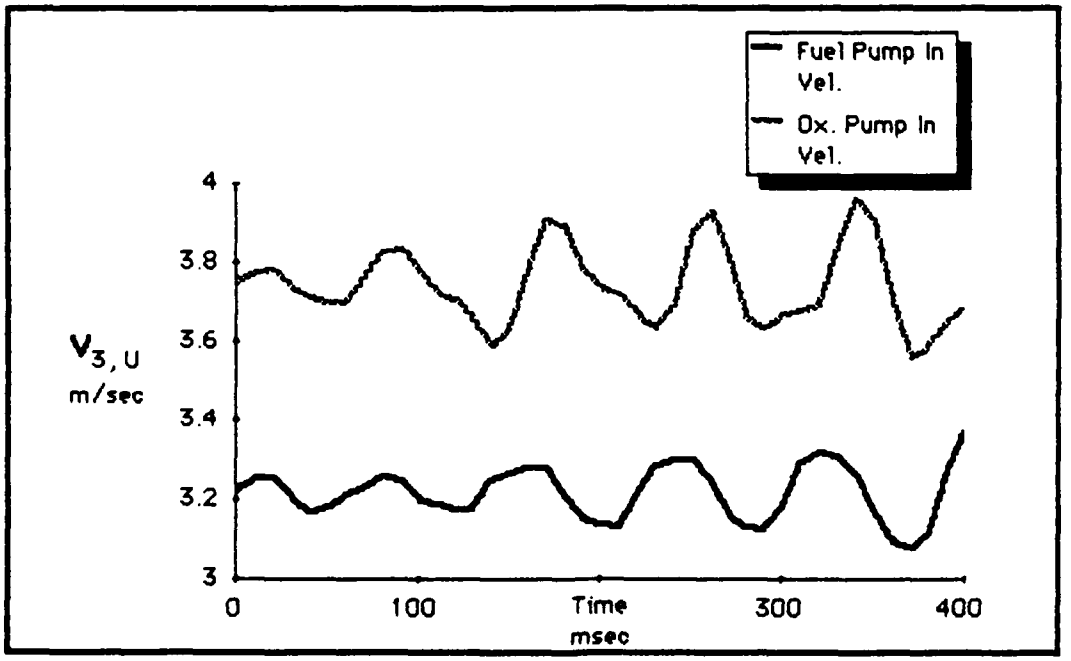

Figure 5.13

Bipropellant system pump inlet velocities (zero compliance).

characteristics had been chosen in Appendix B. The importance of accurate pump characteristics cannot be over stated.

Pump Inlet Velocities ($V_{3,U,F}$ and $V_{3,U,Ox}$). Fig. 5.13 is a plot of the pump inlet velocities for the zero compliance system. As in the case of the inlet pressures, the fuel pump inlet velocity trace is much more sinusoidal than the very non-linear oxidizer pump inlet velocity trace (another manifestation of the oxidizer systems lower sonic velocities). The fuel pump velocity amplitude is approximately 3% of the nominal value while the corresponding oxidizer amplitude is 7% of its nominal value. These very modest variations further indicate a stable system.

Combustion Chamber Pressure ($P_{5,D,F}$ and ($P_{5,D,Ox}$). The chamber pressure transient response is given in Fig. 5.14. This plot is much more complex and non-linear than those for the pump inlets due to the superposition of the combustor dynamics on the pump ouputs. Note also that the magnitude of the chamber pressure oscillation is quite small compared to the mean pressure (another indication of the system's stability).

Injector Outlet Velocities ($V_{5,D,F}$ and ($V_{5,D,Ox}$). The fuel and oxidizer injector outlet velocities for the zero compliance system are given in Fig. 5.15. While both are quite non-linear, these perturbations are a much smaller fraction of the nominal values than were the corresponding pump inlet velocities, attesting to the very stable operation of the pump. The pump is essentially isolating the dishcharge lines and combustor from the modest pump inlet pressure fluctuations.

Component Displacements ($X_{T,F}$). For simplicity, the pump and tank masses and structural coefficients were selected to produce dynamically identical responses with resonances at 10 Hz (see Table 4.4 and Appendix B). Fig. 5.16 plots the displacement of the fuel tank, $X_{T,F}$ in response to the excitation (the oxidizer tank and both pump displacements have responses identical to the fuel tank responses). The transient is very short and the steady state wave form is nearly triangular. The amplitude of the response

VI. Conclusions

This section summarizes the findings of this study and recommends areas for future work. The accuracy and utility of the routines developed in this paper in modeling POGO instability problems of arbitrary complexity has been shown. The following has been accomplished:

1) A general tool has been developed for the study of liquid rocket POGO instability.

2) The routines developed in this paper have been verified by favorable comparison with published data from several sources.

2) A systematic reference for future POGO stability analyses has been presented. Core routines have been written and are available in the Appendix.

Recommendation

The model developed here, while complete, could be extended primarily with the addition of more accurate component models. Furthermore, a complete parametric study would be useful in actually evaluating the effects of various components on the overall stability of a given system.

Bibliography

1. Dorsch, Robert G., Don J. Wood, and Charlene Lightner. "Distributed Parameter Analysis of Pressure and Flow Disturbances in Rocket Propellant Feed Systems," Technical Note TN D-3529. National Aeronautics and Space Administration, Washington, DC (August 1966).

2. Ryan, R.S., L.A. Kiefling, W.A. Jarvinen, and H.J. Buchanan. "Simulation of Saturn V S-II Stage Propellant Feedline Dynamics," Journal of Spacecraft and Rockets, No. 2 (December 1970).

3. Rubin, Sheldon. "Prevention of Coupled Structure-Propulsion Instability (POGO) on the Space Shuttle," Technical Memorandum TM X-52876, Vol. II: 246-262. National Aeronautics and Space Administration, Washington, DC (July 1970).

4. Woods, W.A. "Method of Calculating Liquid Flow Fluctuations in Rocket Motor Supply Pipes," Journal of the American Rocket Scientists, 14: Vol. 31: 1560-1567 (November 1961).

5. Holster, Jesse L. and William J. Astleford. "Analytical Model for Liquid Rocket Propellant Feedline Dynamics," Journal of Spacecraft and Rockets, Vol. 2, No. 2: 180-187 (March 1974).

6. Zielke, W., E.B. Wylie, and R.B. Keller. "Forced and Self-Excited Oscillations in Propellant Lines," Transactions of the ASME, vol. 91D: 671-677 (December 1969).

7. Fashbaugh, R.H. and V.L. Streeter. "Resonance in Liquid Rocket Engine Systems," Transactions of the ASME, vol. 87D: 1011-1017 (December 1965).

8. Zwick, S.A. and M.S. Plesset. "On the Dynamics of Small Vapor Bubbles in Liquids," Journal of Mathematics and Physics, Vol. 33: 308-330 (March 1954).

9. Summerfield, Martin. "A Theory of Unstable Combustion in Liquid Propellant Rocket Systems," Journal of the American Rocket Scientists, Vol. 21: 108-114 (April 1951).

10. Rubin, Sheldon. "Longitudinal Instability of Liquid Rockets Due to Propulsion Feedback (POGO)," Journal of Spacecraft and Rockets, Vol. 3: 1188-1195 (August 1966).

11. Clay Hicks Space Station Task Force. Presentation on Space Station April 1984, National Aeronautics and Space Administration, Washington, DC (April 1984).

12. Ring, Elliot. Rocket Propellant and Pressurization Systems. Englewood Cliffs, New Jersey: Prentice-Hill Inc., 1964.

13. Crocco, L. "Aspects of Combustion Stability in Liquid Propellant Rocket Motors, Parts I and II," Journal of the American Rocket Scientists, Vol. 21: 163-178 (November 1951). Vol. 22: 110-119 (Februarry 1952).

14. Wylie, E.B. and V.L. Streeter. Fluid Transients. New York: McGraw-Hill, Inc., 1978.

15. Ellison, John R. and Daniel L. Balzer. "Liquid Propulsion," AIAA Journal, Vol. 34: 79-83 (December 1983).

16. -----. Liquid Rocket Propulsion: An Evaluation of Our National Capability. An AIAA Position Paper (January 1983).

17. Huzel, Dieter K. and David H. Huang. "Design of Liquid Propellant Rocket Engines (Second Edition)," National Aeronautics and Space Administration, Washington, DC (May 1971).

18. Fang, J. "Application of Combustion Time-Lag Theory to Combustion Stability of Liquid and Gaseous Propellant Rocket Engines," AIAA 22nd Aerospace Sciences Meeting, AIAA paper 84-05110 (Januarry 1984).

19. Bowman, George P. "Thermochemistry (Propulsion Applications)", Lecture Notes, AFIT Department of Mechanical Engineering, WPAFB OH, March 1965.

20. Hill, Philip G. and Carl R. Peterson. Mechanics and Thermodynamics of Propulsion. Reading, Massachussets: Addison-Wesley Publishing Company, 1970.

21. Kit, Boris and Douglas S. Evered. Rocket Propellant Handbook. New York: The MacMillan Company, 1960.

Appendix A: A User's Guide to POGO Analysis Software

This appendix is intended as a guide to applying the routines developed in this paper to arbitrary liquid rocket systems. Although it is true that a completly general model of something as complex and specific as a liquid rocket system is not possible, it is possible to develop core routines to be used in the modeling and simulation of arbitrary systems. The routines documented herein should be viewed as an aid to the analyst in constructing a complete model, not as such a model in themselves. In this spirit, various component modeling routines will be presented and a general framework for their application will be given.

Computational Requirements

The routines used developed in this investigation and detailed in this appendix do not require a great deal of computational power. This is due to the relatively large time steps possible with the method of characteristics fluid flow solution. Also, since only one set of conditions must be stored at any one time, the necessary data storage in arrays and queues is quite small. Transient solutions can be obtained conveniently (with four or five hours of computational time) on even a micro computer. The calculation of steady state solutions will require many more times this computational time and mini or main frame computer must be used.

The code presented here is written in the MS-BASIC™ language (the actual dialect is for the Apple Macintosh™ personal computer). This implementation of BASIC is sufficiently general such that it will run with minor or no modification on most mini and micro computers. Many main frame systems also have BASIC interpreters, although some modification of the routines, especially in the file input-output blocks, will likely be necessary. Note that this version of BASIC assumes double precision (14

digits) unless otherwise specified by the following rule: variables ending in "%", "!", and "#" are of integer, single, and double precision, respectively.

Single Pipe Systems

All systems will consist of a collection of single pipe elements. The complexity arises from the combination of a large number of these elements. A simple routine to evaluate the pressure and velocity at all points internal to an idealized pipe follows.

Initialization Block. Before the routine can be started, the following initialization statements must be executed:

```
10 REM Single Pipe System.
40 GOSUB 200    'Initialization.
41 GOSUB 225    'Calculate Steady State Conditions.
42 SYSTIME=0    'Begin Calculations.
```

Body. The following code will actually apply the initial boundary conditions, calculate the state at the internal sections of the pipe, and apply the terminal boundary conditions.

```
44 IF INT(SYSTIME/DELTATOUT)>INT((SYSTIME-DELTAT)/DELTATOUT)
   THEN GOSUB 300    'Output Results.
45 SYSTIME=SYSTIME+DELTAT    'Increment Time.
46 IF SYSTIME>ENDTIME THEN END    'Stop if Completed.
50 GOSUB 600    'Apply Initial Boundary Condition.
60 FOR IDO%=1 TO NSECTIONS%-1    'Step through all internal
   sections.
70 GOSUB 400    'Get Cp.
73 GOSUB 500    'Get Cm.
75 OLDPRES=PRESSURE(IDO%): OLDVEL=VELOCITY(IDO%)    'Save old
   state (for next section).
80 PRESSURE(IDO%)=(CP+CM)/2    'Calculate new pressure.
90 VELOCITY(IDO%)=(PRESSURE(IDO%)-CM)/(RHO*SOUND)    'Calculate
   new velocity.
```

```
101 NEXT I00%
105 GOSUB 700    'Apply Terminal Boundary Conditon.
110 GOTO 44    'Repeat until finished.
```

Initialization. Before a program can run, values must be assigned to the necessary variables. The data read in will be defined later in this appendix. This section also computes the number of reaches necessary to meet the Courant condition at the specified time step size. This fixes the dimension of the storage arrays the program will require.

```
200 REM Get data and initialize routine.
205 READ DELTAT, TEND, DELTATOUT, RHO, SOUND, LENGTH, DIAM,
    AREA, FRICT, TAUO, PBASE, AMP, FREQ, VGUES, ACCEL, ALPHA,
    TCUT, TAUEXP
210 NSECTIONS%=INT(LENGTH/(DELTAT*(SOUND+VGUES)))    'Use Courant
    Condition to calculate the necessary number of reaches for
    the pipe.
215 THETA=DELTAT/(LENGTH/NSECTIONS%): PSI=THETA*SOUND
    'Calculate Grid Parameters.
220 DIM VELOCITY(NSECTIONS%): DIM PRESSURE(NSECTIONS%)
    'Dimension state arrays.
222 RETURN
```

Steady State Initialization. The finite difference routine requires starting values on which to base its calculations. In this section, the steady state response is calculatated with completely conventional methods. Note that the steady state calculations depend upon the boundary conditions. This particular section assumes an initially constant pressure upstream, and a valve downstream (orifice with decreasing flow coefficient).

```
225 REM Steady State Initialization.
230 VEND=((TAUO^2*(PBASE+RHO*ACCEL*LENGTH*SIN(ALPHA)))/
    (1+(RHO*FRICT*LENGTH*TAUO^2)/(2*DIAM)))^.5    'Calculate
    outlet velocity.
235 PEND=PBASE+RHO*ACCEL*LENGTH*SIN(ALPHA)-(RHO*FRICT*LENGTH*
    VEND^2)/ (2*DIAM)    'Calculate outlet pressure.
240 FOR I00%=0 TO NSECTIONS%
250 PRESSURE(I00%)=PBASE+(PEND-PBASE)*I00%/NSECTIONS%
```

```
    'Interpolate interior pressures.
260 VELOCITY(IDO%)=VEND  'Assign constant interior velocity.
270 NEXT IDO%
275 RETURN
```

Output. This section will of course vary with the user's wishes. The following routine simply prints out the terminal conditions (in scientific notation to 5 significant figures).

```
300 REM Output Routine.
310 PRINT USING "+#.####^^^^_    "; SYSTIME,
    PRESSURE(0),VELOCITY(0),PRESSURE(NSECTIONS%),VELOCITY(NSECTI
    ONS%)
320 RETURN
```

Determination of Cp and Cm. This section calculates the values of Cp and Cm at specified sections of the pipe.

```
400 REM Get Cp.
410 VELR=(VELOCITY(IDO%)-PSI*(VELOCITY(IDO%)-OLDVEL))
    /(1+THETA*(VELOCITY(IDO%)-OLDVEL))   'Calculate Vr.
420 PRESR=PRESSURE(IDO%)-(VELR*THETA+PSI)*(PRESSURE(IDO%)
    -OLDPRES)   'Calculate Pr
430 CP=PRESR+RHO*VELR*(SOUND+ACCEL*SIN(ALPHA)*DELTAT*SOUND/
    VELR-SOUND*FRICT*DELTAT*ABS(VELR)/(2*DIAM))   'Assign Cp
    value.
440 RETURN
500 REM Get Cm.
510 VELS=(VELOCITY(IDO%)-PSI*(VELOCITY(IDO%)-VELOCITY(IDO%+1)))
    / (1-THETA*(VELOCITY(IDO%)-VELOCITY(IDO%+1)))   'Calculate
    Vs.
520 PRESS=PRESSURE(IDO%)+(VELS*THETA-PSI)*
    (PRESSURE(IDO%)-PRESSURE(IDO%+1))   'Calculate Ps
530 CM=PRESS-RHO*VELS*(SOUND+ACCEL*SIN(ALPHA)*DELTAT*SOUND/
    VELS-SOUND*FRICT*DELTAT/(2*DIAM))   'Assign Cm value.
540 RETURN
```

Boundary Conditions. The only remaining issue is the application of the various boundary conditions used to model the end conditions of the pipe. One

initial condition (known pressure) and two terminal conditions (valve closure with and without compliance) will be presented.

Initial Condition. The initial boundary condition for this system is that of a known (oscillatory) pressure. The following code matches the known upstream pressure to the downstream conditions (based on Cm).

```
600 REM Initial Boundary Condtion.
610 IDO%=0: GOSUB 500   'Get Cm.
615 OLDVEL=VELOCITY(0): OLDPRES=PRESSURE(0)
620 PRESSURE(0)=PBASE+AMP*SIN(6.2832*FREQ*SYSTIME)   'Calculate
    upstream pressure.
630 VELOCITY(0)=(PRESSURE(0)-CM)/(RHO*SOUND)   'Match velocity
    to downstream conditions.
640 RETURN
```

Valve Closure with Zero Compliance. The exponential valve closure is applied to the outlet flow coefficient and the conditions are matched.

```
700 REM Terminal B.C.
710 IDO%=NSECTIONS%: GOSUB 400   'Get Cp.
712 OLDPRES=PRESSURE(NSECTIONS%): OLDVEL=VELOCITY(NSECTIONS%)
    'Save old state for next iteration.
715 IF SYSTIME<TCUT THEN TAU=TAU0*(1-SYSTIME/TCUT)^TAUEXP ELSE
    TAU=0   'Calculate flow coefficient.
720 PRESSURE(NSECTIONS%)=(((RHO^2*SOUND^2*TAU^2+4*CP)^.5-
    RHO*SOUND*TAU)/2)^2   'Match pressure.
730 VELOCITY(NSECTIONS%)=(CP-PRESSURE(NSECTIONS%))/(RHO*SOUND)
    'Calculate velocity.
740 RETURN
```

Valve Clossure with Compliance. This boundary condition routine allows the valve inflow and outflow to differ (using the compliance relations developed previously), integrates the resulting pressure rate of change (at averaged conditions), and matches the resulting conditions.

```
700 REM Terminal B.C.
710 IDO%=NSECTIONS%: GOSUB 400   'Get Cp.
711 CPMID=(OLDCP+CP)/2   'Calculate average Cp.
```

```
712 OLDPRES=PRESSURE(NSECTIONS%): MIDPRES=OLDPRES:
    OLDVEL=VELOCITY(NSECTIONS%)   'Guess at end conditions.
715 IF SYSTIME<TCUT THEN TAU=TAU0*(1-SYSTIME/TCUT)^TAUEXP ELSE
    TAU=0   'Calculate flow coefficient.
720 PRESSURE(NSECTIONS%)=OLDPRES+DELTAT*(MIDPRES^2*AREA*((CPMID
    -MIDPRES)/ (RHO*SOUND)-TAU*(MIDPRES)^.5)/(PNOT*MUNOT))
    'Integrate pressure rate of change.
721 IF ABS((PRESSURE(NSECTIONS%)+OLDPRES)/2-MIDPRES)>TOL1 THEN
    MIDPRES=(PRESSURE(NSECTIONS%)+OLDPRES)/2: GOTO 720   'Check
    accuracy of guess, repeat if insufficient.
730 VELOCITY(NSECTIONS%)=TAU*(PRESSURE(NSECTIONS%))^.5  'Match
    velocity.
740 RETURN
```

Application to a Typical Liquid Rocket

In this section the code used to model a bipropellant liquid rocket (see previous sections) will be presented and analyzed. The purpose of this section is to facilitate the application of the methods and software developed in this paper to other systems. The reader will note the great similarity between the routines for this complex system and those for the simple pipe. The essential difference is that most simple variables from the last program are arrays in this case. A detailed list of all program variables, both those used for the reading of data and those internal to the routine, will be presented at the end of this section.

Dynamic Response Routine. The complete liquid rocket model consists of two routines: a dynamic routine employing finite difference methods, and a steady-state routine to initialize the finite difference model. The dynamic routine simply reads the initial values and other parameters from the text (ASCII) file "Steady Results". The program text follows:

```
10 REM BASIC PROGRAM POGO.
15 COMMON NDAT%, DATFILE$(), NDAT2%, DATFILE2$(), PFILE$,
    REMOTE%   'Allows remote calling from another routine (to
    gather many steady state data points automatically).
```

```
20 GOSUB 345   'DEFINE VARIABLES AND READ STEADY STATE RESULTS.
25 GOSUB 170   'Get user input.
30 GOSUB 1430   'Initialize all functions.
35 REM BEGIN ROUTINE.
40 IF INT(SYSTIME/DELTATOUT)>INT((SYSTIME-DELTAT)/DELTATOUT)
   THEN GOSUB 1300   'Print output file.
45 SYSTIME=SYSTIME+DELTAT: IF SYSTIME>TEND THEN 1375   'If
   completed then quit.
50 GOSUB 945   'Establish chamber properties.
55 GOSUB 1200   'Establish structural response.
60 FOR IDO%=FUEL% TO OXIDIZER%
65 ON (IDO%+1) GOSUB 650,650   'Boundary Conditions Zero
   (ullage conditions).
70 FOR DELM%=1 TO NELMS%(IDO%)
75 ELEMENT%=DELM%
80 GOSUB 630   'Get PSI and THETA (dependant on local sonic
   velocity).
85 GOSUB 120   'Step through sections (finite difference
   routine).
90 IF ELEMENT%=NELMS%(IDO%) THEN 100   'If completed, goto
   terminal B.C.
95 IF IDO%=FUEL% THEN ON ELEMENT% GOSUB 685,740,810,740 ELSE ON
   ELEMENT% GOSUB 685,740,810,740   'These are the boundary
   condition subroutines.100 NEXT DELM%   'Get next element.
105 NEXT IDO%   'Goto next subsystem (fuel or oxidizer) or
   terminate finite difference portion.
110 GOSUB 1030   'Chamber Boundary Conditions (apply terminal
   boundary condition).
115 GOTO 35   'Repeat for next time step.

120 REM Finite difference routine.
125 FOR ID1%=NSECTIONS%(IDO%,ELEMENT%)+1 TO
   NSECTIONS%(IDO%,ELEMENT%+1)-2   'Increment through all
   internal sections of the present element.
130 INTPRES=PRESSURE(ID1%): INTVEL=VELOCITY(ID1%)   'Save
   intermediate pressure and velocity for next section.
135 GOSUB 580   'Get CP.
140 GOSUB 605   'Get CM.
145 PRESSURE(ID1%)=(CP+CM)/2
```

```
150 VELOCITY(ID1%)=(PRESSURE(ID1%)-CM)/(SOUND(IDO%,ELEMENT%)
    *RHO(IDO%))
155 OLDPRES(IDO%)=INTPRES: OLDVEL(IDO%)=INTVEL    'Pass values.
160 NEXT ID1%    'Goto next section.
165 RETURN

170 REM Get user's input.
175 IF REMOTE% THEN OPEN "INSTRUCTIONS" FOR INPUT AS #99  'Check
    for remote operation.
180 IF REMOTE% THEN INPUT #99, FREQ, TSTART, TEND, DELTATOUT,
    NDAT%: GOTO 230    'Read remote operating instructions and
    branch.
185 CLS: CALL TEXTFONT(0): CALL TEXTSIZE(18)    'Just formatting
    stuff.
190 PRINT: PRINT TAB(11);"POGO ANALYSIS ROUTINE"
195 CALL TEXTSIZE(12): PRINT: PRINT TAB(5);"Drive Frequency: ";:
    INPUT; "",FREQ
200 PRINT: PRINT TAB(5);"Start Time: ";: INPUT; "",TSTART: PRINT
    "   End Time: ";: INPUT "", TEND
205 PRINT: PRINT TAB(5);"Output Time Increment: [ >";DELTAT;"]
    ";: INPUT "", DELTATOUT
210 IF DELTATOUT<DELTAT THEN 205    'Branch if choice of time
    increment is unacceptable.
215 PRINT: PRINT TAB(5);"This will
    generate";INT((TEND-SYSTIME)/DELTATOUT)+1;"data points.  OK
    ?  (Y/N)": RES$=INPUT$(1)    'Allow user to confirm before
    it's too late.
220 IF RES$<>"Y" AND RES$<>"y" THEN 170    'If error, try again.
225 PRINT: PRINT TAB(5);"Number of data series to generate
    (excluding TIME & ACCEL): ";: INPUT "",NDAT%
230 DIM DATP%(NDAT%): DIM DATFILE$(NDAT%): NDAT2%=1: DIM
    DATFILE2$(5)
250 OPEN "O", #1,"Times",32    'Open and initialize ouput files.
255 OPEN "O", #2,"Accels",32    'Initialize structural ouput
    files.
260 OPEN "O", #3,"Fuel Tank Disp.",10: CLOSE #3
265 OPEN "O", #3, "Fuel Pump Disp.",10: CLOSE #3
270 OPEN "O", #3, "Ox. Tank Disp.",10: CLOSE #3
275 OPEN "O", #3, "Ox. Pump Disp.",10: CLOSE #3
280 FOR IDO%=1 TO NDAT%    '
```

```
285 IF REMOTE% THEN INPUT #99, SIDE%, ELEMENT%, SEC%: GOTO 300
    'Get remote particulars.
287 REM Get information on each ouput file to be generated.
290 PRINT: PRINT TAB(5);"SIDE: (F/O) ";: RES$=INPUT$(1): IF
    RES$="F" OR RES$="f" THEN SIDE%=FUEL% ELSE SIDE%=OXIDIZER%
295 PRINT RES$;"   ELEMENT: ";: INPUT;"",ELEMENT%: PRINT "
    SECTION: ";: INPUT; "",SEC%
300 DATP%(IDO%)=NSECTIONS%(SIDE%,ELEMENT%)+SEC%
305 IF REMOTE% THEN INPUT #99, DATFILE$(IDO%): GOTO 315
310 PRINT "   FILE: ";: INPUT "",DATFILE$(IDO%)
315 OPEN "O",#2*IDO%+1,DATFILE$(IDO%)+".PRES": CLOSE #2*IDO%+1
    'Initialize ouput files.
320 OPEN "O",#2*IDO%+2,DATFILE$(IDO%)+".VEL": CLOSE #2*IDO%+2
325 NEXT IDO%
330 CLS   'Clear the screen.
335 IF REMOTE% THEN CLOSE #99
340 RETURN

345 REM STEADY STATE RESULTS (input the steady state conditions
    as detailed in the file "Steady Results".
347 REM Dimension arrays.
350 DIM OLDCM1(1): DIM OLDCP1(1): DIM OLDVEL(1): DIM OLDPRES(1):
    DIM OLDVEL1(1): DIM RHO(1): DIM ULLAGE(1): DIM NPUMP%(1):
    DIM AREAINJECT(1): DIM TAUU1(1): DIM TAUU2(1): DIM
    TAUINJECT(1): DIM PNOT1(1): DIM NUNOT1(1): DIM TDENDO(1):
    DIM TUENDO(1)
355 DIM BZERO(1): DIM BONE(1): DIM BTWO(1): DIM BTHREE(1): DIM
    DELTAPO(1): DIM UELPO(1)  DIM PRESPO(1): DIM TOLO(3): DIM
    MASSP(1): DIM MASST(1): DIM NELMS%(1): DIM TANKSPR(1): DIM
    TANKDAMP(1): DIM PUMPSPR(1): DIM PUMPDAMP(1): DIM TOL4(1)
360 DIM PDENDO(1): DIM PUENDO(1): DIM TOL4(1): DIM TOL5(1): DIM
    TOL6(1): DIM TOL7(1): DIM NUNOTO(1): DIM PNOTO(1): DIM
    TOL3(1): DIM OLDCP2(1): DIM MAXCPRES(1): DIM MAXPPRES(1):
    DIM MINCPRES(1): DIM MINPPRES(1)
362 REM Read data on run.
365 READ TRUE%, FALSE%, THETAG, RGAS, TOL2, TAUC, MININC
370 FOR IDO%=0 TO 1
375 READ PNOT1(IDO%), NUNOT1(IDO%), TOL3(IDO%), PNOTO(IDO%),
    NUNOTO(IDO%), TOL4(IDO%)
380 NEXT IDO%
```

```
382 REM Read steady conditions from the results file.
385 OPEN "I", #1, "Steady Results"
387 REM Read various parameters.
390 INPUT #1, FUEL%, OXIDIZER%, DELTAT, NELMS%(FUEL%),
    NELMS%(OXIDIZER%), CSTAR0, CSTARSLOPE, MIXTURE0, CTHRUST,
    LSTAR, CHAMVOL, GEE, MASSSTR, SYSTEMTHRUST
395 IF NELMS%(FUEL%)>=NELMS%(OXIDIZER%) THEN
    MNELM%=NELMS%(FUEL%) ELSE MNELM%=NELMS%(OXIDIZER%)   'Find
    most complex system.
400 DIM LENGTH(1,MNELM%): DIM ALPHA(1,MNELM%): DIM NSECTIONS%(1,
    MNELM%+1): DIM DISPLACE(1, MNELM%): DIM SVELOCITY(1,MNELM%)
405 QSIZE%=INT(TAUC/DELTAT)+3   'Calculate the size of the
    velocity queue (allows for the combustor dead time).
410 DIM ACCEL(1,MNELM%): DIM VELQUEUE(1, QSIZE%): DIM
    SOUND(1,MNELM%): DIM DIAM(1, MNELM%): DIM AREA(1, MNELM%):
    DIM FRICT(1,MNELM%)
415 ID3%=0
417 REM Read more parameters.
420 FOR ID0%=FUEL% TO OXIDIZER%
425 INPUT #1, RHO(ID0%), ULLAGE(ID0%), NPUMP%(ID0%),
    AREAINJECT(ID0%), TAUV1(ID0%), TAUV2(ID0%), TAUINJECT(ID0%),
    BZERO(ID0%), BONE(ID0%), BTWO(ID0%), BTHREE(ID0%),
    DELTAPO(ID0%), VELPO(ID0%), PRESPO(ID0%)
430 INPUT #1, TANKSPR(ID0%), TANKDAMP(ID0%), MASST(ID0%),
    PUMPSPR(ID0%), PUMPDAMP(ID0%), MASSP(ID0%), ACCEL(ID0%,0)
435 FOR ID1%=1 TO NELMS%(ID0%)
440 INPUT #1, AREA(ID0%,ID1%), DIAM(ID0%,ID1%),
    LENGTH(ID0%,ID1%), ALPHA(ID0%,ID1%), DISPLACE(ID0%,ID1%),
    SVELOCITY(ID0%,ID1%), ACCEL(ID0%,ID1%), SOUND(ID0%,ID1%),
    ID2%, FRICT(ID0%,ID1%)
445 NSECTIONS%(ID0%,ID1%)=ID3%   'Count up the total number of
    sections (for all elements, i.e. calculate total storage
    requirements).
450 ID3%=ID3%+ID2%+1
455 NEXT ID1%
460 NSECTIONS%(ID0%,ID1%)=ID3%: ID3%=ID3%+1
465 NEXT ID0%
470 DIM PRESSURE(ID3%-1): DIM VELOCITY(ID3%-1)
475 FOR ID0%=0 TO ID3%-1
480 INPUT #1, PRESSURE(ID0%), VELOCITY(ID0%)   'Input steady
```

```
    state values.
 85 NEXT IDO%
 90 CLOSE #1
 92 REM Initialize velocity queue.
 95 FOR IDO%=FUEL% TO OXIDIZER%
 00 FOR ID1%=0 TO INT(TAUC/DELTAT)+3
 05 VELQUEUE(IDO%,ID1%)=
    VELOCITY(NSECTIONS%(IDO%,NELMS%(IDO%)+1))
 10 NEXT ID1%
 15 NEXT IDO%
 17 REM Initialize various variables needed in program.
 20 FOR IDO%=FUEL% TO OXIDIZER%
 25 ELEMENT%=NPUMP%(IDO%)-1: ID1%=NSECTIONS%(IDO%,ELEMENT%+1)-1
 30 GOSUB 630: OLDVEL(IDO%)=VELOCITY(ID1%-1):
    OLDPRES(IDO%)=PRESSURE(ID1%-1): GOSUB 580   'Get CP.
 35 OLDCP1(IDO%)=CP: ELEMENT%=ELEMENT%+1: ID1%=ID1%+1: GOSUB
    630: GOSUB 605   'Get CM.
 40 OLDCM1(IDO%)=CM
 45 ELEMENT%=NELMS%(IDO%): ID1%=NSECTIONS%(IDO%,ELEMENT%+1)-1
 50 GOSUB 630: OLDVEL(IDO%)=VELOCITY(ID1%-1):
    OLDPRES(IDO%)=PRESSURE(ID1%-1): GOSUB 580   'Get Cp.
 55 OLDCP2(IDO%)=CP
 70 NEXT IDO%
 75 RETURN

 80 REM Find CP based on local conditions.
 85 VELR=(VELOCITY(ID1%)-PSI*(VELOCITY(ID1%)-OLDVEL(IDO%)))/
    (1+THETA*(VELOCITY(ID1%)-OLDVEL(IDO%)))   'Caculate Ur.
 90 PRESR=PRESSURE(ID1%)-(VELR*THETA+PSI)*(PRESSURE(ID1%)-
    OLDPRES(IDO%))   'Calculate Pr.
 95 CP=PRESR+RHO(IDO%)*VELR*(SOUND(IDO%,ELEMENT%)+
    (ACCEL(IDO%,ELEMENT%)+ACCEL(IDO%,0))*DELTAT*
    SIN(ALPHA(IDO%,ELEMENT%))*SOUND(IDO%,ELEMENT%)/VELR-
    SOUND(IDO%,ELEMENT%) *FRICT(IDO%,ELEMENT%)*DELTAT*ABS(VELR)/
    (2*DIAM(IDO%,ELEMENT%))).   'Calculate Cp.
00 RETURN
```

AD-A153 121 A CLOSED LOOP ANALYSIS OF POGO INSTABILITY(U) AIR FORCE 2/2
INST OF TECH WRIGHT-PATTERSON AFB OH SCHOOL OF
ENGINEERING D A ROSENBERG DEC 84 AFIT/GA/AA/84D-9

UNCLASSIFIED F/G 21/9.1 NL

END

FILMED

DTIC

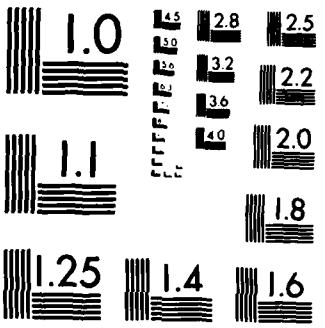

```
605 REM Get CM.
610 VELS=(VELOCITY(ID1%)-PSI*(VELOCITY(ID1%)-
    VELOCITY(ID1%+1)))/(1-THETA*(VELOCITY(ID1%)-
    VELOCITY(ID1%+1)))   'Calculate Us.
615 PRESS=PRESSURE(ID1%)+(VELS*THETA-PSI)*
    (PRESSURE(ID1%)-PRESSURE(ID1%+1))   'Calculate Ps.
620 CM=PRESS-RHO(IDO%)*VELS*(SOUND(IDO%,ELEMENT%)
    +(ACCEL(IDO%,ELEMENT%)+ACCEL(IDO%,0))*DELTAT*
    SIN(ALPHA(IDO%,ELEMENT%))*SOUND(IDO%,ELEMENT%)/VELS-
    SOUND(IDO%,ELEMENT%)*FRICT(IDO%,ELEMENT%) *DELTAT*ABS(VELS)/
    (2*DIAM(IDO%,ELEMENT%)))   'Calculate Cm.
625 RETURN

630 REM Get PSI and THETA.
635 THETA=DELTAT/(LENGTH(IDO%,ELEMENT%)
    /(NSECTIONS%(IDO%,ELEMENT%+1)-1- NSECTIONS%(IDO%,ELEMENT%)))
640 PSI=SOUND(IDO%,ELEMENT%)*THETA
645 RETURN
```

Boundary Conditions. This section of code deserves special attention as it applies the boundary conditions to the interfaces between system elements. In practice, each boundary condition must be evaluated and the resulting equations (some will be differential equations) must be solved before code can be written. A group of "typical" boundary conditions is given here, although it is recognized that many more will be developed by future users in order to solve more complex conditions.

```
650 REM Boundary Conditons Fuel and Oxidizer Zero (ullage
    pressures).
655 ELEMENT%=1: GOSUB 630   'Get Psi, Theta.
660 ID1%=NSECTIONS%(IDO%,1): GOSUB 605   'Get Cm.
665 OLDPRES(IDO%)=PRESSURE(ID1%): OLDVEL(IDO%)=VELOCITY(ID1%)
670 PRESSURE(ID1%)=ULLAGE(IDO%)   'Match pressure.
675 VELOCITY(ID1%)=(PRESSURE(ID1%)-CM)/(SOUND(IDO%,ELEMENT%)*
    RHO(IDO%))   'Calculate velocity.
680 RETURN

685 REM Boundary Conditions Fuel and Oxidizer 1 (area change
```

```
    with relative motion).
690 GOSUB 580   'Get Cp.
695 ID1%=ID1%+1: ELEMENT%=ELEMENT%+1: GOSUB 630: GOSUB 605
    'Get Cm.
700 OLDPRES(ID0%)=PRESSURE(ID1%): OLDVEL(ID0%)=VELOCITY(ID1%)
705 BETA=AREA(ID0%,ELEMENT%)/AREA(ID0%,ELEMENT%-1)   'Area
    ratio.
707 REM Compute quadratic coefficients.
710 A=1-BETA^2
715 B=2*(SOUND(ID0%,ELEMENT%)+BETA*SOUND(ID0%,ELEMENT%-1)+
    BETA*SVELOCITY(ID0%,1)*(SIN(ALPHA(ID0%,ELEMENT%-1))-
    BETA*SIN(ALPHA(ID0%,ELEMENT%))))
720 C=2*(CM-CP)/RHO(ID0%)-SVELOCITY(ID0%,1)^2*(SIN(ALPHA(ID0%,
    ELEMENT%-1))-BETA*SIN(ALPHA(ID0%,ELEMENT%)))^2-2*SOUND(ID0%,
    ELEMENT%-1)*SVELOCITY(ID0%,1)*(SIN(ALPHA(ID0%,ELEMENT%-1))-
    BETA*SIN(ALPHA(ID0%,ELEMENT%)))
725 VELOCITY(ID1%)=(-B+(B^2-4*A*C)^.5)/(2*A):
    PRESSURE(ID1%)=CM+RHO(ID0%)*SOUND(ID0%,ELEMENT%)*VELOCITY(ID
    1%)   'Calculate downstream velocity and pressure.
730 VELOCITY(ID1%-1)=BETA*VELOCITY(ID1%)-SVELOCITY(ID0%,1)*
    (SIN(ALPHA(ID0%,ELEMENT%-1))-BETA*SIN(ALPHA(ID0%,ELEMENT%)))
    :
    PRESSURE(ID1%-1)=CP-RHO(ID0%)*SOUND(ID0%,ELEMENT%-1)*VELOCIT
    Y(ID1%-1)   'Calculate upstream velocity and pressure.
735 RETURN

740 REM Boundary Conditions Fuel and Oxidizer 2, 5 (valve).
745 GOSUB 580   'Get Cp.
750 ID1%=ID1%+1: ELEMENT%=ELEMENT%+1: GOSUB 630: GOSUB 605
    'Get Cm.
755 OLDVEL(ID0%)=VELOCITY(ID1%): OLDPRES(ID0%)=PRESSURE(ID1%)
760 IF ELEMENT%=3 THEN TAU=TAUV1(ID0%) ELSE TAU=TAUV2(ID0%)
765 BETA=AREA(ID0%,ELEMENT%)/AREA(ID0%,ELEMENT%-1)   'Area
    ratio.
767 REM Calculate quadratic coefficients.
770 A=1/(TAU)^2
775 B=RHO(ID0%)*(SOUND(ID0%,ELEMENT%-1)*BETA+
    SOUND(ID0%,ELEMENT%))
780 C=CM-CP
785 VELOCITY(ID1%)=(-B+(B^2-4*A*C)^.5)/(2*A)   'Compute
```

```
    velocities.
790 VELOCITY(ID1%-1)=BETA*VELOCITY(ID1%)
795 PRESSURE(ID1%-1)=CP-RHO(IDO%)*SOUND(IDO%,ELEMENT%-1)*
    VELOCITY(ID1%-1)    'Compute pressures.
800 PRESSURE(ID1%)=CM+RHO(IDO%)*SOUND(IDO%,ELEMENT%)*
    VELOCITY(ID1%)
805 RETURN

810 REM Boundary Conditions Fuel and Oxidizer 3 (Pump with
    relative motion and lumped compliance (isothermal bubble
    expansion)).
815 GOSUB 580    'Get Cp.
820 ID1%=ID1%+1: ELEMENT%=ELEMENT%+1: GOSUB 630: GOSUB 605
    'Get Cm.
825 OLDPRES(IDO%)=PRESSURE(ID1%): OLDVEL(IDO%)=VELOCITY(ID1%)
830 BETA=AREA(IDO%,ELEMENT%)/AREA(IDO%,ELEMENT%-1)
835 DELTAP=DELTAPO(IDO%)-BZERO(IDO%)*
    (VELOCITY(NSECTIONS%(IDO%,NPUMP%(IDO%)))-VELPO(IDO%))^2-
    (BONE(IDO%)-(PRESSURE(NSECTIONS%(IDO%,NPUMP%(IDO%))-1)-
    PRESPO(IDO%))/(BTWO(IDO%)+ BTHREE(IDO%)*
    (PRESSURE(NSECTIONS%(IDO%,NPUMP%(IDO%))-1)-PRESPO(IDO%))))
    'Compute pump pressure rise.
840 IF PNOTO(IDO%)*NUNOTO(IDO%)>1 THEN 870    'Branch for non
    zero compliance.
845 VELOCITY(ID1%)=(DELTAP+CP-CM+RHO(IDO%)*
    SOUND(IDO%,ELEMENT%-1)*SVELOCITY(IDO%,NPUMP%(IDO%))*
    (SIN(ALPHA(IDO%,ELEMENT%-1))-BETA*SIN(ALHA(IDO%,ELEMENT%))))
    /(RHO(IDO%)*(SOUND(IDO%,ELEMENT%)+SOUND(IDO%,ELEMENT%-1)*
    BETA))    'Compute zero compliance downstream velocity.
850 PRESSURE(ID1%)=CM+RHO(IDO%)*SOUND(IDO%,ELEMENT%)*
    VELOCITY(ID1%)    'Compute zero compliance downstream
    velocity.
855 VELOCITY(ID1%-1)=VELOCITY(ID1%)*BETA-
    SVELOCITY(IDO%,NPUMP%(IDO%))*(SIN(ALPHA(IDO%,ELEMENT%-1))-
    BETA*SIN(ALPHA(IDO%,ELEMENT%)))    'Compute zero compliance
    upstream velocity.
860 PRESSURE(ID1%-1)=CP-RHO(IDO%)*SOUND(IDO%,ELEMENT%-1)*
    VELOCITY(ID1%-1)    'Compute zero compliance upstream
    pressure.
865 GOTO 925    'Branch.
```

```
870 CPMID=(OLDCP1(IDO%)+CP)/2: CMMID=(OLDCM1(IDO%)+CM)/2
    'Compute averaged conditions.
875 ENDPRES=PRESSURE(ID1%-1)   'First guess.
880 ENDPRES1= ENDPRES: GOSUB 1460   'Calculate NendPres2.
885 NENDPRES1=NENDPRES2: ENDPRES=ENDPRES*1.00001:
    ENDPRES2=ENDPRES: GOSUB 1460   'Calculate Nendpres2 for
    second guess.
890 A=(NENDPRES1-NENDPRES2)/(ENDPRES1-ENDPRES2):
    B=NENDPRES1-A*ENDPRES1   'Compute linear regression
    coefficients.
895 ENDPRES=B/(1-A): ENDPRES1=ENDPRES2: NENDPRES1=NENDPRES2:
    GOSUB 1460   'Linearly interpolate next guess and try it.
900 IF ABS(NENDPRES2-ENDPRES)> TOL4(IDO%) THEN ENDPRES2=ENDPRES:
    GOTO 890   'Iterate untill sufficient accuracy is achieved.
915 PRESSURE(ID1%-1)=ENDPRES: VELOCITY(ID1%-1)=INVEL   'Compute
    upstream pressure and velocity.
920 PRESSURE(ID1%)=ENDPRES+DELTAP: VELOCITY(ID1%)=OUTVEL
    'Compute downstream pressure and velocity.
925 OLDCM1(IDO%)=CM: OLDCP1(IDO%)=CP   'Save old values for next
    time.
940 RETURN

945 REM Old Chamber Velocities (Chamber dynamics).
950 OLDTHRUST=SYSTEMTHRUST   'Save old thrust.
955 FOR IDO%=FUEL% TO OXIDIZER%
960 BACKTIME=TAUC: GOSUB 1155   'Get delayed injection
    velocities from queue.
965 OLDVEL1(IDO%)=OLDVEL: BACKTIME=TAUC+DELTAT: GOSUB 1155
    'Get older delayed velocity from queue.
970 OLDVEL1(IDO%)=(OLDVEL+OLDVEL1(IDO%))/2   'Compute averaged
    velocities.
975 NEXT IDO%
980 CSTAR=CSTAR0+CSTARSLOPE*(RHO(OXIDIZER%)*
    AREAINJECT(OXIDIZER%)*OLDVEL1(OXIDIZER%)/(RHO(FUEL%)*
    AREAINJECT(FUEL%)*OLDVEL1(FUEL%))- MIXTURE0)   'Compute
    median chamber exit velocity.
985 TCHAM=LSTAR*CSTAR/(THETAG*RGAS)   'Compute median chamber
    temperature.
```

```
990 SYSTEMTHRUST=(RHO(OXIDIZER%)*AREAINJECT(OXIDIZER%)*
    OLDVEL1(OXIDIZER%)+RHO(FUEL%)*AREAINJECT(FUEL%)*
    OLDVEL1(FUEL%))*CSTAR*CTHRUST   'Compute median thrust.
995 ID1%=NSECTIONS%(FUEL%,NELMS%(FUEL%)+1):
    ID2%=NSECTIONS%(OXIDIZER%,NELMS%(OXIDIZER%)+1)   'Exit plane
    indicies.
1000 MIDPRES=PRESSURE(ID1%)   'Guess median pressure.
1005 ENDPRES=PRESSURE(ID1%)+DELTAT*(RGAS*TCHAM*(RHO(FUEL%)*
    AREAINJECT(FUEL%)*OLDVEL1(FUEL%)+RHO(OXIDIZER%)*
    AREAINJECT(OXIDIZER%)*OLDVEL1(OXIDIZER%))/CHAMVOL-
    (RGAS*TCHAM*MIDPRES/(LSTAR*CSTAR)))   'Integrate
    endpressure.
1010 IF ABS(MIDPRES-(ENDPRES+PRESSURE(ID1%))/2)>TOL2 THEN
    MIDPRES=(ENDPRES+PRESSURE(ID1%))/2: GOTO 1005   'Iterate
    untill sufficient accuracy is obtained.
1015 OLDCPRES(FUEL%)=PRESSURE(ID1%):
    OLDCPRES(OXIDIZER%)=PRESSURE(ID2%)   'Save old values.
1020 PRESSURE(ID1%)=ENDPRES: PRESSURE(ID2%)=ENDPRES   'Save new
    chamber pressure.
1025 RETURN

1030 REM Chamber B.C's (injector with lumped compliance).
1035 FOR IDO%=FUEL% TO OXIDIZER%
1040 ELEMENT%=NELMS%(IDO%)
1045 ID1%=NSECTIONS%(IDO%,NELMS%(IDO%)+1)-1
1050 GOSUB 630: GOSUB 580   'Get Cp.
1055 IF PNOT1(IDO%)*NUNOT1(IDO%)>1 THEN 1080   'Branch for non
    zero compliance.
1057 REM Compute quadratic coefficients.
1060 A=1: B=RHO(IDO%)*TAUINJECT(IDO%)^2*SOUND(IDO%,ELEMENT%)*
    AREAINJECT(IDO%)/ AREA(IDO%,ELEMENT%):
    C=-TAUINJECT(IDO%)^2*(CP-PRESSURE(ID1%+1))
1065 VELOCITY(ID1%+1)=(-B+(B^2-4*A*C)^.5)/(2*A):
    VELOCITY(ID1%)=VELOCITY(ID1%+1)*AREAINJECT(IDO%)/
    AREA(IDO%,ELEMENT%)   'Compute zero compliance velocities.
1070 PRESSURE(ID1%)=CP-RHO(IDO%)*SOUND(IDO%,ELEMENT%)*
    VELOCITY(ID1%)   'Compute zero compliance upstream pressure.
1075 GOTO 1125   'Branch.
1080 CPMID=(CP+OLDCP2(IDO%))/2   'Compute aveage value for Cp.
```

```
1085 ENDPRES1=PRESSURE(ID1%):
     NENDPRES1=FNENDPRES(FNMIDPRES(ENDPRES1))   'First guess and
     result.
1090 ENDPRES2=ENDPRES1*1.00001:
     NENDPRES2=FNENDPRES(FNMIDPRES(ENDPRES2))   'Second guess and
     result.
1095 A=(NENDPRES1-NENDPRES2)/(ENDPRES1-ENDPRES2):
     B=NENDPRES1-A*ENDPRES1   'Compute linear regression
     coefficients.
1100 ENDPRES=B/(1-A): NENDPRES=FNENDPRES(FNMIDPRES(ENDPRES))
     'Compute next guess and try it.
1105 IF ABS(ENDPRES-NENDPRES)>TOL3(IDO%) THEN ENDPRES1=ENDPRES2:
     NENDPRES1=NENDPRES2: ENDPRES2=ENDPRES: NENDPRES2=NENDPRES:
     GOTO 1095   'Iterate untill sufficient accuracy is obtained.
1110 PRESSURE(ID1%)=ENDPRES   'Save old value.
1115 VELOCITY(ID1%)=(CP-PRESSURE(ID1%))/(RHO(IDO%)*
     SOUND(IDO%,ELEMENT%))   'Compute upstream velocity.
1120 VELOCITY(ID1%+1)=TAUINJECT(IDO%)*(PRESSURE(ID1%)-
     PRESSURE(ID1%+1))^.5   'Calculate downstream velocity.
1125 GOSUB 1180   'Load velocity queue with new values.
1130 OLDCP2(IDO%)=CP   'Save old value.
1145 NEXT IDO%
1150 RETURN

1155 REM Velocity queue retriever.
1057 REM Find bracketing indicies.
1160 ID2%=(INT(BACKTIME/DELTAT-1) MOD QSIZE%)+1
1165 ID3%=(INT(BACKTIME/DELTAT-2) MOD QSIZE%)+1
1170 OLDVEL=VELQUEUE(IDO%,ID2%)+(BACKTIME/DELTAT-INT(BACKTIME/
     DELTAT))* (VELQUEUE(IDO%,ID3%)-VELQUEUE(IDO%,ID2%))
     'Retrieve and interpolate.
1175 RETURN

1180 REM Load velqueue.
1185 ID2%= (INT(SYSTIME/DELTAT-1) MOD QSIZE%)+1   'Compute index.
1190 VELQUEUE(IDO%,ID2%)=VELOCITY(ID1%+1)   'Load velocity queue.
1195 RETURN

1200 REM Structural response (5 degree of freedom
     spring-mass-dashpot model).
```

```
1205 NINCS%=DELTAT/MININC: NINCS%=-INT(-NINCS%): IF NINCS%<1 THEN
     NINCS%=1   'Compute number of minor increments corresponding
     to the major time step size (for greater accuracy).
1210 FOR ID1%=0 TO NINCS%
1215 REACT=0   'Sum all reactions (relative to the vehicle
     structure).
1220 FOR ID0%=FUEL% TO OXIDIZER%
1225 REACT=REACT+TANKSPR(ID0%)*DISPLACE(ID0%,1)+TANKDAMP(ID0%)*
     SVELOCITY(ID0%,1)+PUMPSPR(ID0%)*DISPLACE(ID0%,NPUMP%(ID0%))+
     PUMPDAMP(ID0%)*SVELOCITY(ID0%,NPUMP%(ID0%))   'Sum tank and
     pump reaction forces.
1230 NEXT ID0%
1235 ACCEL(0,0)=(REACT+OLDTHRUST+(SYSTEMTHRUST-OLDTHRUST)*
     (ID1%/NINCS%)+FNEXCITE(SYSTIME-DELTAT+DELTAT*(ID1%/NINCS%)))
     /MASSSTR   'Compute structure acceleration.
1240 FOR ID0%=FUEL% TO OXIDIZER%
1245 ACCEL(ID0%,1)=-(TANKSPR(ID0%)*DISPLACE(ID0%,1)+
     TANKDAMP(ID0%)*SVELOCITY(ID0%,1))/MASST(ID0%)-ACCEL(0,0)
     'Compute tank accelerations.
1250 ACCEL(ID0%,NPUMP%(ID0%))=-(PUMPSPR(ID0%)*
     DISPLACE(ID0%,NPUMP%(ID0%))+PUMPDAMP(ID0%)*
     SVELOCITY(ID0%,NPUMP%(ID0%)))/MASSP(ID0%)-ACCEL(0,0)
     'Compute pump accelerations.
1255 IF ID1%=NINCS% THEN 1280   'If last element then branch.
1260 DISPLACE(ID0%,1)=DISPLACE(ID0%,1)+SVELOCITY(ID0%,1)*DELTAT/
     NINCS%+ACCEL(ID0%,1)*(DELTAT/NINCS%)^2/2   'Calculate
     displacement.
1265 SVELOCITY(ID0%,1)=SVELOCITY(ID0%,1)+ACCEL(ID0%,1)*DELTAT/
     NINCS%   'Calculate velocity.
1270 DISPLACE(ID0%,NPUMP%(ID0%))=DISPLACE(ID0%,NPUMP%(ID0%))+
     SVELOCITY(ID0%,NPUMP%(ID0%))*DELTAT/NINCS%+
     ACCEL(ID0%,NPUMP%(ID0%))* (DELTAT/NINCS%)^2/2   'Calculate
     displacement.
1275 SVELOCITY(ID0%,NPUMP%(ID0%))=SVELOCITY(ID0%,NPUMP%(ID0%))+
     ACCEL(ID0%,NPUMP%(ID0%))*DELTAT/NINCS%   'Calculate
     velocity.
1280 NEXT ID0%
1285 NEXT ID1%
1290 ACCEL(1,0)=ACCEL(0,0)   'Avoid a possible confusion.
1295 RETURN
```

```
1300 REM Output results.
1305 PRINT #1, SYSTIME;: PRINT USING "+#.###^^^^_
     ";SYSTIME;ACCEL(0,0);
1310 PRINT #2, ACCEL(0,0);
1315 OPEN "A", #3, "Fuel Tank Disp.",10: PRINT #3,
     DISPLACE(FUEL%,1);: CLOSE #3
1320 OPEN "A", #3, "Ox. Tank Disp.",10: PRINT #3,
     DISPLACE(OXIDIZER%,1);: CLOSE #3
1325 OPEN "A", #3, "Fuel Pump Disp.",10: PRINT #3,
     DISPLACE(FUEL%,NPUMP%(FUEL%));: CLOSE #3
1330 OPEN "A", #3, "Ox. Pump Disp.",10: PRINT #3,
     DISPLACE(OXIDIZER%,NPUMP%(OXIDIZER%));: CLOSE #3
1335 FOR IDO%=1 TO NDAT%
1340 OPEN "A", #IDO%*2+1, DATFILE$(IDO%)+".PRES", 10: OPEN "A",
     #IDO%*2+2, DATFILE$(IDO%)+".VEL", 10
1345 PRINT #2*IDO%+1, PRESSURE(DATP%(IDO%));: PRINT USING
     "+#.###^^^^_    ";PRESSURE(DATP%(IDO%));
1350 PRINT #2*IDO%+2, VELOCITY(DATP%(IDO%));: PRINT USING
     "+#.###^^^^_    ";VELOCITY(DATP%(IDO%));
1355 CLOSE #IDO%*2+1: CLOSE #IDO%*2+2
1360 NEXT IDO%
1365 PRINT
1370 RETURN

1375 REM End of routine. Chain to plot routine.
1380 CLOSE #1: CLOSE #2
1400 BEEP: BEEP: BEEP   'Wake user.
1405 END
1410 REM Pogo Data
1415 DATA -1, 0, 0.0015, 5.8867E+3, 1, 0.004, 0.0001
1420 DATA 58.333E+6, 0, 0.1, 180.237E+3, 0, 0.01
1422 REM "Soft" DATA 58.333E+6, 50E-6, 0.1, 180.237E+3,
     283.13E-6, 0.01
1425 DATA 58.333E+6, 0, 0.1, 326.93E+3, 0, 0.01
1427 REM "Soft" DATA 58.333E+6, 50E-6. 0.1, 326.93E+3, 283.13E-6,
     0.01

1430 REM Function Initialization.
1435 DEF FNEXCITE(ATIME)=50000!*SIN(ATIME*FREQ*2*3.1416)
     'Excitation.
```

```
1440 REM 50000!*SIN(ATIME*50*2*3.1416)
1445 DEF FNENDPRES(MIDPRES)=PRESSURE(ID1%)+DELTAT*MIDPRES^2/
     (PNOT1(IDO%)*NUNOT1(IDO%))*((CPMID-MIDPRES)/(RHO(IDO%)*SOUND
     (IDO%,ELEMENT%))*AREA(IDO%,NELMS%(IDO%))-TAUINJECT(IDO%)*
     (MIDPRES-(PRESSURE(ID1%+1)+OLDCPRES(IDO%))/2)^.5*
     AREAINJECT(IDO%))   'Used for injector b.c.
1450 DEF FNMIDPRES(ENDPRES)=(ENDPRES+PRESSURE(ID1%))/2   'Used
     for injector b.c.
1455 RETURN

1460 REM NewPres routine.
1465 MIDPRES=(PRESSURE(ID1%-1)+ENDPRES)/2   'Average pressure.
1470 INVEL=(CPMID-MIDPRES)/(RHO(IDO%)*SOUND(IDO%,ELEMENT%-1))
     'Inflow rate.
1475 OUTVEL=(MIDPRES+DELTAP-CMMID)/(RHO(IDO%)*
     SOUND(IDO%,ELEMENT%))   'Outflow rate.
1480 STORATE=AREA(IDO%,ELEMENT%-1)*(INVEL-BETA*OUTVEL+
     SVELOCITY(IDO%,NPUMP%(IDO%))*(SIN(ALPHA(IDO%,ELEMENT%-1))-
     BETA*SIN(ALPHA(IDO%, ELEMENT%))))   'Storage rate corrected
     for relative velocity.
1485 NENDPRES2=PRESSURE(ID1%-1)+DELTAT*MIDPRES^2/(PNOTO(IDO%)*
     NUNOTO(IDO%))*STORATE
1490 RETURN
```

Steady State Routine. The dynamic response routine requires that initial operating conditions and other parameters be available in the text file "Steady Results". The following program reads in this data, computes initial conditions, and writes this file.

```
10 REM Steady State Initialization Program.
20 GOSUB 830   'Read data and initialize variables.
30 GOSUB 690   'Input user data, etc.
40 GOSUB 400   'Initialize functions.
60 GOSUB 1170   'Get New MDOT's.
70 FOR IDO%=FUEL% TO OXIDIZER%: INTMDOT(IDO%)=MDOT(IDO%):
   INTNMDOT(IDO%)=NMDOT(IDO%): MDOT(IDO%)=1.01*MDOT(IDO%): NEXT
   IDO%   'Save old values.
80 REM Begin loop.
90 GOSUB 1170   'Get New MDOT's.
100 IF ABS(NMDOT(FUEL%)-MDOT(FUEL%))<TOLO(FUEL%) AND
   ABS(NMDOT(OXIDIZER%)-MDOT(OXIDIZER%))<TOLO(OXIDIZER%) THEN
   180   'Branch is sufficient accuracy has been obtained.
105 REM Compute next guess.
110 FOR IDO%=FUEL% TO OXIDIZER%
115 REM Determine Linear Regression Coefficients.
120 A=(INTNMDOT(IDO%)-NMDOT(IDO%))/(INTMDOT(IDO%)-MDOT(IDO%))
130 B=INTNMDOT(IDO%)-A*(INTMDOT(IDO%))
140 INTNMDOT(IDO%)=NMDOT(IDO%): INTMDOT(IDO%)=MDOT(IDO%)   'Save
   old guess.
150 MDOT(IDO%)=B/(1-A)   'Linearly interpolate new guess.
160 NEXT IDO%
170 GOTO 80   'Repeat.
180 GOSUB 590   'Fill data registers.
190 OPEN "Steady Results" FOR OUTPUT AS #1   'Open output file.
195 REM Write parameters to output file.
200 PRINT #1, FUEL%; OXIDIZER%; DELTAT; NELMS%(FUEL%);
   NELMS%(OXIDIZER%); CSTAR0; CSTARSLOPE; MIXTURE0; CTHRUST;
   LSTAR; CHAMVOL; GEE; STRMASS; SYSTEMTHRUST;
210 FOR IDO%=FUEL% TO OXIDIZER%
220 PRINT #1, AH0(IDO%); ULLAGE(IDO%); NPUMP%(IDO%);
   AREAINJECT(IDO%); TAUV1(IDO%); TAUV2(IDO%); TAUINJECT(IDO%);
230 PRINT #1, BZERO(IDO%); BONE(IDO%); BTWO(IDO%); BTHREE(IDO%);
   DELTAPO(IDO%); VELPO(IDO%); PRESPO(IDO%); TANKSPR(IDO%);
```

```
    TANKDAMP(ID0%); TANKMASS(ID0%); PUMPSPR(ID0%);
    PUMPDAMP(ID0%); PUMPMASS(ID0%); ACCEL(ID0%,0)
240 FOR ID1%=1 TO NELMS%(ID0%)
250 IF ID1%=1 THEN
    DISPLACE(ID0%,ID1%)=-ACCEL(ID0%,0)*TANKMASS(ID0%)/TANKSPR(ID
    0%)   'Compute tank displacements.
260 IF ID1%=4 THEN
    DISPLACE(ID0%,ID1%)=-ACCEL(ID0%,0)*PUMPMASS(ID0%)/PUMPSPR(ID
    0%)   'Compute pump displacements.
270 PRINT #1, AREA(ID0%,ID1%); DIAM(ID0%,ID1%);
    LENGTH(ID0%,ID1%); ALPHA(ID0%,ID1%); DISPLACE(ID0%,ID1%);
    SVELOCITY(ID0%,ID1%); ACCEL(ID0%,ID1%); SOUND(ID0%,ID1%);
    NSECTIONS%(ID0%,ID1%); FRICT(ID0%,ID1%);
280 NEXT ID1%
290 NEXT ID0%
300 FOR ID0%=FUEL% TO OXIDIZER%
310 FOR ID1%=1 TO NELMS%(ID0%)
320 FOR ID2%=0 TO NSECTIONS%(ID0%,ID1%)
330 PRINT #1, PRESSURE(ID0%,ID1%,ID2%);
    VELOCITY(ID0%,ID1%,ID2%);   'Write initial conditions.
340 NEXT ID2%
350 NEXT ID1%
360 PRINT #1, CPRES; MDOT(ID0%)/(AREAINJECT(ID0%)*RHO(ID0%));
    'Write initial chamber pressure and injector velocities.
370 NEXT ID0%
380 CLOSE #1
390 CHAIN "Pogo"   'Run the dynamic response routine.

400 REM  Initialize all functions.
410 DEF FNDELP(ID0%,ID1%)=RHO(ID0%)*ACCEL(0,0)*
    LENGTH(ID0%,ID1%)*SIN(ALPHA(ID0%,ID1%))-RHO(ID0%)*
    LENGTH(ID0%,ID1%)*FRICT(ID0%,ID1%)/(2*DIAM(ID0%,ID1%))*
    (MDOT(ID0%)/(RHO(ID0%)*AREA(ID0%,ID1%)))^2   'Compute
    pressure rise accross element.
420 DEF FNVEL(ID0%,ID1%)=MDOT(ID0%)/(RHO(ID0%)*AREA(ID0%,ID1%))
    'Local velocity.
430 RETURN

440 REM Calculate Injector Pressures.
450 FOR ID0%=FUEL% TO OXIDIZER%
```

```
455 REM Work through elements to determine injector pressure for
    a particular flow condition.
460 PRESSURE(IDO%,1,0)=ULLAGE(IDO%)   'Ullage pressure.
470 PRESSURE(IDO%,1,NSECTIONS%(IDO%,1))=PRESSURE(IDO%,1,0)+
    FNDELP(IDO%,1)   'Sump pressures.
480 PRESSURE(IDO%,2,0)=PRESSURE(IDO%,1,NSECTIONS%(IDO%,1))+
    RHO(IDO%)*(FNVEL(IDO%,1)^2-FNVEL(IDO%,2)^2)/2   'Area change
    boundary condition.
490 PRESSURE(IDO%,2,NSECTIONS%(IDO%,2))=PRESSURE(IDO%,2,0)+
    FNDELP(IDO%,2)   'Pressure at feedline valve.
500 PRESSURE(IDO%,3,0)=PRESSURE(IDO%,2,NSECTIONS%(IDO%,2))-
    (FNVEL(IDO%,3)/TAUV1(IDO%))^2   'Valve b.c.
510 PRESSURE(IDO%,3,NSECTIONS%(IDO%,3))=PRESSURE(IDO%,3,0)+
    FNDELP(IDO%,3)   'Pump inlet pressure.
520 DELTAP=DELTAPO(IDO%)-BZERO(IDO%)*(FNVEL(IDO%,4)-
    VELPO(IDO%))^2-
    (BONE(IDO%)-(PRESSURE(IDO%,3,NSECTIONS%(IDO%,3))-
    PRESPO(IDO%))/(BTWO(IDO%)+BTHREE(IDO%)*
    (PRESSURE(IDO%,3,NSECTIONS%(IDO%,3))- PRESPO(IDO%))))
    'Pump pressure rise.
530 PRESSURE(IDO%,4,0)=PRESSURE(IDO%,3,NSECTIONS%(IDO%,3))+
    DELTAP   'Pump ouput pressure.
540 PRESSURE(IDO%,4,NSECTIONS%(IDO%,4))=PRESSURE(IDO%,4,0)+
    FNDELP(IDO%,4)   'Pressure at throttle valve.
550 PRESSURE(IDO%,5,0)=PRESSURE(IDO%,4,NSECTIONS%(IDO%,4))-
    (FNVEL(IDO%,5)/TAUV2(IDO%))^2   'Valve b.c.
560 PRESSURE(IDO%,5,NSECTIONS%(IDO%,5))=PRESSURE(IDO%,5,0)+
    FNDELP(IDO%,5)   'Injector pressure.
570 NEXT IDO%
    RETURN

590 REM Fill data arrays.
600 FOR IDO%=FUEL% TO OXIDIZER%
610 FOR ID1%=1 TO NELMS%(IDO%)
620 FOR ID2%=0 TO NSECTIONS%(IDO%,ID1%)
630 PRESSURE(IDO%,ID1%,ID2%)=PRESSURE(IDO%,ID1%,0)+ID2%/
    NSECTIONS%(IDO%,ID1%)*
    (PRESSURE(IDO%,ID1%,NSECTIONS%(IDO%,ID1%))-
    PRESSURE(IDO%,ID1%,0))   'Linearly interpolate local
    pressures.
```

Spring and Damper Constants. The spring constants of Table 4.5 are calculated to produce the specified component natural frequency, ω_n, which is 62.83 rad/sec (10 Hz) for both pumps and both tanks:

$$C = \zeta\, 2\sqrt{kM} \qquad [A.15]$$

The damping constants of Fig. 4.5 are calculated to satisfy the 10% of critical damping specification (ζ=0.1):

$$k = \omega_n^2\, M \qquad [A.16]$$

This completes the description of the bipropellant rocket system required by the POGO analysis routine described in Appendix A.

Setting the nominal pump ouput velocities in [3.17] to their steady state values

$$V_{Po} = \frac{\dot{M}\pi}{4\rho D^2} \qquad [A.12]$$

$$V_{Po,F} = \underline{12.896} \text{ m/sec}$$

$$V_{Po,Ox} = \underline{15.006} \text{ m/sec}$$

The nominal pump pressure rise is equal to the difference between the steady state pump output pressure minus the steady state pump inlet pressure:

$$\Delta P_o = P_{3,D} - P_{3,U} \qquad [A.13]$$

$$\Delta P_{o,F} = \underline{58.153} \text{ MPa}$$

$$\Delta P_{o,Ox} = \underline{58.006} \text{ MPa}$$

The only remaining pump parameters to be determined are the constants **B0**, **B1**, **B2**, and **B3** which are defined in [3.17]. The constant **B0** is set to 50,000 Kg/m^3 for both fuel and oxidizer pumps. This constant sets the slope of the pump pressure rise roll off and, in this case, results in the very broad roll offs shown in Fig. 4.8. For simplicity, **B1** is taken as 0.0 Pa and **B2** as 0.5. It was found that these values allow the sharp pump pressure rise roll off with decreasing pump inlet pressure, as shown in Fig. 4.9. The values of **B3** are $5 \cdot 10^{-6}$ and $2.5 \cdot 10^{-6}$ 1/Pa, respectively. These values place the pump cavitation points (the vertical lines in Fig. 4.9) 100 KPa and 200 KPa below the nominal pump inlet pressures of the fuel and oxidizer systems.

Line Thicknesses. The line thicknesses displayed in Table 4.5 are adjusted to achieve the sonic velocities specified in Table 4.3. This is done by solving [4.2] for the line wall thickness, **t**:

$$t = \frac{KD}{\gamma(K/\rho a^2 - 1)} \qquad [A.14]$$

Propellant Pumps. Figure 4.6A schematically depicts the fluid lines of the bipropellant rocket system . The pressures at the interfaces 0 (ullage pressure) and 5 (combustor) are known. The upstream pressures at interfaces 3 ($P_{3,U,F}$ and $P_{3,U,Ox}$) are the pump inlet pressures while the downstream pressures at interfaces 3 ($P_{3,D,F}$ and $P_{3,D,Ox}$) are the pump output pressures. These pressures must be found in order to define the pump's characteristics in [3.17]. Noting that the feed and throttle valves are open and can be ignored, the steady state pressure loss equations[22] (which are just the steady state case of the Navier–Stokes equations used in the method of characteristics solution of Section II) can be used to obtain the pump inlet and output pressures:

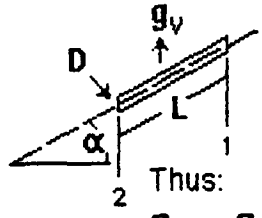

For a single pipe:

$$P_2 = P_1 + \rho g_V \sin\alpha - 1/2\,\rho V^2 \frac{L}{D} f$$

Thus:

$$P_{3,U} = P_{0,U} + \rho g_V \sin\alpha_T - 1/2\,\rho V^2 \frac{L}{D}_T f_T + \rho g_V \sin\alpha_{L1} - 1/2\,\rho V^2 \frac{L}{D}_{L1} f_{L1} + \rho g_V \sin\alpha_{L2} - 1/2\,\rho V^2 \frac{L}{D}_{L2} f_{L2} \qquad [A.10]$$

$P_{3,U,F} = \underline{180.24}$ KPa $P_{3,U,Ox} = \underline{326.93}$ KPa

Similarly,

$P_{3,D,F} = \underline{58.153}$ MPa $P_{3,D,Ox} = \underline{58.006}$ MPa

Setting the nominal pump inlet pressures in [3.17] to their steady state values

$$P_{Po,F} = \underline{180.24} \text{ KPa} \quad P_{Po,Ox} = \underline{326.93} \text{ KPa} \qquad [A.11]$$

For steady state conditions, the rate of change of the combustion chamber pressure given by [3.18] must equal zero. Rearanging [3.18]

$$Vol_C = \frac{L^* \dot{M}_{Total} C_o^*}{P_C} = \underline{0.100}\ m^3 \qquad [A.6]$$

Propellant Injectors. Using the definition of injector pressure drop and the specified chamber pressure

$$\Delta P_{inj} = \frac{0.4\, P_C}{0.6} = \underline{23.33}\ MPa \qquad [A.7]$$

The injector diameters can be calculated using the following continuity relation, the injection velocity, and the fuel and oxidizer mass flow rates. Note, the diameters are rounded to the nearest millimeter.

$$D_{inj} = \frac{4}{\pi}\sqrt{\frac{\dot{M}}{\rho V_{inj}}} \qquad [A.8]$$

$$D_{inj,F} = \underline{45}\ mm$$

$$D_{inj,Ox} = \underline{27}\ mm$$

Back substituting these rounded diameters to obtain the actual injection velocities (thus the fuel and oxidizer will not be injected at exactly 150 m/sec but the mass flow rates will be accurate) the injector flow constants can be calculated:

$$\tau_{inj} = \frac{4}{\pi}\sqrt{\frac{\dot{M}}{\rho D_{inj}^2 \Delta P_{inj}}} \qquad [A.9]$$

$$V_{inj,F} = \underline{29.66 \cdot 10^{-3}}\ (m^3/Kg)^{1/2}$$

$$V_{inj,Ox} = \underline{30.79 \cdot 10^{-3}}\ (m^3/Kg)^{1/2}$$

Mass Flow Rates. The total mass flow rate, $\dot{M}$ is given by[20:357]

$$\dot{M}_{Total} = \frac{F}{C_o^* C_T} = \underline{113.36} \text{ Kg/sec} \qquad [A.1]$$

Combining the definition of mixure ratio and the fact that the total mass flow rate is the sum of the fuel and oxidizer mass flow rates

$$\dot{M}_F = \frac{\dot{M}_{Total}}{(1+MR)} = \underline{16.18} \text{ Kg/sec} \qquad [A.2]$$

$$\dot{M}_{Ox} = \dot{M}_F MR = \underline{97.07} \text{ Kg/sec}$$

Since the fuel and oxidizer tank masses were assumed equal to the masses of the propellants stored:

$$M = \dot{M} \tau_b \qquad [A.3]$$

$$M_{T,F} = \underline{3[illegible]0} \text{ Kg}$$

$$M_{T,Ox} = \underline{25,800} \text{ Kg}$$

All component masses are now known allowing the calculation of the steady state vehicle acceleration, g_V:

$$g_V = \frac{F}{M_S + M_{T,F} + M_{T,Ox} + M_{P,F} + M_{P,Ox}} \qquad [A.4]$$

$$= \underline{19.31} \text{ m/sec}^2$$

Chamber Properties. From the definition of the gas residence time, θ_g, for steady state conditions

$$L^* = \frac{\theta_g R T_C}{C_o^*} = \underline{7.00} \text{ m} \qquad [A.5]$$

injector is 150 m/sec. This high velocity improves the efficiency of the propellant mixing process[12]. These values were chosen for simplicity and in actual practice, the injector flow coefficients would be known. This would automaticaly specify injection velocities (for a given injector pressure drop).

Relative Component Motion. The tanks and pumps are tied to the structure by means of springs (lumped stiffneses) and dashpots (lumped damping elements) as depicted in Fig. 4.7. For simplicity, all spring and damping constants will be selected to produce identical natural frequencies for the fuel and oxidizer pump and tank motions. The natural frequency is taken as 10 Hz while the damping will be 10% of the critical value. The natural frequency was selected to produce a resonance within the limited range of excitation frequencies that are examined in Section V. The structure includes all parts of the rocket system other than the pumps and tanks, i.e. fluid lines, supporting structure and payload. The structure mass is 3000 Kg while both pump masses are taken as 100 Kg. The tank masses are assumed equal to the mass of the propellants contained, neglecting the tanks' structural masses. For this system, the tanks contain enough propellant for 200 sec of burn time, therefore, the tank structural masses constitute an insignificant part of the total tank masses. Note that the structural mass fraction (including payload as part of the structure) is approximately 12% which is typical for an OTV mission[11].

Calculated Values

The bipropellant POGO analysis routine detailed in Appendix A requires still more parameter values (see Tables 4.4 and 4.5). In this section, relationships taken from the literature will be used to calculate these values from those initial values given to define the system.

propellants to obtain high specific impulses (high exhaust velocities). The fuel density is taken as 71 Kg/m^3 and the bulk modulus as 102.6 MPa while the corresponding oxidizer values are 1140 Kg/m^3 and 1.642 GPa [21]. The steady state mixture ratio (oxidizer mass flow rate devided by the fuel mass flow rate) is 6:1 (8:1 being Stoichiometric)[11,21]. As described by [3.19], the effective exhaust velocity is modeled as a linear function of mixture ratio whose slope, C^*_{slope} is taken as 75 m/sec while the gas constant, R of the exhaust gas is 5.89 KJ/Kg·K for purposes of this analysis[21]. Both the fuel and oxidizer ullage pressures, P_{ull} (the gas pressure at the top of both tanks) are 150 KPa as in the Dorsch example[1].

Fluid Lines and Tanks. The lengths, diameters, sound speeds, orientations and friction factors of the system lines and tanks given in Table 4.3 represent a typical system. Note that the feed lines are longer and larger in diameter than the high pressure discharge lines. Also, the feed lines are oriented parallel to the rockets longitudinal axis which will make the pump inlet pressures sensitive to vehicle acceleration variations, since the hydrostatic pressure at the bottom of the feed lines (pump inlet pressure) is proportional to the vehicle acceleration. The sound speeds in the fuel lines are chosen to be similar to those of the monopropellant system modeled by Dorsch, et al.[1], while the oxidizer sonic velocities are taken as approximately one-half as large as the fuel sonic velocities simply to provide a contrast between the fuel and oxidizer systems. The sonic velocities are a function of the Young's modulus and thickness of the line material. The line material Young's modulus is 10 GPa (a representative value)[12]. The tank lengths correspond to the volumes required to supply 200 seconds of steady state propellant flow (see calculated parameters). The friction factors are taken from the Dorsch system[1].

Valves and Injectors. For this analysis, both the feed and throttle valves (Fig. 4.6) are assumed to be open. This is accomplished by using a relatively large number (100 $(m^3/Kg)^{1/2}$ in this analysis) for the valve flow constants of the POGO routine. The propellant injector pressure drops are taken as 40% of their respective upstream (end of discharge line) pressures (see Dorsch monopropellant system[1]). The injection velocity for each

Appendix B: Bipropellant Liquid Rocket System Parameters

In this appendix, parameter values describing the bipropellant liquid rocket system depicted in Figs. 4.6 and 4.7 will be calculated from those values given in Table 4.3. The values defining the system will first be justified and then liquid rocket relationships will be given for the calculation of other parameters required by the bipropellant POGO analysis routine documented in Appendix A.

Initial Values

Before any numerical analysis can be attempted, values must be assigned to parameters describing the system. The bipropellant liquid rocket described in this thesis is intended to represent a "typical" system. As such, its descriptive parameters do not necessarily correspond to any actual rocket and this system is examined solely to demonstrate the application of the bipropellant POGO analysis routine developed in this investigation.

Rocket Engine Properties. The steady state thrust of the system is taken as 500,000 N with a steady state effective exhaust velocity, C_0^* of 4,415 m/sec (corresponding to a specific impulse of 450 sec) and thrust coefficient, C_T of 0.999. The steady state chamber pressure is 35 MPa (5000 psia) while the chamber temperature is 3500 K. These values are typical of the high performance OTV's and OMV's being researched today[11,16]. The values for the chamber dead time, τ_c and gas residence time, θ_g are taken as 4 msec and 1.5 msec, respectively. These values are very similar to those for the monopropellant system analyzed by Dorsch, et al.[1].

Propellants. The system employs liquid hydrogen fuel and liquid oxygen as the oxidizer since most OTV and OMV concepts employ these

Steady State Data Statements. The following values must appear in the data statements in the order shown: **FUEL%, OXIDIZER%, CSTAR0, CSTARSLOPE, MIXTURE0, CTHRUST, LSTAR, CHAMVOL, STRMASS.**

The following set of data must next appear twice: first for the fuel system and second for the oxidizer system: **NELMS%, BULK,RHO,ULLAGE, NPUMP%, AREAINJECT, TAUV1, TAUV2, TAUINJECT, BZERO, BONE, BTWO, BTHREE, DELTAP0, VELP0, PRESP0, TOL1, TANKMASS, TANKSPR, TANKDAMP, PUMPMASS, PUMPSPR, PUMPDAMP.**

The following data must appear once for each element in the fuel and oxidizer systems: **YOUNG, THICK, AREA, DIAM, LENGTH, ALPHA, FRICT.**

Dynamic Response Data Statements. The following data must appear first: **TRUE%, FALSE%, THETAG, RGAS, TOL2, TAUC, MININC.**

The following data must appear once for the fuel system and once for the oxidizer system: **PNOT1, NUNOT1, TOL3, PNOT0, NUNOT0, TOL1.**

Array Variables.

ACCEL: component acceleration
AREA: component area
BONE: pump coefficient
BTWO: pump coefficient
BZERO: pump coefficient
DELTAPO: nom. pump pres. rise
DISPLACE: component displacement
FALSE%: logical value (=0)
FUEL%: fuel index (=0)
INTNMDOT: intermediate mass rate
MDOT: current mass rate
NMDOT: final mass rate
NSECTIONS%: section index
NUNOT1: injector bubble nom. volume
OLDCP1: old Cp value
OLDCPRES: old chamber pressure
PNOTO: pump bubble nom. pres.
PRESPO: nom. pump inlet pres.
PUMPDAMP: pump damping constant
PUMPSPR: pump spring constant
SOUND: sonic velocity
TANKDAMP: tank damping constant
TANKSPR: tank spring constant
TAUV1: feed line valve flow const.
THETAG: gas residence time
TOL1: pump match pres. tolerance
TOL4: pump inlet pres. tolerance
ULLAGE: ullage pressure
VELPO: nom. pump velocity
YOUNG: component Young's modulus

ALPHA: component orient. angle
AREAINJECT: injector area
BTHREE: pump coefficient
BULK: fluid bulk modulus
DELMS%: element index
DIAM: component diameter
ELEMENT%: element index
FRICT: component friction factor
INTMDOT: intermediate mass rate
LENGTH: component length
NELM%: # of elements in system
NPUMP%: pump element ID #
NUNOTO: pump bubble nom. volume
OLDCM1: old Cp value
OLDCP2: old Cp value
OXIDIZER%: oxidizer index (=1)
PNOT1: injector bubble nom. pres.
PRESSURE: pressures
PUMPMASS: pump mass
RHO: fluid density
SVELOCITY: structure velocity
TANKMASS: tank mass
TAUINJECT: injector flow constant
TAUV2: throttle valve flow const.
TOLO: mass flow match tolerance
TOL3: injector match pres. tol.
TRUE%: logical value (=-1)
VELOCITY: velocities
VELQUEUE: velocity queue

Program Variables

This section lists all of the variables used in the steady state and dynamic response routines. The identity and meaning of each program variable will be given, and the input order will be specified for those variables whose values are read from data statements.

Simple Variables.

ATIME: time parameter
BETA: area ratio
CM: current value of Cm
CP: current value of Cp
CPRES: chamber pressure
CSTAR0: nominal exhaust velocity
CTHRUST: thrust coefficient
DELTAT: time step
ENDPRES: pressure (intermediate)
ENDPRES2: pressure (int.)
ID1%: counter
ID3%: counter
INVEL: pump inlet velocity
MIDPRESS: pressure (average)
MIXTURE: current mixture ratio
MNELM%: largest # of elements
NENDPRES1: pressure (intermediate)
NEWPRESS: pressure (terminal)
OLDTHRUST: last thrust value
PRESR: Pr
PSI: grid parameter
REACT: total reaction force
RGAS: chamber gas constant
SIDE%: designator (fuel=0, ox.=1)
STRMASS: structure mass
TAU: orafice constant
TCHAM: chamber temperature
THETA: grid mesh ratio
TOL2: combustor pres. tolerance
VELR: Vr

BACKTIME: Velocity queue param.
CHAMVOL: chamber volume
CMMID: Cm (intermediate)
CPMID: Cp (intermediate)
CSTAR: current exhaust velocity
CSTARSLOPE: local slope
DELTAP: pump pressure rise
DELTATOUT: output time step
ENDPRES1: pressure (int.)
ID0%: counter
ID2%: counter
INTPRES: pressure (intermediate)
LSTAR: chamber char. length
MININC: min. structural time step
MIXTUREZERO: nom. mixture ratio
MNSECT%: largest # of sections
NENDPRES2: pressure (int.)
NINCS%: # of minor timesteps
OUTVEL: pump outlet velocity
PRESS: Ps
QSIZE%: size of velocity queue
RES$: a user response string
SEC%: section
STORATE: pump inlet storage rate
SYSTEMTHRUST: thrust
TAUC: chamber dead time
TEND: end time
THICK: pipe wall thicknes
TSART: begin time
VELS: Vs

```
1080 DATA 1E+10, 644.37E-6, 70.686E-3, 0.3, 8, 1.5708, 0.03
1090 DATA 1E+10, 644.37E-6, 70.686E-3, 0.3, 8, 1.5708, 0.03
1100 DATA 1E+10, 1.9718E-3, 17.671E-3, 0.15, 1, 0, 0.002
1110 DATA 1E+10, 1.9718E-3, 17.671E-3, 0.15, 1, 0, 0.002
1120 DATA 1E+10, 1.9245E-3, 7.0686, 3, 2.4093, 1.5708, 0.03
1130 DATA 1E+10, 305.05E-6, 22.698E-3, 0.17, 3, 1.5708, 0.03
1140 DATA 1E+10, 305.05E-6, 22.698E-3, 0.17, 3, 1.5708, 0.03
1150 DATA 1E+10, 506.58E-6, 5.6745E-3, 0.085, 1, 0, 0.002
1160 DATA 1E+10, 506.58E-6, 5.6745E-3, 0.085, 1, 0, 0.002

1170 REM Thrust determination.
1180 MIXTURE=MDOT(OXIDIZER%)/MDOT(FUEL%)   'Compute mixture
     ratio.
1185
     SYSTEMTHRUST=(MDOT(FUEL%)+MDOT(OXIDIZER%))*(CSTAR0+CSTARSLOP
     E* (MDOT(OXIDIZER%)/MDOT(FUEL%)-MIXTURE0))*CTHRUST
     'Determine thrust.
1190 ACCEL(FUEL%,0)=SYSTEMTHRUST/(STRMASS+TANKMASS(FUEL%)+
     TANKMASS(OXIDIZER%)+PUMPMASS(FUEL%)+PUMPMASS(OXIDIZER%))
     'Get system acceleration.
1200 ACCEL(OXIDIZER%,0)=ACCEL(FUEL%,0)
1210 CSTAR=CSTAR0+CSTARSLOPE*(MIXTURE-MIXTURE0)   'Operating
     exhaust velocity.
1220 CPRES=LSTAR*CSTAR/CHAMVOL*(MDOT(FULE%)+MDOT(OXIDIZER%))
     'Operating chamber pressure.
1230 GOSUB 440   'Get Injector Pressures.
1240 FOR IDO%=FUEL% TO OXIDIZER%
1250 MMDOT(IDO%)=TAUINJECT(IDO%)*
     (PRESSURE(IDO%,MELMS%(IDO%),MSECTIONS%(IDO%,MELMS%(IDO%)))-
     CPRES)^.5*AREAINJECT(IDO%)*RHO(IDO%)   'Compute mass flow
     rate.
1260 NEXT IDO%
1270 RETURN
1280 END
```

```
870 FOR ID0%=FUEL% TO OXIDIZER%
880 READ NELMS%(ID0%), BULK(ID0%), RHO(ID0%), ULLAGE(ID0%),
    NPUMP%(ID0%), AREAINJECT(ID0%), TAUV1(ID0%), TAUV2(ID0%),
    TAUINJECT(ID0%), BZERO(ID0%), CONE(ID0%), BTWO(ID0%),
    BTHREE(ID0%)
890 READ DELTAPO(ID0%), VELPO(ID0%), PRESPO(ID0%), TOLO(ID0%),
    TANKMASS(ID0%), TANKSPR(ID0%), TANKDAMP(ID0%),
    PUMPMASS(ID0%), PUMPSPR(ID0%), PUMPDAMP(ID0%)
900 NEXT ID0%
910 IF NELMS%(FUEL%)>NELMS%(OXIDIZER%) THEN MNELM%=NELMS%(FUEL%)
    ELSE MNELM%=NELMS%(OXIDIZER%)
920 DIM AREA(1,MNELM%): DIM DIAM(1,MNELM%): DIM
    LENGTH(1,MNELM%): DIM ALPHA(1,MNELM%): DIM
    DISPLACE(1,MNELM%): DIM SVELOCITY(1,MNELM%): DIM
    ACCEL(1,MNELM%): DIM SOUND(1,MNELM%): DIM NSECTIONS%(1,
    MNELM%): DIM FRICT(1, MNELM%)
930 FOR ID0%=FUEL% TO OXIDIZER%
940 FOR ID1%=1 TO NELMS%(ID0%)
950 READ YOUNG, THICK, AREA(ID0%,ID1%), DIAM(ID0%,ID1%),
    LENGTH(ID0%,ID1%), ALPHA(ID0%,ID1%), FRICT(ID0%,ID1%)
960 SOUND(ID0%,ID1%)=(BULK(ID0%)/(RHO(ID0%)*(1+BULK(ID0%)*
    DIAM(ID0%,ID1%)/(YOUNG*THICK))))^.5   'Compute local sonic
    velocity.
970 NEXT ID1%
980 MDOT(ID0%)=VELPO(ID0%)*AREA(ID0%,NPUMP%(ID0%))*RHO(ID0%)
    'First guess for system flow.
990 NEXT ID0%
1000 RETURN

1010 REM Data for steady state problem.
1020 DATA 0, 1, 4415, 75, 6, 0.999, 7, 0.1, 3000
1030 DATA 5, 102.24E+6, 71, 150E+3, 4, 1.5904E-3, 100, 100,
     29.664E-3,  50000, 0, 0.5, 5E-6
1040 DATA 58.153E+6, 12.896, 180.24E+3, 0.1, 3236, 12.774E+6,
     40.663E+3, 100, 394.78E+3, 1.2566E+3
1050 DATA 5, 1.6416E+9, 1140, 150E+3, 4, 572.56E-6, 100, 100,
     30.787E-3, 50000, 0, 0.5, 2.2033E-6
1060 DATA 58.006E+6, 15.006, 326.93E+3, 0.1, 19414, 76.643E+6,
     243.96E+3, 100, 394.78E+3, 1.2566E+3
1070 DATA 1E+10, 2.0448E-3, 7.0686, 3, 6.4478, 1.5708, 0.03
```

```
640 VELOCITY(ID0%,ID1%,ID2%)=FNVEL(ID0%,ID1%)   'Element
    velocities.
650 NEXT ID2%
660 NEXT ID1%
670 NEXT ID0%
680 RETURN

690 REM Input user data and calculate required number of
    sections.
700 CLS: CALL TEXTFONT(0): CALL TEXTSIZE(18): PRINT: PRINT
    TAB(5);"Steady State Initialization"
710 CALL TEXTSIZE(12): PRINT: PRINT
720 PRINT TAB(5);"Time Increment: ";: INPUT "",DELTAT
730 MNSECT%=0
740 FOR ID0%=FUEL% TO OXIDIZER%
750 FOR ID1%=1 TO NELMS%(ID0%)
760 NSECTIONS%(ID0%,ID1%)=INT(LENGTH(ID0%,ID1%)/(DELTAT*
    (SOUND(ID0%,ID1%)+MDOT(ID0%)/(RHO(ID0%)*AREA(ID0%,ID1%)))))
    'Compute number of sections based on Courant condition.
770 IF NSECTIONS%(ID0%,ID1%)=0 THEN PRINT TAB(5);"Time Increment
    too large.": END   'Quit if response is unacceptable.
780 IF NSECTIONS%(ID0%,ID1%)>MNSECT% THEN
    MNSECT%=NSECTIONS%(ID0%,ID1%)   'Determine system with
    maximum number of sections.
790 NEXT ID1%
800 NEXT ID0%
810 DIM VELOCITY(1,MNELM%,MNSECT%): DIM
    PRESSURE(1,MNELM%,MNSECT%)
820 RETURN

830 REM Input data and dimension arrays.
840 READ FUEL%, OXIDIZER%, CSTAR0, CSTARSLOPE, MIXTURE0,
    CTHRUST, LSTAR, CHAMVOL, STRMASS
850 DIM NELMS%(1): DIM RHO(1): DIM ULLAGE(1): DIM NPUMP%(1): DIM
    AREAINJECT(1): DIM TAUV1(1): DIM TAUV2(1): DIM TAUINJECT(1):
    DIM MDOT(1): DIM BZERO(1): DIM BONE(1): DIM BTWO(1): DIM
    BTHREE(1): DIM INTMDOT(1): DIM NMDOT(1): DIM INTNMDOT(1)
860 DIM DELTAP0(1): DIM VELP0(1): DIM PRESP0(1): DIM PUMPSPR(1):
    DIM PUMPDAMP(1): DIM TANKSPR(1): DIM TANKDAMP(1): DIM
    PUMPMASS(1): DIM TANKMASS(1): DIM BULK(1)
```

Vita

Second Lieutenant David A. Rosenberg was born on 21 May 1959 in Tulsa, Oklahoma. He graduated from high school in Danville, California, in 1978 and attended the University of California, at Berkeley, where he received the degree of Bachelor of Science in Mechanical Engineering in December 1982. He received a commission in the USAF through AF OTS in May 1983, entering the resident program at AFIT immediately thereafter.

Permanent address: 231 Vagabond Ct.
Danville, CA 94526

UNCLASSIFIED

SECURITY CLASSIFICATION OF THIS PAGE

REPORT DOCUMENTATION PAGE

1a. REPORT SECURITY CLASSIFICATION UNCLASSIFIED	1b. RESTRICTIVE MARKINGS
2a. SECURITY CLASSIFICATION AUTHORITY	3. DISTRIBUTION/AVAILABILITY OF REPORT Approved for public release; distribution unlimited.
2b. DECLASSIFICATION/DOWNGRADING SCHEDULE	
4. PERFORMING ORGANIZATION REPORT NUMBER(S) AFIT/GA/AA/84D-9	5. MONITORING ORGANIZATION REPORT NUMBER(S)
6a. NAME OF PERFORMING ORGANIZATION School of Engineering 6b. OFFICE SYMBOL (If applicable) AFIT/EN	7a. NAME OF MONITORING ORGANIZATION
6c. ADDRESS (City, State and ZIP Code) Air Force Institute of Technology Wright Patterson AFB, Ohio 45433	7b. ADDRESS (City, State and ZIP Code)
8a. NAME OF FUNDING/SPONSORING ORGANIZATION 8b. OFFICE SYMBOL (If applicable)	9. PROCUREMENT INSTRUMENT IDENTIFICATION NUMBER
8c. ADDRESS (City, State and ZIP Code)	10. SOURCE OF FUNDING NOS. PROGRAM ELEMENT NO. / PROJECT NO. / TASK NO. / WORK UNIT NO.
11. TITLE (Include Security Classification) See Box 19	
12. PERSONAL AUTHOR(S) David A. Rosenberg, B.S., 2d Lt, USAF	
13a. TYPE OF REPORT MS Thesis 13b. TIME COVERED FROM _____ TO _____	14. DATE OF REPORT (Yr., Mo., Day) 1984 December 15. PAGE COUNT 124
16. SUPPLEMENTARY NOTATION	

17. COSATI CODES			18. SUBJECT TERMS (Continue on reverse if necessary and identify by block number)
FIELD	GROUP	SUB. GR.	Liquid Rockets, POGO Instability, Method of Characteristics, Finite Difference
21	08	1	

19. ABSTRACT (Continue on reverse if necessary and identify by block number)

Title: A CLOSED LOOP ANALYSIS OF POGO INSTABILITY

Thesis Chairman: Milton E. Franke, PhD

Approved for public release: IAW AFR 190-17.

LYNN E. WOLAVER
Dean for Research and Professional Development
Air Force Institute of Technology (AIC)
Wright-Patterson AFB OH 45433

20. DISTRIBUTION/AVAILABILITY OF ABSTRACT UNCLASSIFIED/UNLIMITED ☒ SAME AS RPT. ☐ DTIC USERS ☐	21. ABSTRACT SECURITY CLASSIFICATION UNCLASSIFIED
22a. NAME OF RESPONSIBLE INDIVIDUAL Milton E. Franke, PhD	22b. TELEPHONE NUMBER (Include Area Code) 22c. OFFICE SYMBOL AFIT/ENY

DD FORM 1473, 83 APR EDITION OF 1 JAN 73 IS OBSOLETE.

UNCLASSIFIED

SECURITY CLASSIFICATION OF THIS PAGE

In this thesis, a generalized computer code for the simulation of POGO instability in liquid rockets was generated and verified. The term POGO refers to the out of phase motion of the ends of a liquid rocket, which can build to a dangerous magnitude due to propulsion feed back. The elimination of any POGO instability will be of great importance in the development of future liquid rocket systems such as OTV's and OMV's. The model detailed in this investigation is based on a method of characteristics solution of the simplified Navier-Stokes equations. The resulting non-linear differential equations were solved using first order finite difference methods. This solution was applied to the fluid lines of several liquid rocket systems. Boundary conditions, based on component models used generally throughout the literature were developed to link these fluid lines.

The computer routines were verified by comparison with published results from several sources. The results of numerous runs agreed quite well with the published data, even in very non-linear systems with large disturbance amplitudes.

As an aid to future investigators the routines developed in this thesis were applied to a typical bipropellant liquid rocket system. Both the transient and the steady state responses of this system to sinusoidal thrust variations were obtained. A relatively limited parametric study was performed and indicated the extreme parametric sensitivity of the model to input thrust variation. Two factors were most important: The pump operating points and the chamber dead time, the stability of the system being greatly decreased with a large dead time or by operation near the cavitation point.

A user's guide was compiled which details the software developed here. Its purpose is to facilitate the application of these routines to other systems by future investigators.

END

FILMED

5-85

DTIC